NOTICE

The quality of this microform is heavily dependent upon the quality of the original thesis submitted for microfilming. Every effort has been made to ensure the highest quality of reproduction possible.

If pages are missing, contact the university which granted the degree.

Some pages may have indistinct print especially if the original pages were typed with a poor typewriter ribbon or if the university sent us an inferior photocopy.

Reproduction in full or in part of this microform is governed by the Canadian Copyright Act, R.S.C. 1970, c. C-30, and subsequent amendments.

AVIS

La qualité de cette microforme dépend grandement de la qualité de la thèse soumise au microfilmage. Nous avons tout fait pour assurer une qualité supérieure de reproduction.

S'il manque des pages, veuillez communiquer avec l'université qui a conféré le grade.

La qualité d'impression de certaines pages peut laisser à désirer, surtout si les pages originales ont été dactylographiées à l'aide d'un ruban usé ou si l'université nous a fait parvenir une photocopie de qualité inférieure.

La reproduction, même partielle, de cette microforme est soumise à la Loi canadienne sur le droit d'auteur, SRC 1970, c. C-30, et ses amendements subséquents.

Canada

Feasibility Investigation of a New Concept of Ignition Chamber for Diesel Engine Using Compressed Methane as Combustible

Michel Pharand

A Thesis

in

The Department

of

Mechanical Engineering

Presented in Partial Fulfilment of the Requirements
for the Degree of Master of Applied Science at
Concordia University
Montreal, Quebec, Canada

September 1993

ISBN 0-315-87279-9

ABSTRACT

Feasibility Investigation of a New Concept of Ignition Chamber for Diesel Engine Using Compressed Methane as Combustible

Michel Pharand

The need for low emission vehicles has prompted research in the field of alternate fuels. Gaseous fuels such as hydrogen and methane are needed to replace liquid hydrocarbon fuels, whose emissions have been scientifically linked to causing environmental damage. A great deal of research is focused on the use of the diesel engine because it represents the most energy efficient power plant. Ignition problems have been encountered with gaseous fuels such as hydrogen and methane, when used in diesel engines.

This thesis addresses the problem of ignition when injecting compressed methane in a compression ignition engine. The objective of this thesis is to test the feasibility of a new type of ignition chamber to be used with a diesel engine. To support the ignition of the injected fuel charge, a spark plug is placed inside the ignition chamber instead of the standard glow plug which is normally utilized in a diesel engine. To test the new prototype, a modified single cylinder diesel engine with the ignition system controlled by a microprocessor has been fitted with this new chamber. To further support this analysis, the method of schlieren photography has been used to visualize the

gas flow path taking place in this ignition chamber. The test engine as well a the schlieren photography setup, served not only as investigation tools, but also as optimizing instruments for this new ignition chamber concept. The method and strategy used to develop this prototype is fully discussed in this thesis. Finally, recommendations for further work are made based on the test results.

ACKNOWLEDGMENTS

The author would like to express his gratitude to the many individuals who helped in the preparation of this thesis, for their involvement, support, and encouragement. In particular, special thanks is extended to Dr.T.Krepec, my supervisor, whose support, guidance, and financial assistance throughout my graduate studies made this thesis possible. I am grateful to Bendix Avalex inc. for their financial support via the contract given to the Fuel Control Laboratory at Concordia University. I thank my co-workers from the Fuel Control Laboratory, Dr.A.Georgantas and H.Kekedjian, who provided consulting and assistance in writing some softwares. I also wish to thank Dr.R.A.Neemeh for his consultation in the field of gas dynamics. Also, many thanks to P.Lawn for his help in setting up the schlieren photography equipment and use of the Dr.A.J.Saber Aerospace and Propulsion Laboratory at Concordia University.

I am indebted to my mother, Aline Pharand, for her love and financial support in difficult times. And to my long time friends Vern Bélanger and Grégoire Blais, for their moral support which proved invaluable.

Finally, but not least, I am especially grateful to Cortina Jone for her continual patience, understanding and assistance. In particular, her background in engineering and computer science served as an invaluable asset in proofreading this thesis.

TABLE OF CONTENTS

LIST OF FIGURES ix

LIST OF TABLES xv

NOMENCLATURE xvi

CHAPTER 1

1.0 INTRODUCTION 1

CHAPTER 2

2.0 LITERATURE STUDY 6

CHAPTER 3

3.0 GAS IGNITION CONCEPTS 13

3.1 Introduction 13

3.2 Design Strategy 15

3.3 Proposed Ignition Chamber Design 16

3.3.1 Ricardo Hydra Engine 17
3.3.1.1 Pilot Injection Ignition Chamber 18
3.3.1.2 Turbulent Ignition Chamber . . . 20

3.3.2 Peugeot Indenor Diesel Engine 22
3.3.2.1 Conventional Swirl Chamber . . . 23
3.3.2.2 Dual Jet Ignition Chamber 24

3.4 New Concept of Ignition Chamber for Gaseous Fuel Application 25

CHAPTER 4

4.0 METHODOLOGY 29

CHAPTER 5

5.0 TEST SETUP FOR IGNITION INVESTIGATION 35

5.1 Experimental Apparatus 35

5.2 Ignition Chamber Design 39

5.3 High Pressure Gas Injector Modifications 43

5.3.1 Calculation of Injected Fuel Dose 47

5.3.2 Experimental Apparatus Used for Calibration of the Gas Injector 52

5.3.3 Calibration Methodology 56

5.3.4 Calibration Results and Discussion . . . 60

5.3.5 Determination of the Gas Jet Angle . . . 61

5.4 Injector Control Circuit 62

5.5 Signal Conditioning Circuit for Measuring the Crankshaft Position 70

5.6 Spark Ignition System Evaluation 74

5.6.1 Spark Ignition Theory 74

5.6.2 Spark Ignition Selection 78

5.6.3 Description of the Apparatus and Testing Methodology 80

5.6.4 Ignition Triggering Circuit 81

5.6.5 Ignition System Tested 85

5.6.6 Test Results 87

5.6.7 Discussion of the Results and Recommendations 88

5.7 Software for MCS-96 Controller 90

CHAPTER 6

6.0 PRELIMINARY ENGINE IGNITION TESTS 98

6.1 Test Results and Discussion 106

CHAPTER 7

7.0 VISUALIZATION OF THE GAS FLOW PATH USING SCHLIEREN PHOTOGRAPHY 115

7.1 Experimental Apparatus 116

7.2 Design of a High Pressure Vessel with Quartz Windows 121

7.3 Ignition Chamber Model Used for the Experiment . 125

7.4 Software for the MCS-96 Controller 127

7.5 Schlieren Photography Operation 131

7.6 Visualization Methodology 132

7.7 Visualization Results 136

7.8 Visualization Results Discussion 143

CHAPTER 8

8.0 FINAL ENGINE IGNITION TESTS 146

8.1 Test Results and Discussion 150

CHAPTER 9

9.0 SUMMARY, CONCLUSION, AND RECOMMENDATIONS 156

REFERENCES 162

APPENDIX A A.1

APPENDIX B B.1

APPENDIX C C.1

APPENDIX D D.1

APPENDIX E E.1

LIST OF FIGURES

CHAPTER 3

Figure 3.1 Basic ignition chamber design proposed for Ricardo Hydra engine 17

Figure 3.2 Pilot injection ignition chamber for Ricardo Hydra engine 19

Figure 3.3 Ignition chamber for Ricardo Hydra engine in action, a. Phase I - Ignition, b. Phase II - Gaseous torch development 19

Figure 3.4 Turbulent ignition chamber from Ricardo Hydra engine 21

Figure 3.5 Turbulent ignition chamber of Ricardo Hydra engine in action a. Phase I - Ignition, b. Phase II - Flame penetration of charge 21

Figure 3.6 Swirl chamber Ricardo Comet of Peugeot Indenor engine 22

Figure 3.7 Ricardo Comet swirl chamber in action a. Phase I - Ignition, b. Phase II - Combustion 23

Figure 3.8 Dual jet ignition chamber for Peugeot Indenor engine 24

Figure 3.9 Dual jet ignition chamber for Peugeot engine in action a. Phase I - Ignition, b. Phase II - Combustion 25

Figure 3.10 Proposed ignition chamber concept 27

Figure 3.11 Ignition chamber concept for the open combustion chamber of the Petters engine 28

CHAPTER 5

Figure 5.1 Petters engine coupled with electric motor for ignition tests 36

Figure 5.2 Optical switch support system using the camshaft to send a signal to the microcontroller . . 36

Figure 5.3 Schematic of the primary setup for ignition testing 38

Figure 5.4 Assembly drawing of the ignition chamber design 40

Figure 5.5 Ignition chamber with injector on modified Petters diesel engine 41

Figure 5.6 Ignition chamber with injector spacers 42

Figure 5.7 Cross sectional view of the injector 45

Figure 5.8 Ignition chamber for Petters engine with injector, spark plug and pressure transducer 46

Figure 5.9 Nozzle modification needed for gaseous fuel . . 51

Figure 5.10 High pressure gas injector, mounted on fuel dose measurement device 53

Figure 5.11 Sectional view of the device used for measuring the fuel dose from the injector 54

Figure 5.12 Schematic representation of the apparatus used for the fuel dose calibration of the injector . 55

Figure 5.13 Calibration curve No.1 58

Figure 5.14 Calibration curve No.2 59

Figure 5.15 Setup used to determine the gas jet cone angle 62

Figure 5.16 Injector triggering circuit, H-bridge type . 64

Figure 5.17 H-bridge circuit performance for ΔP of 14.6 [bar] 65

Figure 5.18 Injector triggering circuit (boost circuit) . 67

Figure 5.19 Boost circuit performance for a ΔP of 28.2 [bar] 68

Figure 5.20 Signal conditioning circuit 73

Figure 5.21 Current characteristics during sparking, the current probe setting is 100 mV/amp 75

Figure 5.22 MOSFET triggering circuit 77

Figure 5.23 Spark evaluation instrument 79

Figure 5.24 Schematic diagram of the apparatus using the MOSFET triggering circuit 82

Figure 5.25 Experimental setup used with MSD ignition box 89

Figure 5.26 JP2 connector for interface between MCS-96 microcontroller and peripheral [28] 92

Figure 5.27 Flow chart for ENGINE program 94

Figure 5.28 Flow chart for ENGINE1 program 97

CHAPTER 6

Figure 6.1 Various injector position 99

Figure 6.2 Spark plug orientation 105

Figure 6.3 Experimental result no.10, CH1-injector pressure, CH2-ignition chamber pressure, CH3-spark plug current, CH4-TDC on falling edge 108

Figure 6.4 Experimental result no.17 109

Figure 6.5 Experimental result no.9 112

Figure 6.6 Experimental result no.19 114

CHAPTER 7

Figure 7.1 Schlieren photography apparatus 117

Figure 7.2 Pressure chamber used for the schlieren photography experiment 118

Figure 7.3 Relief valve used with pressure chamber 122

Figure 7.4 Pressurized chamber for investigation of gaseous jets 124

Figure 7.5 Detailed drawing of the ignition chamber model 126

Figure 7.6 Software flow chart for MCS-96 controller . . 128

Figure 7.7 Different injector nozzle configuration (a) cylindrical nozzle orifice (b) 30° nozzle orifice angle (c) 30° nozzle orifice angle with modified injector pintle 135

Figure 7.8 Cylindrical nozzle orifice, Hole diameter: 0.75 [mm], Distance: position no.7, Injector opened for 0.36 [msec] 137

Figure 7.9 Cylindrical nozzle orifice, Hole diameter: 0.75 [mm], Distance: position no.7, Injector opened for 0.67 [msec] 137

Figure 7.10 Cylindrical nozzle orifice, Hole diameter: 0.75 [mm], Distance: position no.7, Injector opened for 1.60 [msec] 137

Figure 7.11 Cylindrical nozzle orifice, Hole diameter: 0.75 [mm], Distance: position no.5, Injector opened for 0.28 [msec] 138

Figure 7.12 Cylindrical nozzle orifice, Hole diameter: 0.75 [mm], Distance: position no.5, Injector opened for 0.46 [msec] 138

Figure 7.13 Cylindrical nozzle orifice, Hole diameter: 0.75 [mm], Distance: position no.5, Injector opened for 2.10 [msec] 138

Figure 7.14 30° nozzle orifice angle, Hole diameter: 0.75 [mm], Distance: position no.5, Injector opened for 0.67 [msec] 139

Figure 7.15 30° nozzle orifice angle, Hole diameter: 0.75 [mm], Distance: position no.5, Injector opened for 1.60 [msec] 139

Figure 7.16 30° nozzle orifice angle, Hole diameter: 0.75 [mm], Distance: position no.5, Injector opened for 2.10 [msec] 139

Figure 7.17 30°nozzle orifice angle, pintle modified to induce swirl, Hole diameter: 0.75 [mm], Distance: position no.5, Injector opened for 0.67 [msec] . . . 140

Figure 7.18 30° nozzle orifice angle, pintle modified to induce swirl, Hole diameter: 0.75 [mm], Distance: position no.5, Injector opened for 0.92 [msec] . . . 140

Figure 7.19 30° nozzle orifice angle, pintle modified to induce swirl, Hole diameter: 0.75 [mm], Distance: position no.5, Injector opened for 1.60 [msec] . . . 140

CHAPTER 8

Figure 8.1 Redesigned ignition chamber insert 147

Figure 8.2 Experiment result no.23, CH1-injector pressure, CH2-ignition chamber pressure, CH3-spark plug current, CH4-TDC on falling edge 153

Figure 8.3 Pressure distribution in both chambers during ignition, CH1-cylinder pressure, CH2-ignition chamber pressure 154

Figure 8.4 Peak pressure registered in both chambers during ignition, CH1-cylinder pressure, CH2-ignition chamber pressure 155

APPENDIX B

Figure B.1 Ignition chamber body B.1

Figure B.2 Ignition chamber insert B.2

Figure B.3 Fuel injector spacer B.3

Figure B.4 Copper washer (cylinder head and ignition chamber) B.4

Figure B.5 Washer for sealing surface between the fuel injector spacer and the ignition chamber B.5

Figure B.6 Adapter for spark plug to ignition chamber . B.6

APPENDIX C

Figure C.1 Ignition chamber with spacer number 1 . . . . C.1

Figure C.2 Ignition chamber with spacer number 2 . . . . C.2

Figure C.3 Ignition chamber with spacer number 3 . . . . C.3

Figure C.4 Ignition chamber with spacer number 4 . . . . C.4

Figure C.5 Ignition chamber with spacer number 5 . . . . C.5

Figure C.6 Ignition chamber with spacer number 6 . . . . C.6

Figure C.7 Ignition chamber with spacer number 7 . . . . C.7

APPENDIX D

Figure D.1 Pressure transducer drawing D.1

Figure D.2 Technical information for the pressure transducer D.1

Figure D.3 Calibration curve of the injector pressure transducer D.2

Figure D.4 Calibration curve of the ignition chamber pressure transducer D.3

APPENDIX E

Figure E.1 Engine data sheet E.1

LIST OF TABLES

CHAPTER 5

Table 5.1 Conversion table from decimal to hexadecimal . . . 57

Table 5.2 Results obtained from the experiments 87

CHAPTER 6

Table 6.1 Injector position 99

Table 6.2a Initial ignition test results. 101

Table 6.2b Initial ignition test results 102

Table 6.2c Initial ignition test results 103

CHAPTER 7

Table 7.1 Software delay for triggering the light source . 130

CHAPTER 8

Table 8.1 Final ignition test results 149

NOMENCLATURE

A_{fl} - injector flow area, [m^2]

C_d - discharge coefficient

D - diameter, [m]

L - length, [m]

m_a - mass of air, [kg]

m_f - mass of fuel, [kg]

$\dot{m}_f$ - fuel mass flow rate, [kg/sec]

P_f - cylinder pressure at end of compression, [kPa]

P_i - initial cylinder pressure, [kPa]

P_{inj} - injector pressure, [kPa]

r - stoichiometric ratio

T_i - initial cylinder temperature, [K]

V_i - initial cylinder volume, [m^3]

V_f - clearance volume, [m^3]

GREEK SYMBOLS

α - angle, [deg]

Δt - change in time, [sec]

γ - specific heat ratio

η - volumetric efficiency

ρ_{inj} - fuel density in injector, [kg/m^3]

CHAPTER 1

1.0 INTRODUCTION

In recent decades, engineers and scientists have extensively researched the effects of fossil fuel emissions on our environment. Their results show environmental damage arising from our daily use of transportation vehicles. The pollutant CO is poisoning the atmosphere. It has been proven that the CO_2 is partly responsible for causing global warming. Furthermore, NOx and $CH^{\bullet}$ emissions are directly linked to the formation of ground level pollution, commonly known as smog. However, two solutions have slowly emerged from international environmental forums; increasing the use of electrical vehicles and of public transportation systems using alternative fuels.

Electrical vehicles are drawing a lot of attention from industry and the world media as a pollution free propulsion system for transportation. But, at present, this technology can only be implemented on lightweight vehicles and certain public transport vehicles such as city buses and metros. Because of the high cost related to the implementation of this technology and the limited range of the vehicles, electric power does not present a feasible solution for intercity delivery vehicles (intermediate and heavy size trucks for urban and intercity use).

An alternative solution to this problem is the use of alternate fuels such as natural gas, hydrogen, or alcohols. The first two energy sources aforementioned, are the more promising

choices from the point of view of pollutant emission. Emissions from alcohols are not much less pollutant than those from gasoline. Natural gas is found in abundance in Canada, and is relatively inexpensive to extract. In contrast, hydrogen, which can be obtained from water or natural gas, is relatively expensive due to the production process used. Therefore, it is not commercially feasible.

When using a gaseous fuel as combustible for a vehicular internal combustion engine, two problems arise; (1) the on board storage of the fuel and (2) the fuel delivery system. Compressed methane, in a gaseous state, has a lower volumetric energy content as compared to gasoline. Hence, the storage of methane in this state, causes an increase in the weight of the vehicle and occupies a substantially larger volume of the vehicle in order to preserve a comparable vehicle range. Gaseous fuels have a larger specific volume than liquid fuels, thus displaces a greater volume of air when injected into the manifold. Therefore, direct injection of gaseous fuels into the cylinder is a more efficient method of fuel delivery than manifold injection, because there is no displacement of air out of the cylinder.

For spark ignition engines, an extensive amount of technology is readily available, thus the engine conversion can be made without much difficulty. However, for engines operating on diesel cycle, many obstacles are encountered. There are limitations to the time available for proper mixing of the fuel

and air and for ignition. Because the fuel is injected into the cylinder late in the compression cycle, the mixing process between the two fluids should have a very short duration. This effect results in a highly stratified mixture present upon ignition.

For intermediate size diesel engines, with a cylinder capacity between 0.5 to 1 litres, the injection of the fuel can be made via a pre-chamber. The advantages of using a pre-chamber, as opposed to direct injection are significant. The divided chamber increases the mixing rate and accelerates the propagation of the flame front. As a result, an engine can be operated at a higher speed and produce a higher power output.

The primary scope of this thesis will be to investigate the feasibility of a new design of ignition chamber. This includes the experimental approach to be used for testing of a prototype, and the hardware required on the test setup. The investigation of such an ignition chamber will aid in establishing its potential application for gaseous fuel engines, or more specifically, engines using natural gas as combustible.

The obstacle related to the ignition of natural gas is the high energy required to ignite this fuel as compared to diesel fuel. Because of the low cetane number of natural gas, compression ignition is not likely. To overcome this difficulty, ignition has to be supported by other means. Several techniques have been used in the past with certain success, such as glow plug and spark plug. The problem encountered with the glow plug

is its short life span, since it has to be used continuously as opposed to a conventional diesel engine where it is used only for starting. With the spark plug system, the spark discharge is restricted to a single instant; therefore the mixture present in the region of spark electrodes has to be close to stoichiometric. However, spark ignition support applied to gaseous fuel ignition presents the highest potential.

For diesel fuels the mechanisms pertaining to ignition and combustion are well known and documented, but not for gaseous fuels to be used in diesel engines. Ignition of a charge of natural gas is a function of the temperature level present in the ignition chamber. For most diesel engines using typical compression ratio which ranges between 15-23, the air temperature in the cylinder near the end of compression is still not sufficient for self-ignition of the natural gas/air mixture despite the presence of a stoichiometric ratio mixture at some location in the chamber. For this reason, ignition has to be supported by external means.

The proposed concept for this thesis, is to try an ignition chamber with a spark plug commonly used in Otto engines to support ignition. However, the use of a spark plug in a diesel engine creates several problems. One of the problems is the difficulty for sparking to occur across the electrodes because of high air density caused by the high compression ratio.

To fulfill the objective of this thesis the following issues are addressed in the ensuing chapters.

* Establish the problems related to gaseous fuel ignition.
* Find a suitable research engine and an ignition chamber geometry for natural gas ignition.
* Build a research test setup for ignition investigation.
* Investigate the proposed design and optimize its performance, so that 100% reliability in ignition would be obtained.

CHAPTER 2

2.0 LITERATURE STUDY

Since the petroleum crisis in the early 1970's, a general concern about our dependence on imported energy source has been rapidly growing among the population. With transportation systems being of strategic importance in occidental countries, drastic measures had to be taken to decrease our dependence on petroleum importation. A significant increase in the price of the petroleum barrel, compounded with an unstable political situation in many of the crude oil supplying countries has forced most industrialized countries to review their policies with respect to the development of alternate energies [1]*. For these reasons, substantial funding is available for research in alternate energy sources.

In the early 1930's, Sir H.R. Ricardo [2] proposed several designs for improving ignition characteristics of diesel engines. The Comet Mark III and the Comet Mark V combustion chambers, and the Whirlpool designs, have been successfully used over the years by different engine manufacturers. The three aforementioned chamber types are referred to as divided chamber or pre-ignition chamber.

---

* Numbers in square brackets designate references at the end of this thesis.

Their main feature is to improve the mixing process of a diesel engine, thus allowing the achievement of higher engine speeds. Such designs have been used for many decades on conventional diesel engines, and may prove to be strong contenders for gaseous fuel ignition.

There are advantages in using a spark ignition engine, such as to allow time between air and fuel to mix homogeneously before ignition. There are also advantages in using compression ignition engine, because it can use low quality fuels i.e. fuels with low octane number, and the possibility to inject the fuel directly into the cylinder. However, there is a possibility to combine certain features of both engines. They are referred to as hybrid engines. Stratified-Charge engines fall into this category, since they try to use the best characteristics of both cycles.

The Texaco Controlled Combustion System (TCCS) [3] is an example of stratified-charge engine. It uses a bowl-in-piston design as a combustion chamber. Upon injection of the fuel, late in the compression cycle, the mixture present in the chamber is highly stratified, however, the air/fuel ratio near by the spark plug is close to stoichiometric. The fuel is introduced directly into the cylinder and tangentially with respect to the combustion chamber. As a result, fast swirling is created which accelerates the mixing process between the fuel and the air.

Other designs which are falling into the category of stratified charge engine, is the M.A.N.-FM System [4]. This

engine uses a piston cup as combustion chamber and is similar in operation to the TCCS system previously discussed; it also uses a spark plug to support ignition. The fuel injector is positioned such that the fuel is introduced tangentially with respect to the piston cup. The characteristic that distinguishes this type from over the TCCS, is the spark plug location which is placed down stream as opposed to a location beside the fuel injector. This is to allow a maximum of heat transfer to the fuel/air mixture before it reaches the spark plug.

Another design which has known an important commercial success, is the jet-ignition or torch ignition stratified-charge engine [5]. The fuel is introduced in the cylinder via two separate intake valves. A small intake valve is bringing a very rich mixture to a small pre-chamber (really ignition chamber), which has a spark plug mounted into it. The main intake valve is bringing a very lean mixture. The intent of this design is to operate a lean burning engine. The rich mixture is used only to support the flame kernel and bring the flame beyond the critical radius, such that a flame front can develop.

The basic advantage for using an stratified charge engine is that more degrees of freedom are offered to a designer to meet specific requirements such as pollutant emissions, or use of fuel with lower octane requirement [6].

Some examples of added parameters are:

*Fuel injection advance

*Fuel nozzle orientation and number of holes

*Distance between injector and spark plug

*Ratio of cup volume to clearance volume

*Fuel pressure

Recently, a new type of spark plug has been developed by the engineers at Bosch GMBH [7]. It uses the principle, of the divided chamber.

The spark plug consists of the positive electrode covered entirely by a negative electrode, with only a small air volume separating the two electrodes. The hemispherical ignition chamber wall has small holes drilled into it, to allow the air fuel mixture to penetrate the void during the compression cycle. The wall of the chamber performs the role of the ground electrode. Upon ignition, a violent blast causes the oxidized gases to escape the pre-chamber, thus accelerating the mixing process. Experimental results show an increase in flame propagation rate hence, increasing the engine performance.

In spite of the fact that many researchers have oriented their work toward the use of more conventional method for improving ignition of either diesel or gaseous fuels, other methods more complex have been investigated as well for diesel engine applications. For example, the application of a resonance tube for igniting hydrogen in a diesel engine has been

investigated by C.Lisio [8]. These ignition systems are used for gas turbine engines and rocket propulsion systems. Lisio attempted to adapt a resonance tube to produce ignition in a diesel engine. He designed a resonance tube such that an ignition delay of the order of a few millisecond and a gas temperature in excess of 1000 K could be achieved. After having tried different configurations of resonance tubes, Lisio was not able to obtained the desired results. In his conclusion he discussed the difficulties related to the adaptability of this technology towards diesel engine applications.

Investigation of other methods of ignition for application on diesel engine has been done by E. N. Quiros et al. [9]. They suggested a new concept of ignition system based on a toroidal ignition chamber. This method involves circulating the air charge heated by compression in a toroid which has the shape of a converging diverging orifice. The fuel is introduced in the toroid at the throat of the orifice where the air temperature is the highest. Upon combustion of the fuel, the gas mixture enters the diverging part of the chamber such that high gas velocity can be achieved. This method of ignition is a combination between the single chamber and the divided chamber used in diesel engine.

To better understand the ignition and combustion mechanism, knowledge of the concentration distribution of fuel is of paramount importance in diesel engine study. The work done in this field by H. Tanabe et al.[10] has been to study the wall impingement of a jet from a fuel injector. This research focused

on the unsteady behaviour of wall impinging jet, applied to a direct injection diesel engine. In particular, the pressure distribution on the surface from the early stage to the end of injection was the centre of interest. The author used helium and injected it on a surface. The concentration was measured using hot wire anemometry, and a pressure probe to map the pressure. Tanabe et al. reported that the wall jet impingement augments the air entrainment and, as a result, this scheme promotes a faster combustion.

Some investigation using platinum wire has been made by Furuhama and Kobayashi [11]. Using a platinum wire heated to temperature in excess of 1300 K, the investigators obtained hydrogen ignition.

In spite of all the work done in the field of diesel engine ignition using gaseous fuel, several authors including W. L. Mitchell et al.[12], reported that for the ignition of methane and hydrogen, the fast wearing of the glow plug is a persistent problem. To overcome this difficulty, a special high quality glow plug have been designed. However, because of the high cost of the material required, this solution became expensive.

Another approach for solving the ignition problem was the use of the Spark Aided Diesel Engine (SADE) system. It has been demonstrated that using a spark plug instead of a glow plug, excellent results can be obtained, especially in the case of cold engine start. Study carried by Ubong [13] suggests that engine

using SADE system is less sensitive to different fuel properties and provide cleanliness of the exhaust. In addition, the engine combustion is also smoother than with the non-assisted type. Ubong concluded in his investigation that the spark plug gap does not have an impact on the steady state behaviour of the engine. Despite this conclusion, he also tested other ignition systems such as the multiple spark discharge systems and concluded that the significant advantage of using high energy ignition systems is the possibility of obtaining ignition of lean mixtures.

Using an analytical model of ignition system to study the performance of different schemes, A.V. Ward [14] found an efficient method to reduce power losses from ignition systems. He further developed a model of a standard ignition system elaborated by Kalghatgi [15]. Kalghatgi traced the guidelines for an ignition system, and described the different voltage and current phases during sparking. Ward's work deviated from this point, and created a mean to reduce the inefficiencies of a standard ignition system. By doing so, Ward was able to significantly increase the transfer of energy to the mixture during sparking, and has been able to design an ignition system to achieve lean burn in a gasoline engine.

CHAPTER 3

3.0 GAS IGNITION CONCEPTS

An evaluation of different designs was necessary to determine the selection of my experimental design. Before deciding on a specific ignition chamber geometry, several already existing designs have to be considered, bearing in mind their possible conversion toward gaseous fuel application. Furthermore, the possible change in the pre-chamber geometry should be considered, making it more feasible for igniting gaseous fuels. Finally, the problem should be addressed regarding the chamber accessibility inside the engine selected for eventual modifications.

The important part of this investigation is to provide an overview of the air/fuel mixing mechanism involved, before deciding on the actual geometry of an ignition chamber prototype. To achieve this, three typical ignition chambers found on existing engines, have been looked into. This was to help establish a strategy for developing and testing a new concept of spark assisted ignition chamber for gaseous fuel application [16].

3.1 Introduction

It is well known from the literature study that the ignition difficulties cause serious obstacles in developing

combustion systems with high pressure gas injection. These types of systems must be equipped with some kind of ignition supporting device which would initiate the combustion at the proper time and piston position within the combustion chamber and provide the sufficient combustion rate during further stages of the combustion process. The simplest way to support ignition is to apply a conventional spark ignition system as used in gasoline engines. In the gas-injected engine, however, the conditions to ignite the charge are more difficult than in gasoline engines for the following reasons:

1 - The ignition temperature for gaseous fuels is higher than for gasoline. For example, ignition with hydrogen requires approximately 200K higher temperature than for gasoline, and for methane, approximately 100K higher.

2 - High pressure gas injection creates a strong charge stratification in the combustion chamber. The fuel concentration distribution is time dependent and is highly sensitive to the dynamics of the gas motion in the combustion chamber. The air and gas mixing process depends strongly on the in-cylinder charge motion, on the gas jet-air interaction and the geometry of the gas jet itself.

3 - The effectiveness of the spark-ignition depends strongly on the charge motion in the vicinity of

the spark plug at the moment of ignition. The same dependence has been observed in the premixed charge engines. This problem is quantitatively different and more difficult because of the stronger local charge stratification.

3.2 Design Strategy

To overcome the aforementioned ignition difficulties, the following three approaches are suggested.

1 - Use a conventional spark plug as a source of ignition energy but create a proper gas flow conditions to obtain a stoichiometric fuel to air ratio at the spark plug electrodes for the effective flame kernel development.

2 - Apply more unconventional methods to generate the discharge energy and to distribute the flame throughout the combustion chamber.

3 - Facilitate gas ignition by the proper pretreatment of the injected gas fuel dose in order to increase its cetane number, i.e. to improve its ignitability.

Note: The simultaneous use of these three methods can also be considered.

3.3 Proposed Ignition Chamber Design

It is known from the previous investigations (such as for instance Fukuma et al. [17]) that it is very difficult to obtain compression ignition of hydrogen when injected in the main combustion chamber. Literature studies conducted on the investigation of the stratified charge gasoline engines indicate that the improvement of the ignition process can be best achieved by means of a divided combustion chamber. A pre-chamber allows to organize the final air mixing process and the motion of the charge in such a way that it is favourable for the combustion initiation. Moreover, the action of a pre-chamber can also significantly stimulate further combustion process in the main chamber.

Several specific concepts of the pre-chamber ignition systems are introduced below. Systems designed on the basis of the Ricardo Hydra as well as of the Peugeot Indenor engines gives a variety of research possibilities with only minor changes of the original hardware. This in turn, gives the opportunity to investigate the influence of several most important parameters (ignition location point, charge motion intensity, injection jet geometry etc.) on the ignition process.

The basic modification proposal of the pre-chamber ignition systems for both engines are introduced below.

3.3.1 Ricardo Hydra Engine

The basic arrangement of the proposed ignition system is shown in Figure 3.1. The modified hole-type high pressure gas injector is placed in a position which allows to create a moderate size cell which is supposed to serve as the ignition chamber. Appropriate extension of the spark plug electrodes allows for changing of the ignition point position. The spark plug can also be moved outwards to let the ignition point be shielded against the swirling gas motion. The pre-chamber volume can also be changed by varying the injector axial position.

Two different concepts of the ignition chamber are proposed, namely Pilot Injection Ignition Chamber and Turbulent Ignition Chamber.

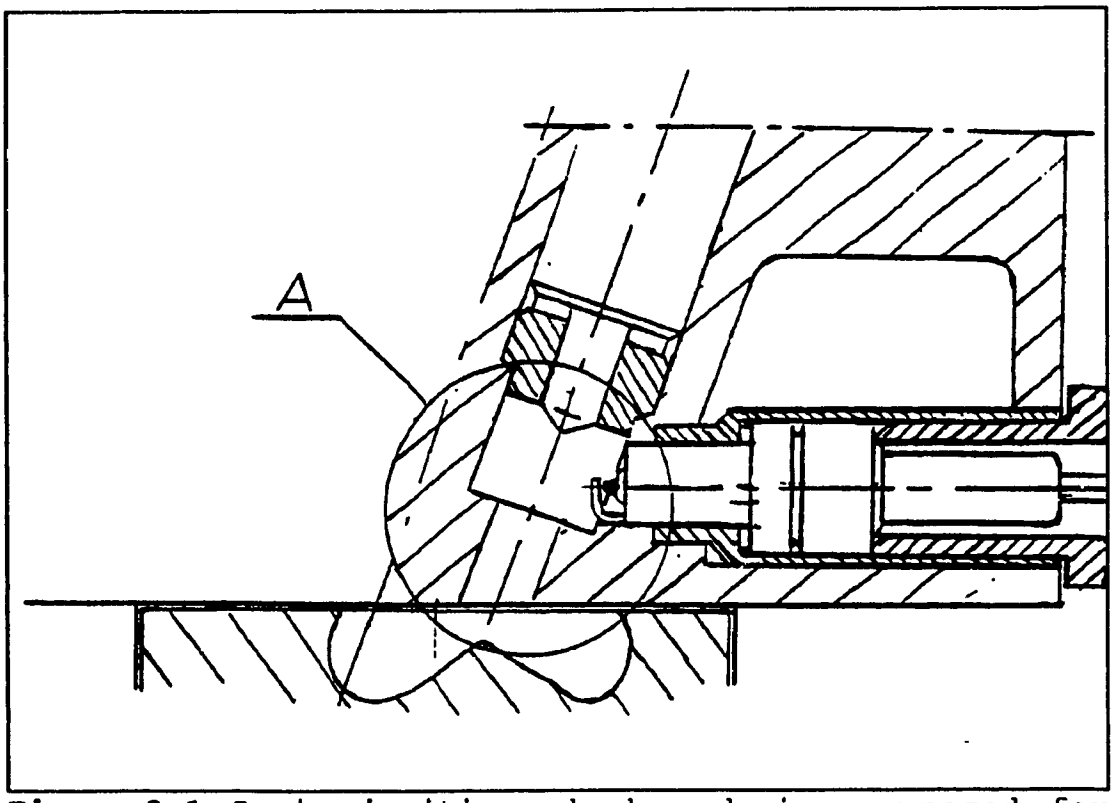

Figure 3.1 Basic ignition chamber design proposed for Ricardo Hydra engine

3.3.1.1 Pilot Injection Ignition Chamber

The schematic of the chamber is shown in Figure 3.2. The chamber is slightly increased in size by moving down its bottom surface. This allows for shortening of the inter-chamber passage, which is machined as open as possible. The action of this pre-chamber (see Figure 3.3) is as follows:

Phase I A pilot dose of gas is injected into the chamber. The proper amount of the injected gas and its spacial distribution result from the suitable design of the injector. It should make it possible to saturate the pre-chamber with the gaseous fuel rather than to create a typical thin gaseous jet during this phase. One should therefore, obtain a close to stoichiometric mixture around the spark plug at the time of ignition. (See Figure 3.3a)

Phase II The mixture in the pre-chamber is ignited. The combustion spreads quickly throughout the whole pre-chamber due to its relatively small volume. Simultaneously, the main injection occurs. The typical gaseous jet enters the pre-chamber and it penetrates it down to the main chamber through the connecting channel. The high temperature combustion gases, contaminated with the chemically active intermediate combustion products, are mixing with the fresh injected gas. This stimulates the jet impingement process, as well as air fuel mixing. It results in a significant increase in burning rate. The toroidal shape of the main piston-part of the combustion chamber, helps to organize the combustion process. The richer

the mixture in the pre-chamber, the more important is the role of the combustion chemistry in this process. (See Figure 3.3)

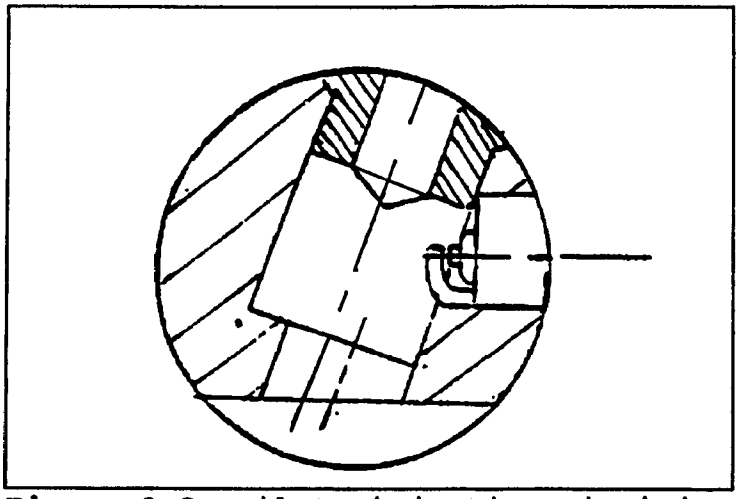

Figure 3.2 Pilot injection ignition chamber for Ricardo Hydra engine

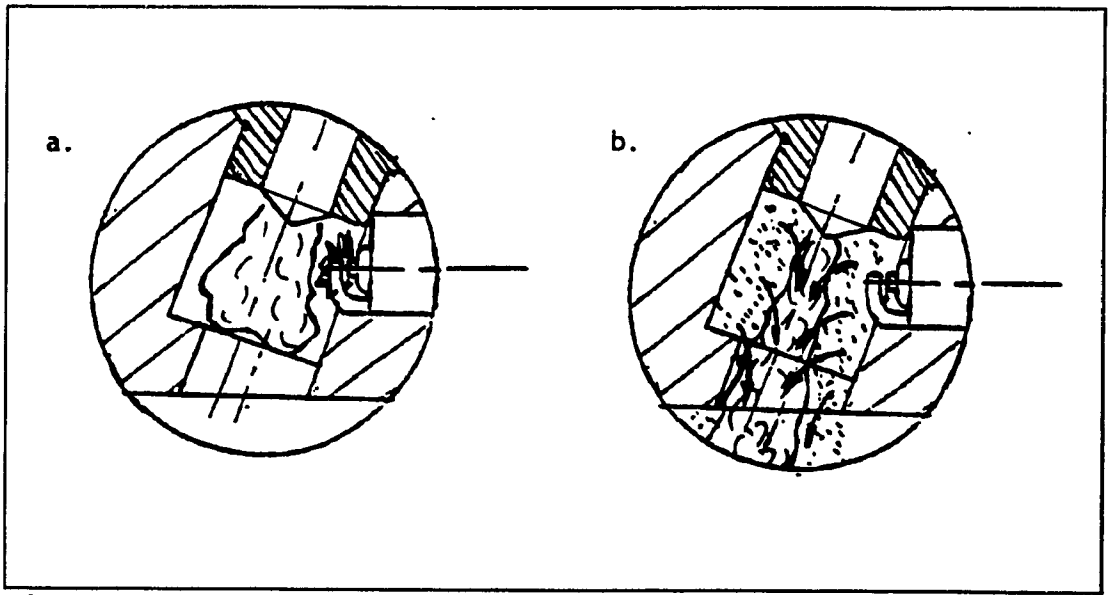

Figure 3.3 Ignition chamber for Ricardo Hydra engine in action, a. Phase I - Ignition, b. Phase II - Gaseous torch development

3.3.1.2 Turbulent Ignition Chamber

The schematic of the chamber is shown in Figure 3.4. The pre-chamber is similar to that of a pilot-injection geometry, but the inter-chamber passage is in general smaller in diameter. The shape of this passage can be modified in the course of the investigation by applying various inserts.

The action of this pre-chamber (see Figure 3.5) is described as follows:

Phase I The single gas jet enters the pre-chamber and it penetrates into the main chamber through the channel. The dynamic motion of the jet generates several toroidal vortices in the pre-chamber axial plane. The outer layer of the jet is being trimmed by the edge of the orifice which has a smaller size than the gas jet diameter at this position. The gas from the outer part of the jet is forced to recirculate and to create several small vortices. This results in a quick air-fuel mixing in the region around the jet where satisfactory conditions for the ignition by a spark plug could be created. (See Figure 3.5a)

Phase II During this phase the torch of burning gases enters the main chamber. It stimulates the rapid mixing of the remaining portion of air and gas and results in instantaneous multi-source ignition. (See Figure 3.5b)

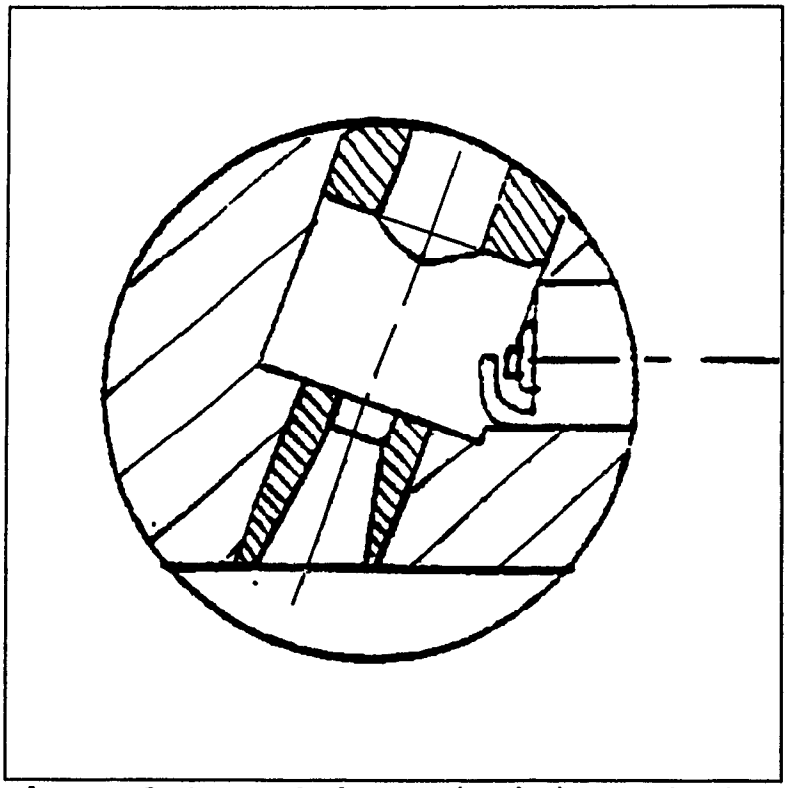

Figure 3.4 Turbulent ignition chamber from Ricardo Hydra engine

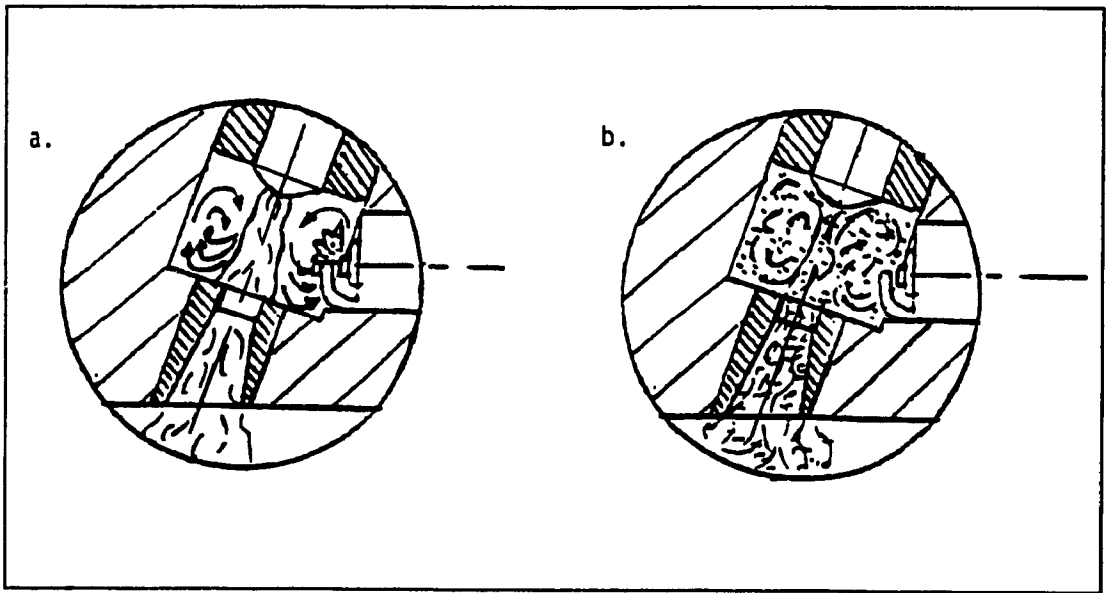

Figure 3.5 Turbulent ignition chamber of Ricardo Hydra engine in action a. Phase I - Ignition, b. Phase II - Flame penetration of charge

3.3.2 Peugeot Indenor Diesel Engine

This is a high compression indirect injection diesel engine and it provides an opportunity to investigate the ignition in an air swirling flow. Basic arrangement of the ignition chamber is schematically shown in Figure 3.6. The original injector is replaced by a high pressure gas injector. The original glow plug is replaced by the conventional spark plug with the same dimensions. The bottom part of the swirl chamber, which is removable, makes it possible to modify the shape of the chamber and the direction of the inter-channel. Also in this case, the appropriate extension of the spark plug electrodes allows for the change of the ignition point position. This can be especially important in the case of the swirling flow, where one can expect a strong radial charge stratification. The pre-chamber volume can also be altered by changing the shape of the bottom part of the pre-chamber. Two different concepts of the ignition chamber are proposed in the next two sections.

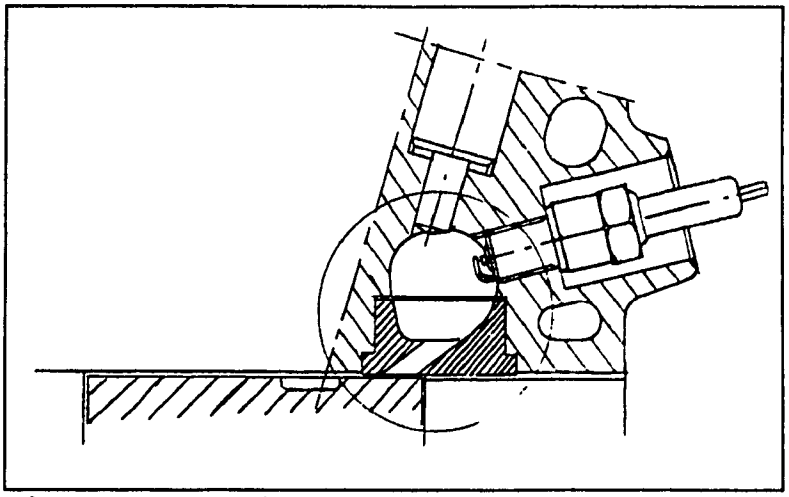

Figure 3.6 Swirl chamber Ricardo Comet of Peugeot Indenor engine

3.3.2.1 Conventional Swirl Chamber

This concept is mainly based on the existing Ricardo Comet swirl chamber which, for this research, will be equipped with the high pressure gas injector and the spark plug for ignition support. The action of the swirl chamber is schematically shown in Figure 3.7a and Figure 3.7b. The sequence of event is different from that which occurs in a diesel engine because the liquid fuel evaporation problem does not exist in the case of gas injection; however, the time available and the fuel distribution pattern within the chamber are critical for the ignition process. That type of ignition chamber has the potential of creating satisfactory conditions for the investigation of correlations between gas injection parameters and ignition point position under well controlled swirling motion of the gas.

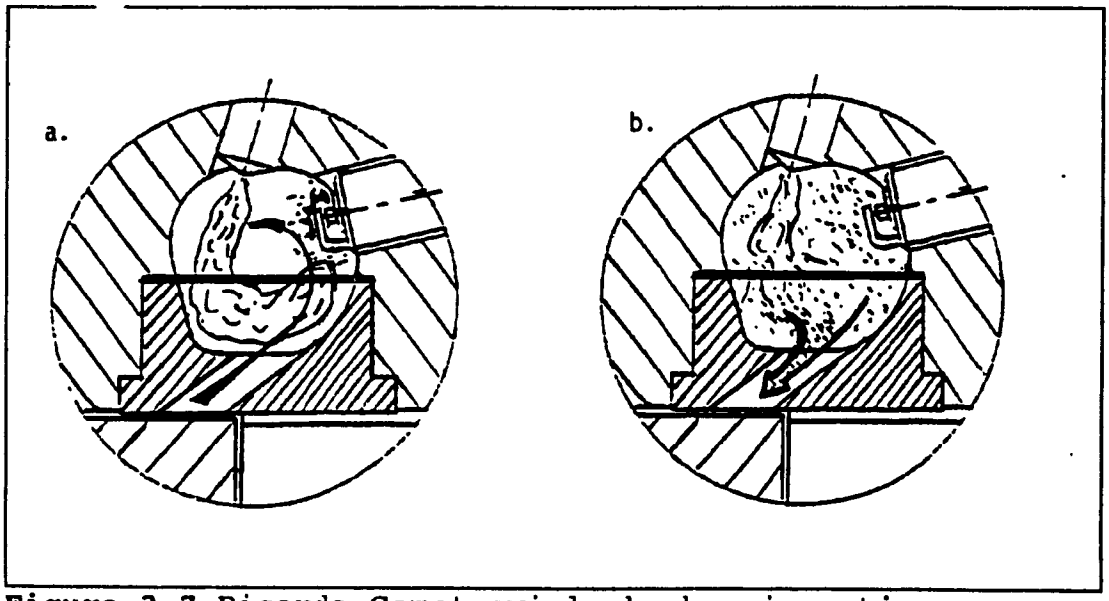

Figure 3.7 Ricardo Comet swirl chamber in action
a. Phase I - Ignition, b. Phase II - Combustion

3.3.2.2 Dual Jet Ignition Chamber

The schematic of such chamber is shown in Figure 3.8. This is an open type chamber and the longitudinal shape of the inter chamber passage is the result of conforming to the shape of the cavity in the piston crown. The shape of the passage, however, could be utilized during investigation of the system previously referred to as the "turbulent ignition chamber". This chamber in action is shown in Figure 3.9.

This system is basically designed to collaborate with a dual jet gas injector. Its operation is similar to that previously described as "pilot injection". The difference is that now the ignition portion of the mixture of the well controlled stoichiometry is created by a separate gaseous jet directed toward the spark plug, instead of the pilot jet generated during the two stage injection. Again, the main gas jet interacts with the burned gas flowing out of the pre-chamber and it stimulates the mixing and combustion process.

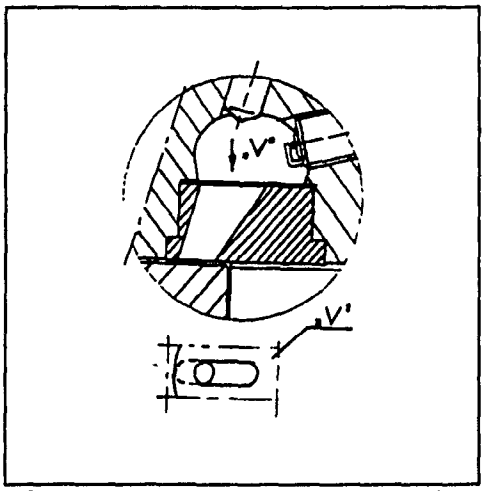

Figure 3.8 Dual jet ignition chamber for Peugeot Indenor engine

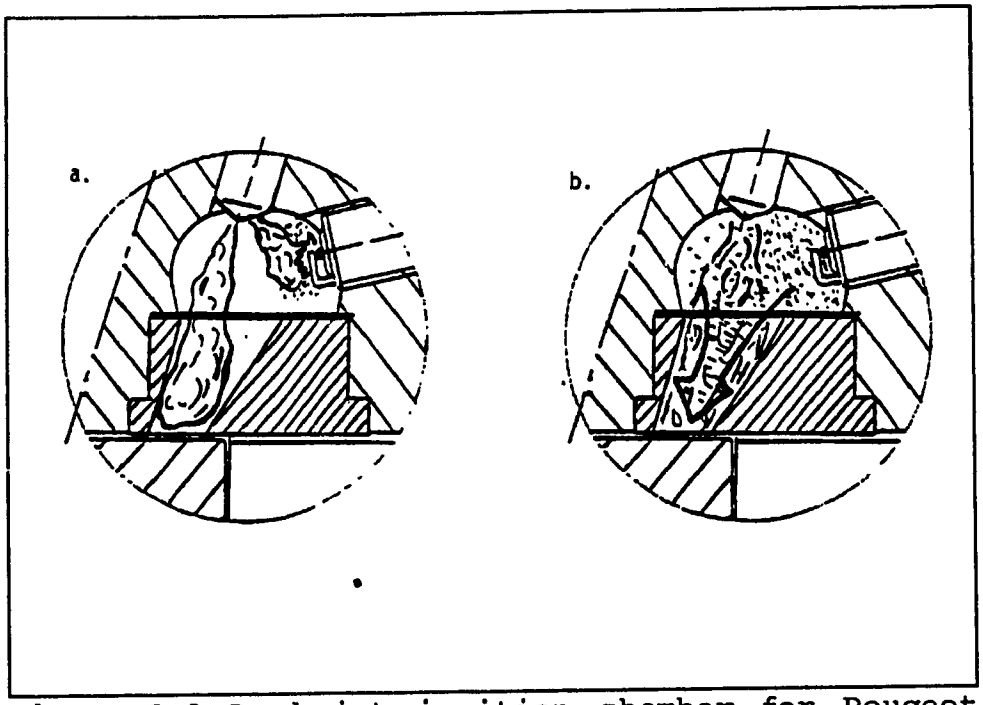

Figure 3.9 Dual jet ignition chamber for Peugeot engine in action a. Phase I - Ignition, b. Phase II - Combustion

3.4 New Concept of Ignition Chamber for Gaseous Fuel Application

This new type of ignition chamber, as shown in Figure 3.10, uses several advantages taken from the existing chambers, reviewed and described in the previous section (3.3). It is similar in geometry to the Ricardo Hydra pre-chamber because of the pilot injection features. This is because the injector is positioned directly above the passage connecting the two chambers. Similarly, this design also uses the swirling feature of the Ricardo Comet, used on the Peugeot Indenor engine. This is by forcing the fuel to flow towards the spark ignition electrode position. The innovative feature of the proposed design, is by using the pilot jet as well as the swirling action

of air incorporated in the same design.

Upon triggering of the injector, the fuel is progressing toward the passage connecting the pre-chamber with the main chamber. At this point, because of the geometry of the chamber, the fuel flow is being divided into two portions. One part of the fuel remains in the chamber and is being forced to create a vortex directed toward the spark plug. The other fuel stream is directed into the main chamber. The advantage of using a swirling feature on this type of chamber, is to augment the time duration for the fuel to be in contact with the hot wall. Under cold starting, this characteristic does not play a significant role, however, during steady state operation this feature becomes advantageous. This is essentially because it is increasing the energetic content of the fuel as it is approaching the spark plug. However, during cold starting this effect is drastically reduced, if not insignificant. To vary the ratio of fuel being delivered to each chamber, the injector position can be changed by using different injector positions which are shown in Figure 3.10.

Since the other chambers evaluated were all accessible only by removing the cylinder head of the engine, such manipulation which is time consuming, is not desirable for research purpose. To overcome this problem, locating the pre-chamber outside the engine seemed appropriate.

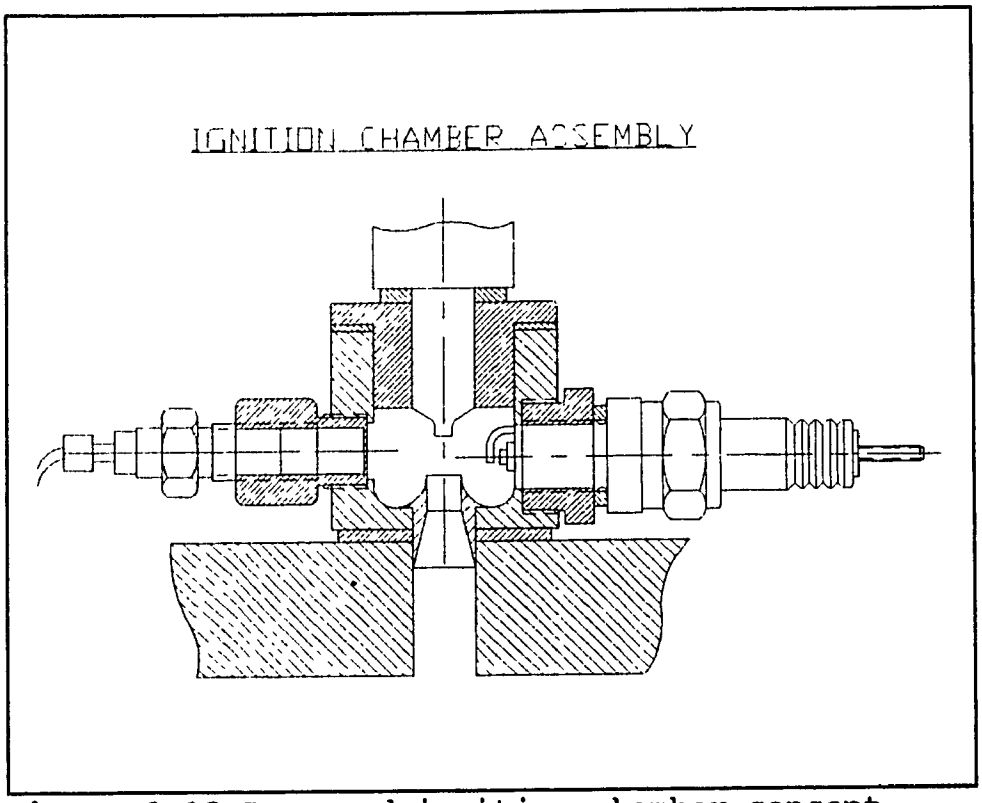

Figure 3.10 Proposed ignition chamber concept

Selecting a single cylinder engine, with the pre-chamber prototype mounted externally was the final decision. The single cylinder engine found is manufactured by Petters in England. The engine has a total displacement of 660.9 [cm^3], and operates on a diesel cycle. The main combustion chamber is placed in the piston crown. Although the engine does not come with an ignition chamber, the modification required to include one is modest. Further description of the engine test setup will be given in the chapter 5 of this thesis.

In order to record any changes in pressure taking place in the chamber because of ignition, a piezoelectric transducer has been placed opposite to the spark plug, as shown in Figure 3.10.

In order to incorporate the concept of ignition chamber in the engine, modification to the Petters cylinder head is necessary. Figure 3.11 shows the location of the igntion chamber on the air cooled cylinder head.

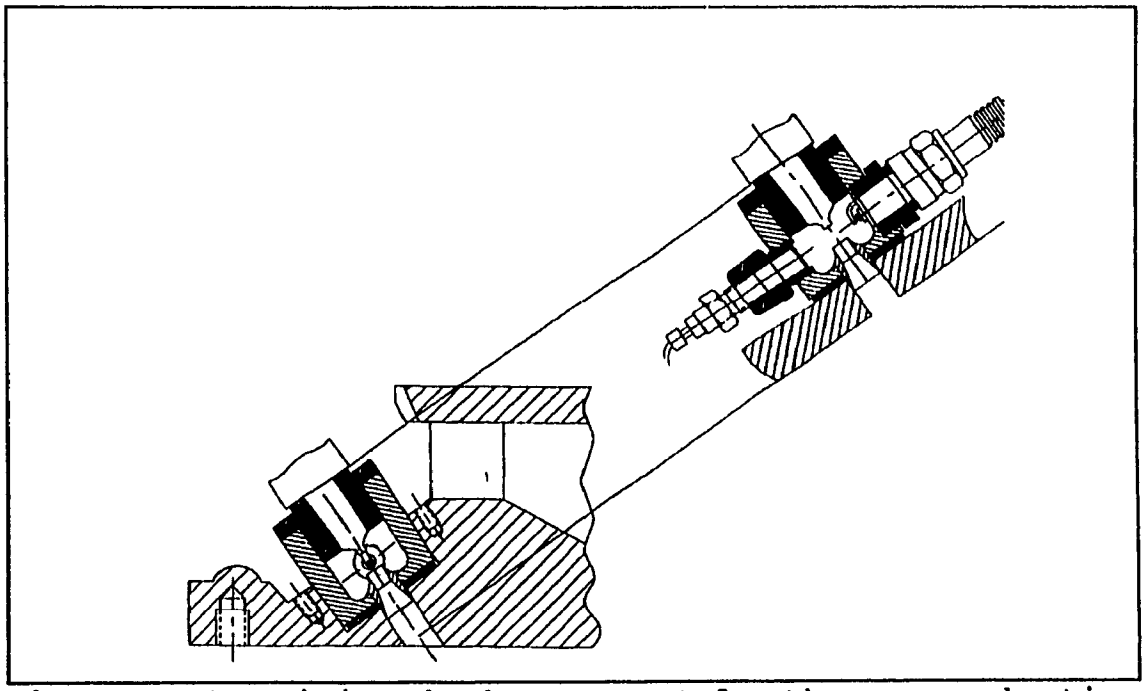

Figure 3.11 Ignition chamber concept for the open combustion chamber of the Petters engine

CHAPTER 4

4.0 METHODOLOGY

The objective of this experiment is to evaluate a new design of ignition chamber with spark ignition support, dedicated for use with gaseous fuels. The method of evaluation consists of determining the ignition quality under cold starting, and at low engine speed. The fuel injection and sparking in the ignition chamber was performed every fifty crankshaft revolutions, so that the engine remained cold during testing. This investigation was oriented only towards the ignition performance of the chamber prototype. More research will be further required to evaluate the combustion characteristic of this design; however, this will not be covered in this thesis.

The new type of ignition chamber proposed for this thesis was investigated on an experimental engine test setup. It consisted of a single cylinder diesel engine, with a prototype of the ignition chamber mounted externally on the cylinder head. This experimental engine was fitted with all the instrumentation required to provide information about the engine operational parameters, such as cylinder pressure and temperature. To indicate the opening of the injector and the fuel discharge process, a pressure transducer was placed in the body of the injector to record the pressure fluctuations. An optical switch was placed on the flywheel of the engine so that a signal is sent

to the data acquisition system in order to locate the TDC position on each graph.

The first phase of this experimental investigation was to obtain ignition from a pre-determined fuel dose injected in the ignition chamber. This required the calibration of the gas injector prior to the experiment. The calibration instrument consisted of a specially designed volume measuring device which uses a piston and cylinder assembly. Upon triggering the injector, using a signal generated by a microcontroller, a piston was displaced from its initial position. By measuring the piston displacement and knowing the piston diameter and the final pressure, the gaseous fuel dose was determined using the thermodynamic tables. A pressure drop recorded by a piezo-electric transducer showed the injector opening and indirectly, the mass of fuel delivered. However, this method of calibration is not intended to show the discharge characteristic of the injector. It can only determine the total fuel dose injected without any knowledge of the transient fuel discharge rate.

The next step was to determine the capability of the solenoid driving circuit used with the gas injector to open the injector at pressures in excess of 70 [bar]. Operating the gas injector at high pressure was required for achieving short injection period in the range of 2 to 3.5 [msec], typical for a diesel engine.

After selecting an amplification circuit and calibrating the injector, selection of a suitable spark

discharge system for the engine was next. Because of the high air density that exists in a diesel engine, as the piston approaches TDC, the air enclosed between the spark plug electrodes acts as a barrier for the current. A standard ignition system may not work as well in such conditions as in an Otto cycle where a spark ignition is normally used. Several spark ignition systems including triggering circuits, have been evaluated for this test engine. This required a specially designed apparatus which was made for this purpose.

The instrument proposed consisted of two electrodes mounted on insulated plate, with one electrode connected to ground. The distance between the electrodes was altered by having the ground electrode mounted on a micrometer head. This device was used to evaluate each ignition system combination.

When testing the engine, it was needed to record the signal for triggering of the ignition coil. This signal provided proof of a spark occurrence at the spark plug. After the coil was triggered, from the secondary coil, a discharge occured between the spark plug electrodes. The arc produced at the spark plug induces a magnetic field around the high voltage wire. Using a DC current probe and sending this signal to the digital storage oscilloscope, accurate recording of a spark presence between the spark plug electrodes was taken.

After the preparatory stages of the experiment were completed, the strategy for the actual engine testing was considered. Several design parameters were changed regarding

the ignition chamber namely, the injector position relative to the ignition chamber, the injection advance, and the spark advance, all are relative to TDC. To allow for more fuel to remain in the ignition chamber, another parameter was changed in the pre-chamber. The inter-passage between the ignition chamber and the main chamber was reduced in diameter. This option was considered only as a last resort, after all other options were exhausted, because of the machining required. To achieve this the insert portion of the ignition chamber was remachined.

At the beginning of the experiment, an initial injector, setting based on the evaluation of the jet cone angle was used with respect to the edge of the ignition chamber. Since the maximum temperature in the cylinder obtained from air compression occurs at TDC, a spark advance of 2 to 3 [msec] was used to allowed fuel to mix in the ignition chamber before ignition. In other words, the spark signal was sent with some delay after the start of injection.

A series of injector spacers were machined to allow for a change in the position of the injector with respect to the swirling part of the ignition chamber. The lowest injector position allowed for virtually no fuel to remain in the ignition chamber, and the highest position provided most of the fuel to remain in the ignition chamber.

Following an analysis of the obtained results, the best spacer was chosen and the spark advance was varied until satisfactory results were obtained. Similarly, the injection

advance was also varied. Although this technique may seem quite arbitrary, the important factor was to vary only one parameter at a time while keeping the others constant. As previously stated, this method is used only to investigate the potential of obtaining ignition with this chamber design.

Because of difficulties in obtaining a repeatable ignition in the preliminary engine experiment, it was decided to use schlieren photography. Schlieren photography allows for visualizing the flow path taking place inside the chamber, to obtain more information about the gas flow characteristics in the ignition chamber. This provided the necessary information to make the appropriate changes to the ignition chamber prototype. Furthermore, schlieren photography was used to investigate different injector nozzle orifice geometry. This provided information about the development of the gas jet while entering the ignition chamber.

Two options were available for schlieren photography, namely installing the apparatus on the engine, or using a special setup off the engine. Because of the difficulties encountered with the modification of the ignition chamber on the engine, it was decided to use the second option. However, that required the design and the manufacturing of a pressurized chamber with quartz windows to simulate the air pressure present during the compression cycle. A model of the ignition chamber was machined and placed inside the pressurized container. After having performed this experiment the results lead to minor modification

of the ignition chamber and a better knowledge of the injector orifice geometry necessary to obtain the desired gas jet shape. A second set of ignition experiments have been performed on the engine, using the same method which was used during the preliminary test.

CHAPTER 5

5.0 TEST SETUP FOR IGNITION INVESTIGATION

The apparatus consists of a modified diesel engine equipped with an experimental ignition chamber. The experimental setup and the instrumentation required is fully explained in section 5.1. All the important parameters required for this experiment are monitored on a digital storage oscilloscope. The parameters observed are: injector pressure, ignition chamber pressure, engine temperature, spark advance, and top dead center position. Upon successful completion of this experiment, the second step would be to optimize the parameters in order to obtain combustion at higher engine speed. If the results would not be satisfactory, schlieren photography is required to better understand the flow mechanism that takes place inside the ignition chamber.

5.1 Experimental Apparatus

The experimental test bed consists of a modified single cylinder diesel engine, fitted with an ignition chamber (as shown in Figure 5.1). The engine is driven by a 2.2 [kW] electric A.C. motor linked via a jaw type coupling.

Figure 5.1 Petters engine coupled with electric motor for ignition tests

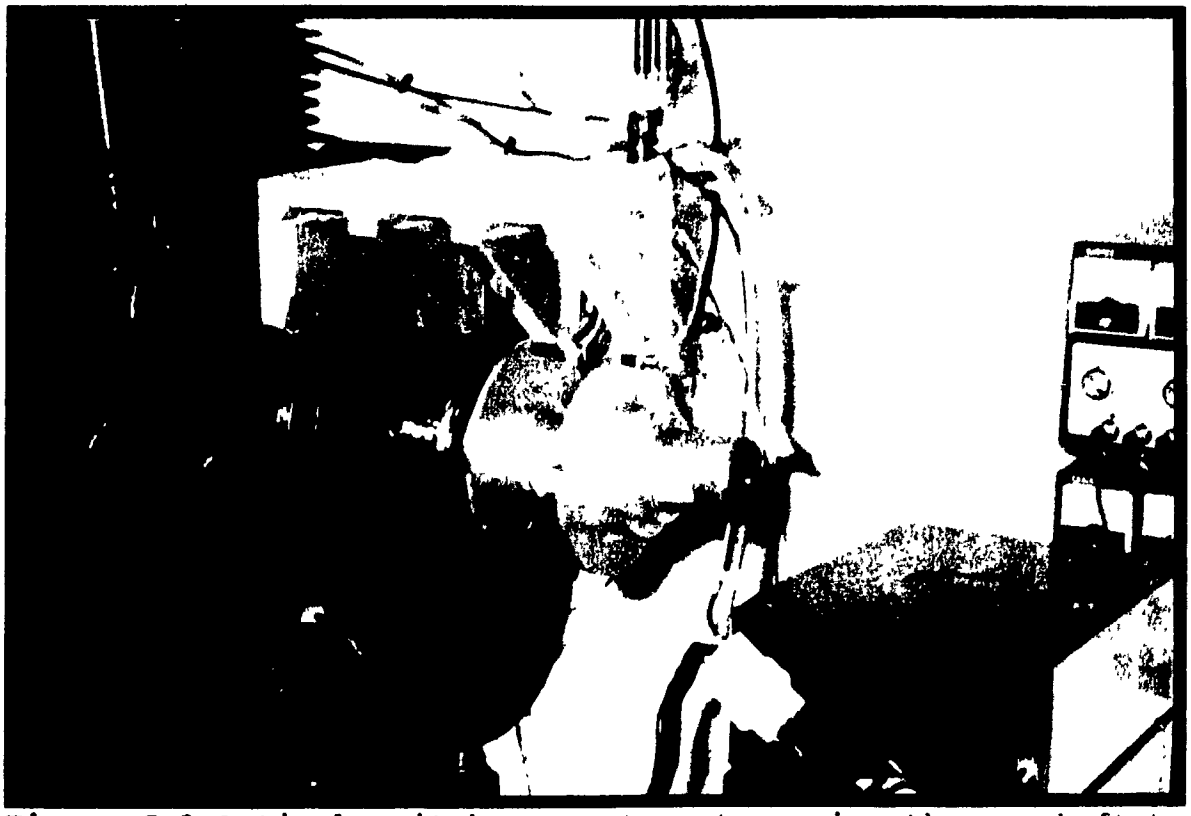

Figure 5.2 Optical switch support system using the camshaft to send a signal to the microcontroller

To reduce the electric motor shaft output speed, and increase the output torque, a 5:1 reduction gear box is used. The crankshaft position is monitored by two optical switches placed on the camshaft that are triggered by a slotted polished disk (see Figure 5.2). The TTL type signal is then conditioned and fed into a microcontroller. The two optical switches are used to activate the fuel injector and the ignition system.

The Intel MCS-96 microcontroller is used as a digital controller for this engine setup. The program is written and assembled in a desktop computer, then downloaded to the controller via a RS-232 serial port. For the interface between the controller and the engine, amplification circuits are necessary. The boost type circuit serves as a triggering system for the fuel injector. Similarly, a control circuit is placed between the controller and the ignition system for triggering the spark plug placed in the ignition chamber (see Figure 5.3).

For capturing the signals from the transducers placed on the engine, a four channel digital oscilloscope manufactured by Tektronics, with a capability of 200 megasample per second is used as the data acquisition system. The data is read by the oscilloscope and stored in its memory. The curves recorded by the oscilloscope can then be downloaded to an external plotter.

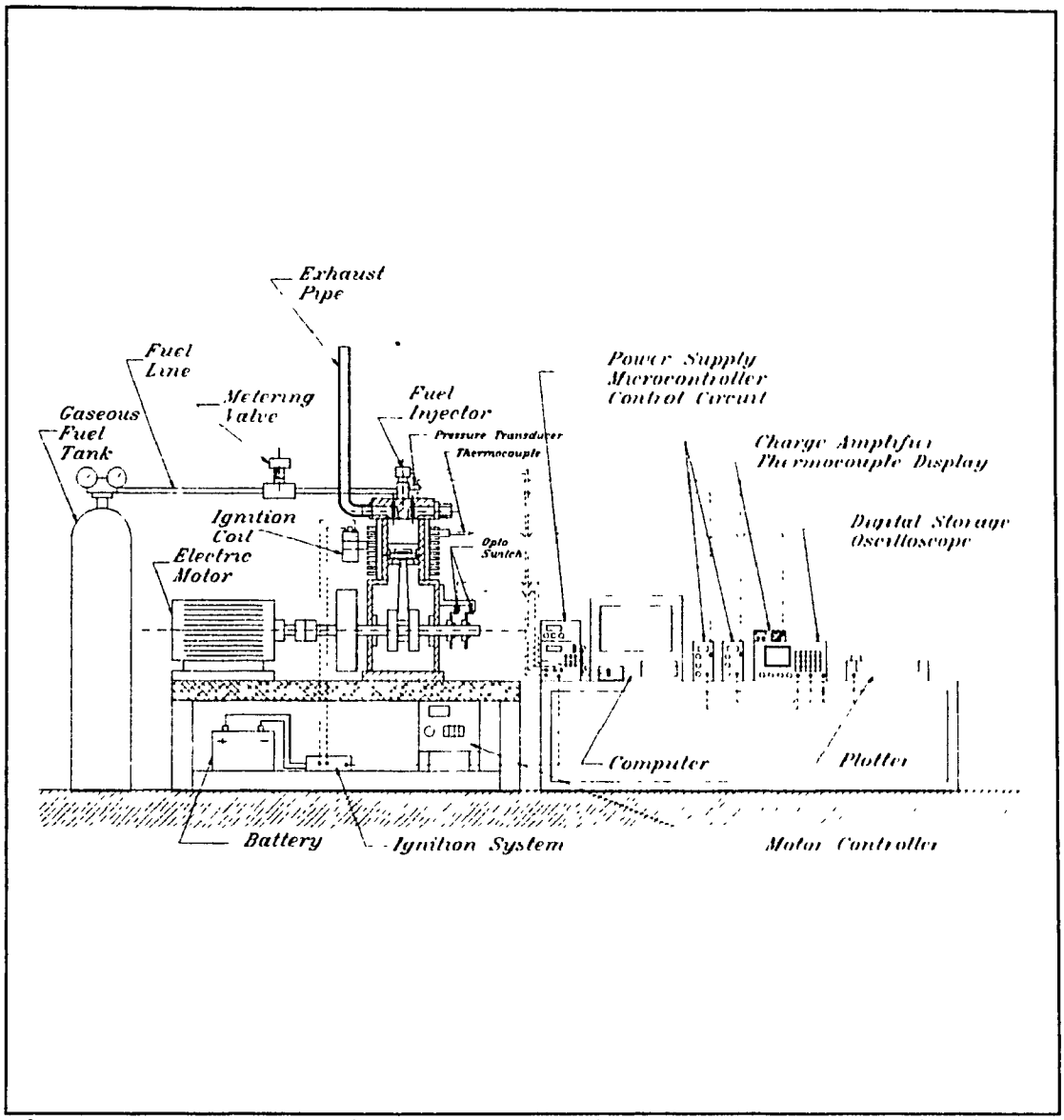

Figure 5.3 Schematic of the primary setup for ignition testing

5.2 Ignition Chamber Design

The role of the ignition chamber in a diesel engine is to ignite a portion of the total fuel, injected into a pre-chamber which is separated from the main chamber by a narrow passage. As a result, faster mixing between air and fuel can be achieved in the main chamber. Upon ignition of a portion of methane in the pre-chamber, a blast of oxidising mixture and a flame front moves rapidly from the ignition chamber (pre-chamber) to the main chamber. The net effect of this scheme is to accelerate the combustion process thus, permitting higher engine speeds.

However, the size of the passage between the two chamber has to be large enough, to reduce the throttling losses caused by the incoming air pushed by the piston upon compression. Also, the volume of the chamber has to be small, such that the engine clearance volume does not increase significantly. Those are the design criteria for the ignition chamber.

The ignition chamber design proposed in this thesis uses the concepts of pilot injection as well as the swirl chamber. The assembly drawing of the chamber design is shown in Figure 5.4. The injector is located on the same center line as the interpassage between the two chambers. This feature is similar to the pilot injection. Similarly, as the gas jet develops upon injection, part of the fuel is shaved off the main gas stream and forced to swirl around the spark plug. This characteristic is similar to the action of a swirl chamber.

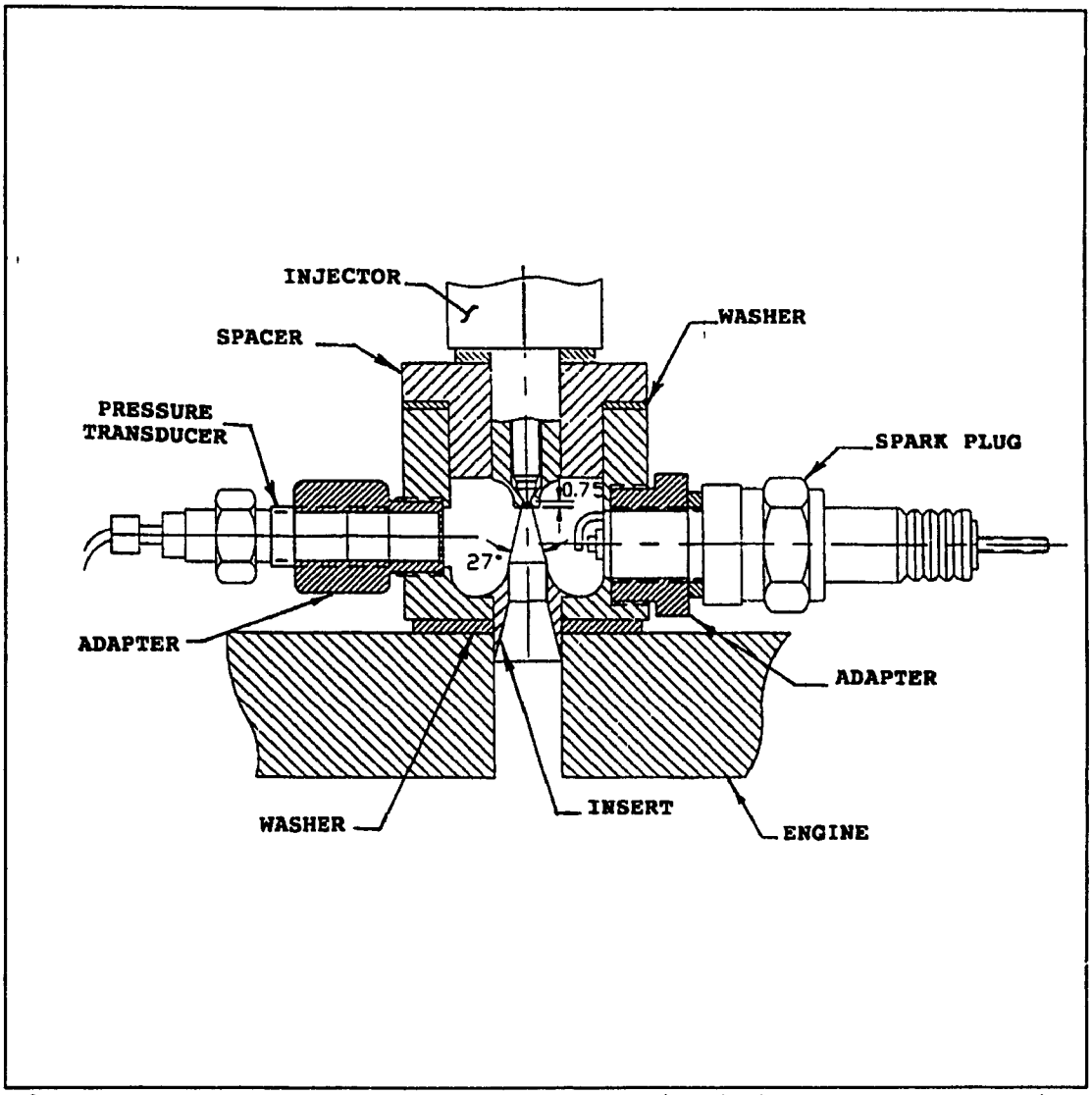

Figure 5.4 Assembly drawing of the ignition chamber design

The design of the Petters single cylinder diesel engine offers the possibility to mount the ignition chamber prototype externally. This advantage is significant for a research purpose, since it minimizes the time required for installing and removing the ignition chamber.

After having modified the cylinder head of the Petters diesel engine (see Figure 5.5), to adapt the new ignition chamber prototype, a copper washer has been machined to be used as a gasket between the ignition chamber and the engine.

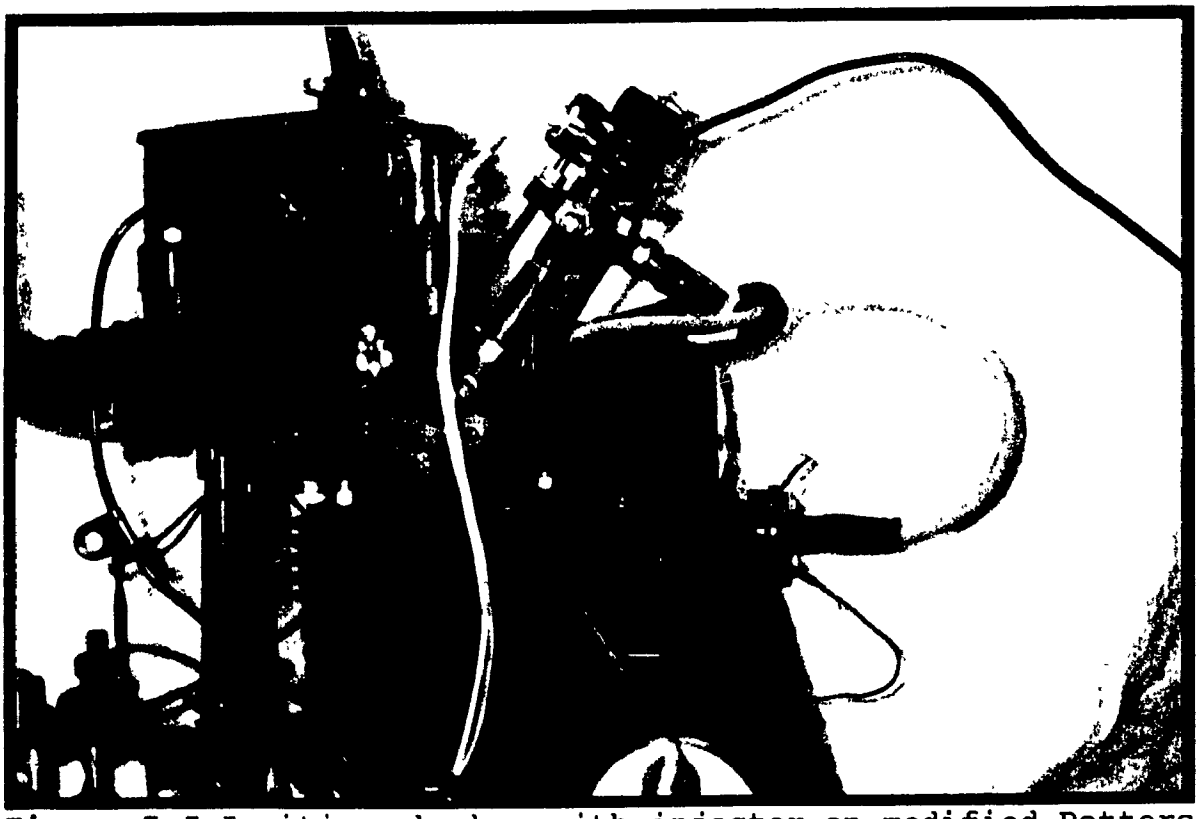

Figure 5.5 Ignition chamber with injector on modified Petters diesel engine

The ignition chamber is held in place via the fuel injector which is retained to the cylinder head with two threaded studs. The torque applied to the studs has to overcome the gas pressure building up in the pre-chamber.

To vary the amount of fuel distributed between the ignition chamber and the main cylinder, a series of spacers have been machined (see Figure 5.6). These spacers causes the injector to be located further away or closer to the shaving insert, depending on the spacer selected. To seal the two surfaces between the ignition chamber body and the spacer, a copper washer has been machined and is used as a gasket.

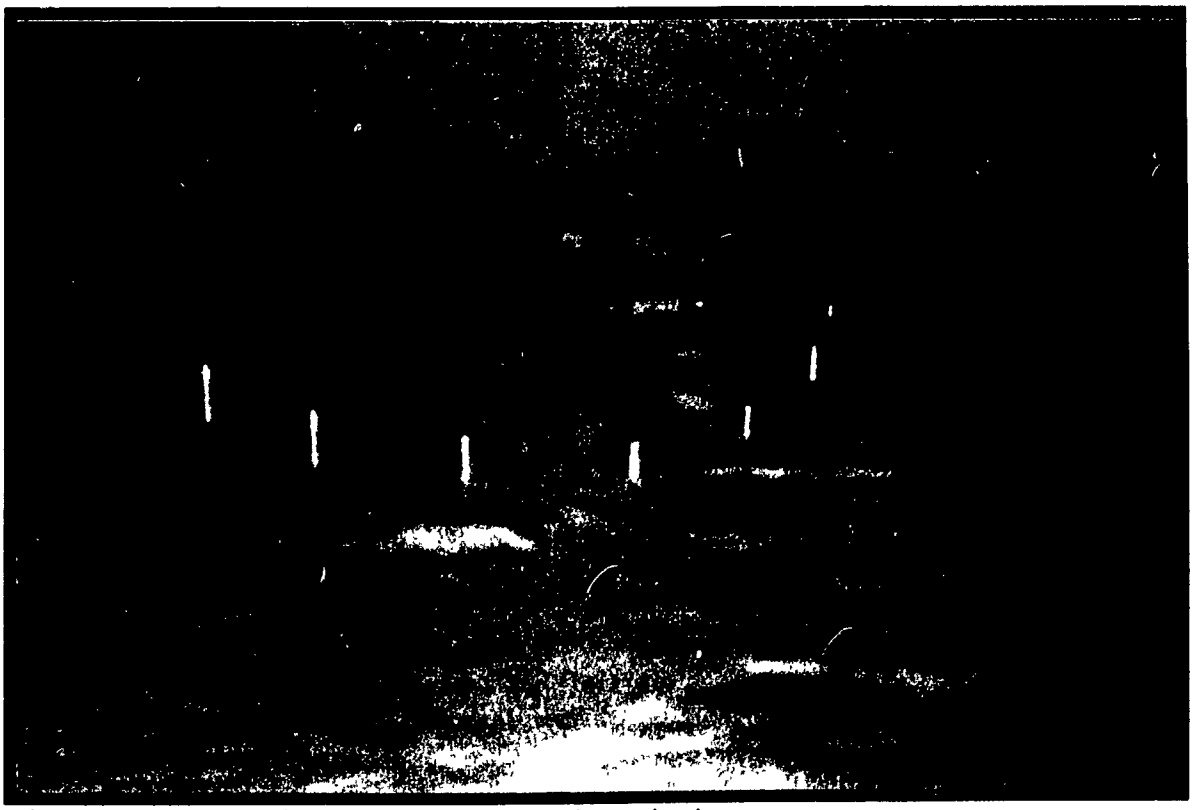

Figure 5.6 Ignition chamber with injector spacers

The steel body of the ignition chamber has been designed to be used with a pressure transducer and a spark ignition system. However, both components mounted on the chamber need to be installed on adapters designed for this purpose. The adaptors are then mounted on the ignition chamber body, and the excess material is removed such that the interior surface of the ignition chamber is uniform.

The fuel shaving insert is also made out of steel, and is press fitted into the ignition chamber body. This insert can be removed and replace with another one. The reason for this is to provide more flexibility to change the size of the passage between two chambers, if necessary.

This design offers significant advantages from a research point of view, first because of its outside cylinder head location , and second because of the ease of modifying the geometry of any component without much work. Refer to Appendix B for ignition chamber detailed drawings.

5.3 High Pressure Gas Injector Modifications

This section is aimed to provide the reader with a background on how the gas injector operates, and the type of flow mechanism involved in this process. This injector has been built from modified CAV-Lucas fuel injector components, such as the nozzle and the body. This injector has been developed and tested in the Fuel Control Laboratory (FCL) at Concordia University.

Aside from the conventional FCL gas injector design and modifications, another modification was necessary to improve the original design. A more efficient sealing system, to bring the power to the solenoid, had to be designed such that the injector would not leak gas. This is required to contain the high pressure gases at the junction where the lead wires exit, to power the injector solenoid. Figure 5.7 shows a sectional view of the injector used on this test rig. Figure 5.8 shows the gas injector with ignition chamber.

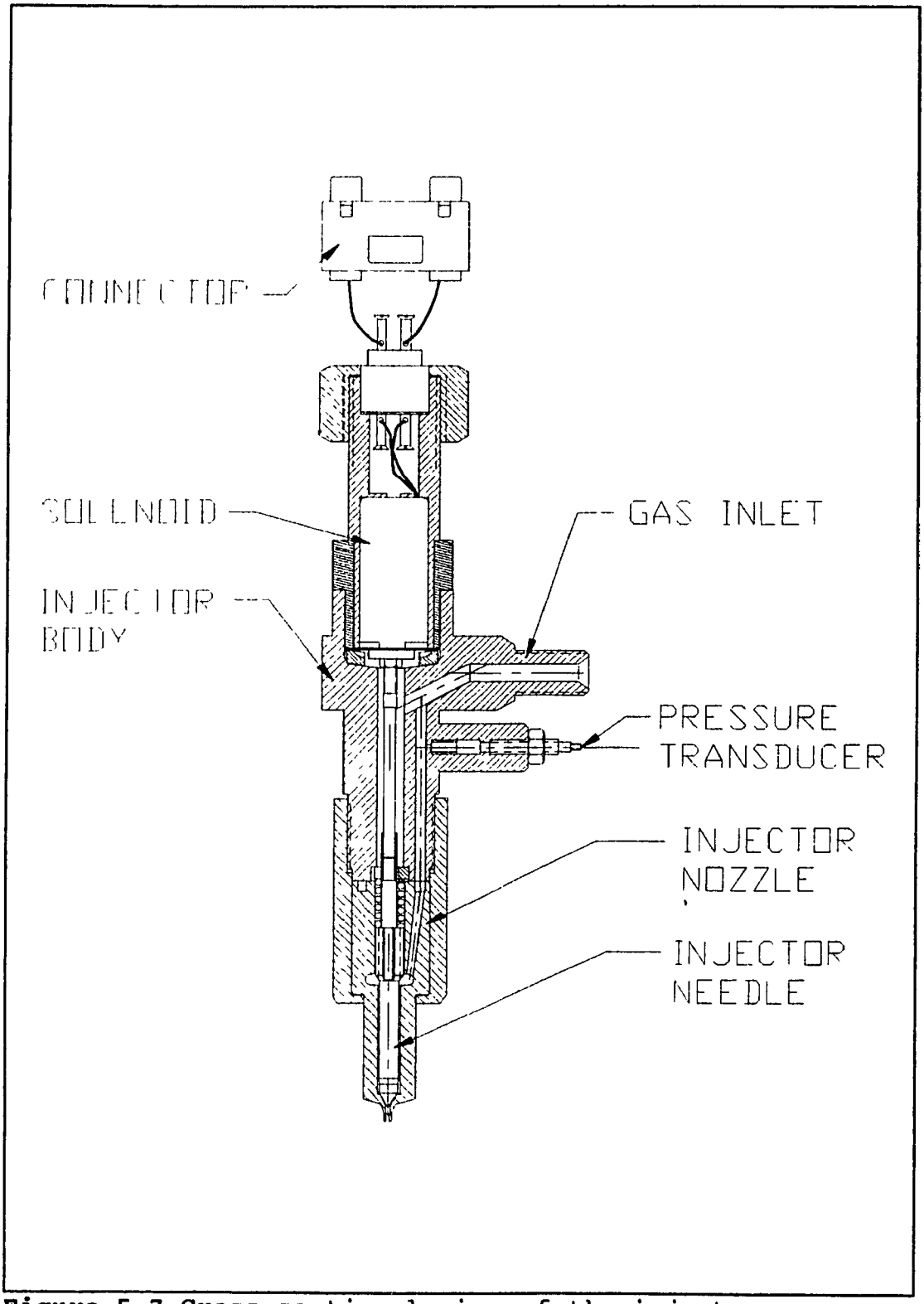

Figure 5.7 Cross sectional view of the injector

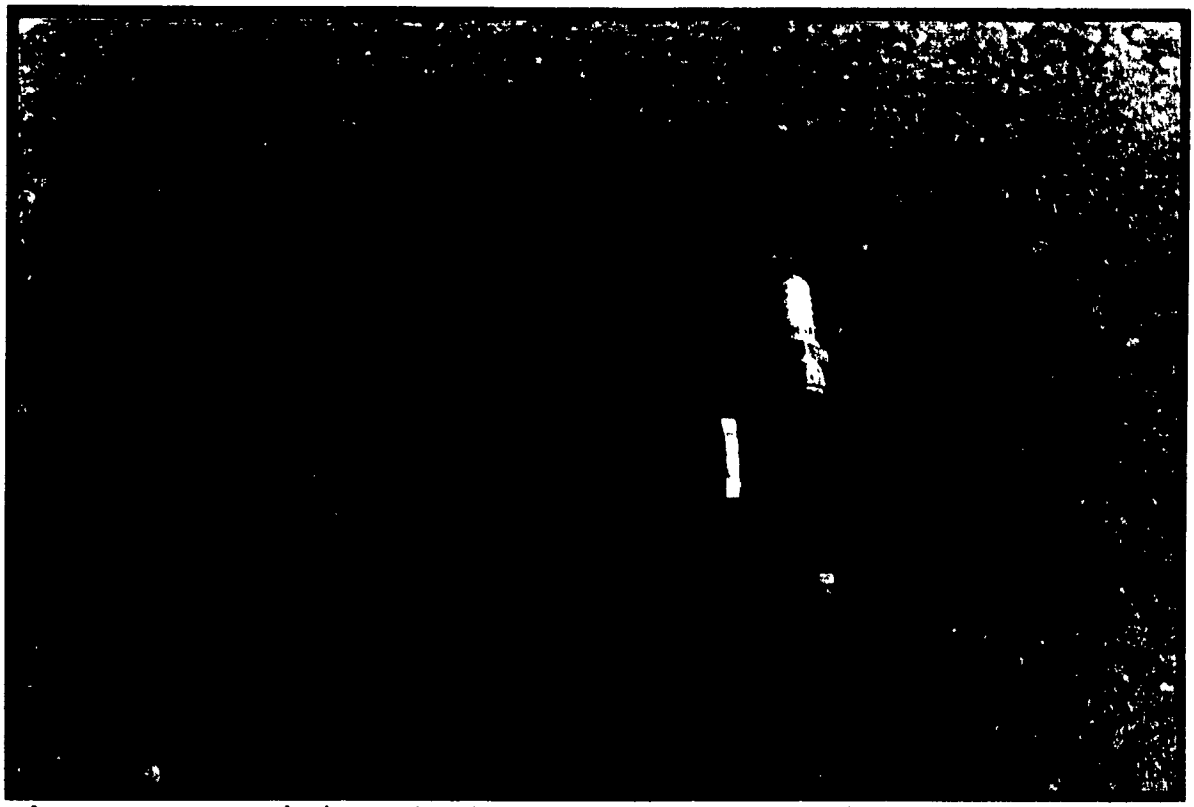

Figure 5.8 Ignition chamber for Petters engine with injector, spark plug and pressure transducer

This injector features solenoid operation, so that it can be controlled electronically instead of the conventional hydraulic actuation. The solenoid must overcome the spring preload force needed for the closure of the injector, the high differential gas pressure needed for diesel injection, and should also provide fast dynamic action such that the necessary quantity of fuel needed can be delivered in less than 4 [msec].

The other consideration when using gaseous fuel, is the compressibility effect. If excessive throttling occurs inside the injector, shock waves may occur at some places other than the nozzle orifice; this would cause a significant

fluctuation in the fuel dose. For this reason, sonic flow has to be present only at the nozzle orifice of the injector. This is an important consideration when using gas injectors in an internal combustion engine. For a sonic flow at the injector orifice, the fuel flow rate delivered to the cylinder is a function of the injector internal pressure only; any fluctuations in the cylinder pressure would not affect the fuel dose delivered. Whereas for the subsonic case, the fuel flow rate is a function of the back pressure as well as the injector internal pressure.

5.3.1 Calculation of Injected Fuel Dose

The calculation is used to size the injector nozzle orifice, required to deliver the correct fuel dose. From the given parameters of the diesel engine used on this setup, the required fuel dose can be determined.

The diesel engine used here is manufactured by Petters England, model PH1. It is a single cylinder engine with a total capacity of 660.9 [cm^3] and a compression ratio of 16.5:1 (see Appendix E for further details). However, the actual compression ratio of the modified test engine is significantly less, because of the added volume of the ignition chamber.

The fuel dose for this engine can be found in the following way. The equation of reaction between the oxygen and methane (since natural gas is made of 95% of methane, one can assume pure methane) is:

$$CH_4 + 2O_2 \rightarrow CO_2 + 2H_2O \qquad \textbf{(5.1)}$$

From mass balance one gets:

$$18 + 64 \rightarrow 46 + 36 \qquad \textbf{(5.2)}$$

From the mass balance in (5.2), dividing through by 18, results in an O_2 to CH_4 ratio of 3.556. Since there is 0.21 O_2 per 1 unit of air, the stoichiometric fuel to air ratio is 16.9 [kg] of air to 1 [kg] of CH_4. Having calculated this quantity, one can now solve for the fuel dose.

Since the total displacement volume of the cylinder, the cylinder pressure and the type of fuel are known, using the state equation, the fuel dose delivered to the cylinder can be determined. However, for a diesel engine 30% excess air is required. The equation to find the mass of air in the cylinder is:

$$m_a = \eta \, (P_i V_i / R T_i)$$

where R = 0.287 [kJ/kg*K] (for air)

For $P_i = 90$ [kPa]

$V_i = 660.9$ [cm^3]

$T_i = 293$ K

$\eta = 0.9$ (cylinder volumetric efficiercy)

one can determine the mass of air to be $m_a = 660.9$ [mg of air]. The equation of air to fuel ratio is:

$$m_f = m_a / (1.3*r)$$

where r is the stoichiometric ratio previously found to be 16.9. Therefore the dose of fuel is calculated to be $m_f = 30.08$ [mg] of

methane.

The critical ratio for sonic flow in methane is found using the following equation:

$$\frac{P_{inj}}{P_f} = \left(1 + \frac{\gamma - 1}{2}\right)^{\frac{\gamma}{\gamma - 1}} \qquad \textbf{(5.3)}$$

For methane, γ is equal to 1.32. Therefore the critical pressure ratio is 1.845 or $P_f/P_{inj} = 0.542$.

The compression process for a diesel engine can be approximated by an adiabatic compression, which follows the equation:

$$\frac{P_f}{P_i} = \left(\frac{V_i}{V_f}\right)^{\gamma} \qquad \textbf{(5.4)}$$

In equation 5.4 the ratio v_i over v_f represents the compression ratio, which is 13:1 for the engine used on this setup Therefore, for an initial pressure of 0.9 [bar], the final pressure P_f is 26.6 [bar] according to equation 5.4. Using the result found in equation 5.3, one can find the lowest injector pressure such that sonic flow occurs at the nozzle orifice. The minimum pressure is 49 [bar]. The next step involved in these calculations is to determine the injector flow area from the previous results obtained. The angle for the injection duration assumed should not last more than 35° of crank angle, at an engine speed of 2000 [rpm]:

$$\Delta t = \frac{35^\circ / injection}{360^\circ / rev} * \frac{60 \text{ sec/min}}{2000 rev/\text{min}} \qquad (5.5)$$

From equation 5.5 the time of injection is found to be 3 msec/ injection. Knowing the time of injection and the dose of fuel, one can find the average flow rate to be:

$$\dot{m}_f = \frac{m_f}{\Delta t} \qquad (5.6)$$

The mass flow rate is therefore, 10.03 [g of CH_4/sec]. Finally the orifice flow area can be computed from equation 5.7:

$$A_{fl} = \frac{\dot{m}_f}{C_d \sqrt{\frac{2\ \gamma\ P_{inj}\ \rho_{inj}}{(\gamma + 1)} \left(\frac{2}{(\gamma + 1)}\right)^{\frac{2}{(\gamma - 1)}}}} \qquad (5.7)$$

$$A_{fl} = 870.1 \times 10^{-9}\ [m^2]$$

In equation 5.7 it is important to point out that the density ρ_{inj} cannot be calculated from the state equation because of the high pressure present in the injector. This requires to use the thermodynamic tables for CH_4 . For a flow area of A_{fl} = 870.1 x 10^{-9} [m^2], this circular area can be expressed as a nozzle orifice diameter of 1.05 [mm]. This diameter is located at the throat of the diverging part of the orifice.

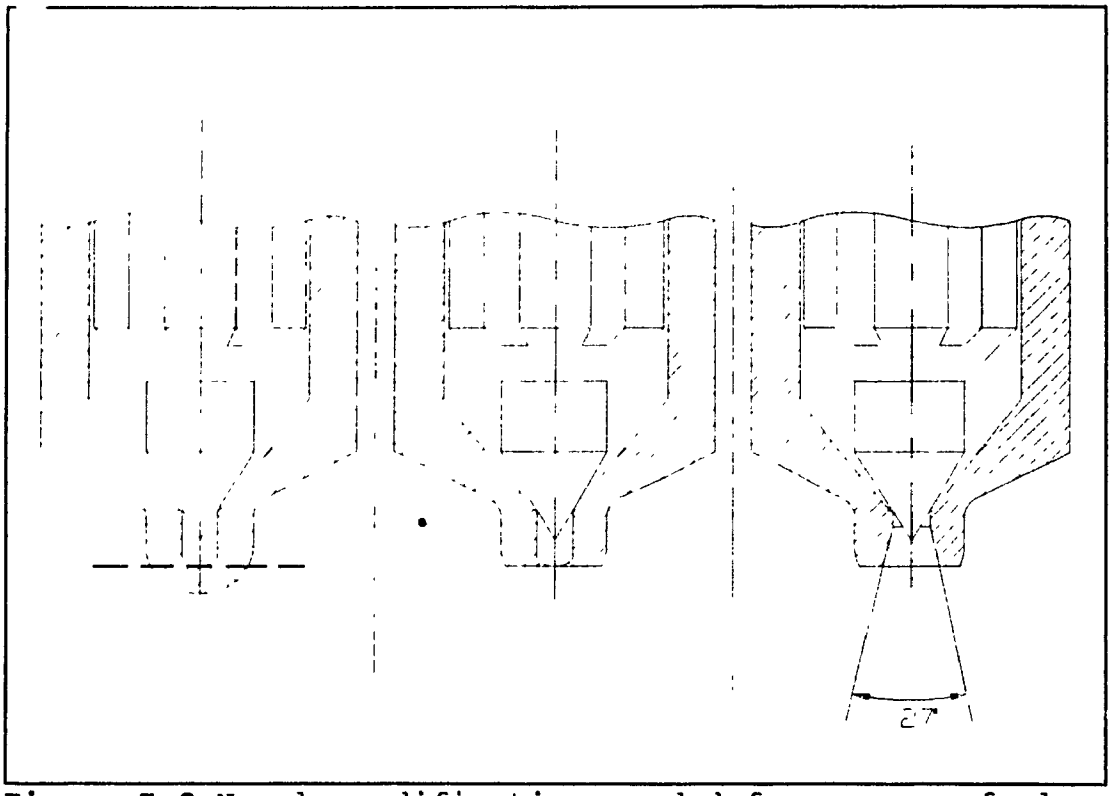

Figure 5.9 Nozzle modification needed for gaseous fuel

Knowing this dimension, one can now modify the standard CAV-Lucas nozzle orifice for the flow diameter found above. Figure 5.9 shows the procedure involved for this modification. The modification shown, is required since gaseous fuels have a much larger specific volume than liquids. Because of this consideration, the flow area has to be increased substantially.

5.3.2 Experimental Apparatus Used for Calibration of the Gas Injector

The calibration instrument for the fuel dose measurement is shown in Figure 5.11. This setup is operated by a microcontroller via a triggering amplifier placed between the injector and the controller.

After finding the flow area for the injector, the next process is to calibrate the injector. This calibration requires an experimental apparatus for measuring the fuel dose delivered by the injector. The apparatus proposed in this section is made of a piston cylinder assembly (see Figure 5.10), whereupon triggering of the injector, the fuel delivered by the injector displaces the piston by a certain distance. The piston displacement is measured with a dial indicator thus, allowing to measure the fuel dose. The fuel dose control is achieved by increasing or decreasing the injector opening time through the software delay. This delay adjusts a pulse width such that a measured fuel dose is delivered to the cylinder.

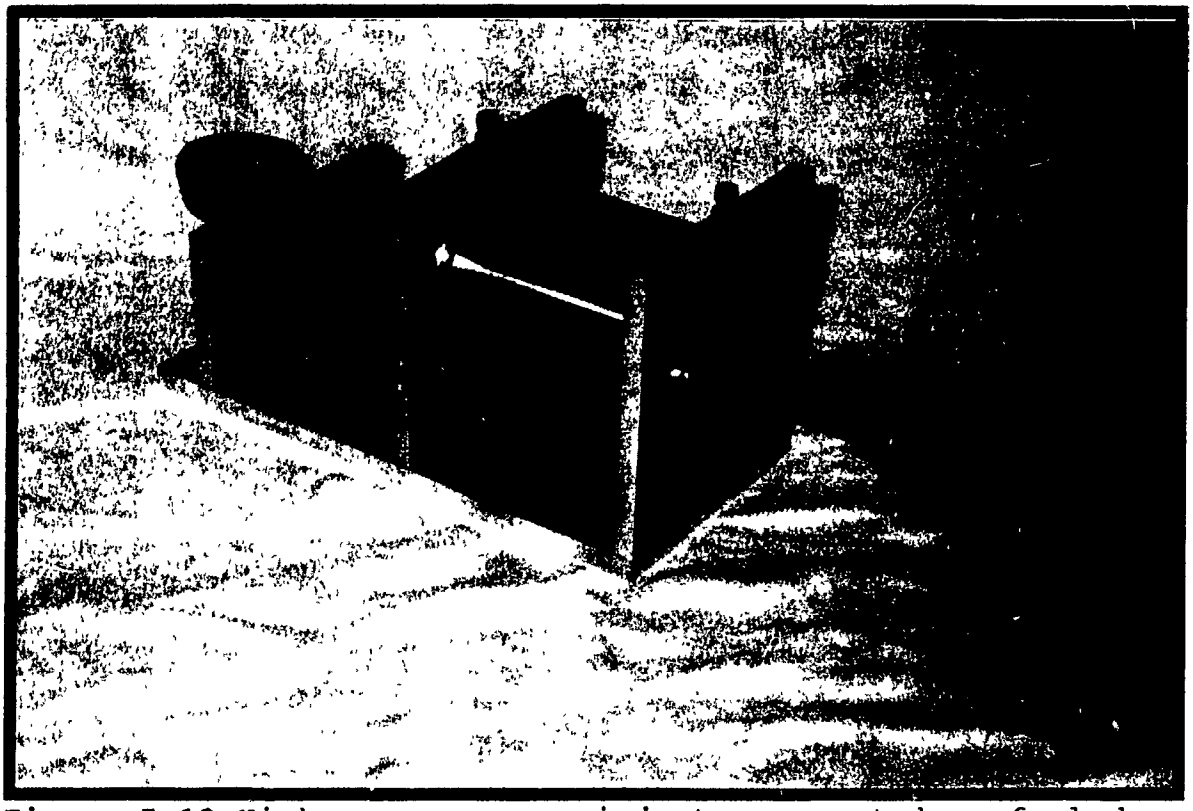

Figure 5.10 High pressure gas injector, mounted on fuel dose measurement device

To measure the displacement of the piston, a dial gage indicator is used to record the initial and the final position of the piston. The cylinder shown in Figure 5.11 allows for a back pressure to be applied using shop air. This is needed for a more accurate measurement of the fuel dose.

The advantage of this device over other systems which have been used by D.Miele [19] and Tebelis [20], to calibrate a gaseous fuel injector, is that the back pressure caused by the increase in cylinder pressure can be simulated. However, because of this large back pressure, the device has a tendency to leak. Since the proposed instrument can simulate the back pressure, it is possible to achieve a better injector calibration.

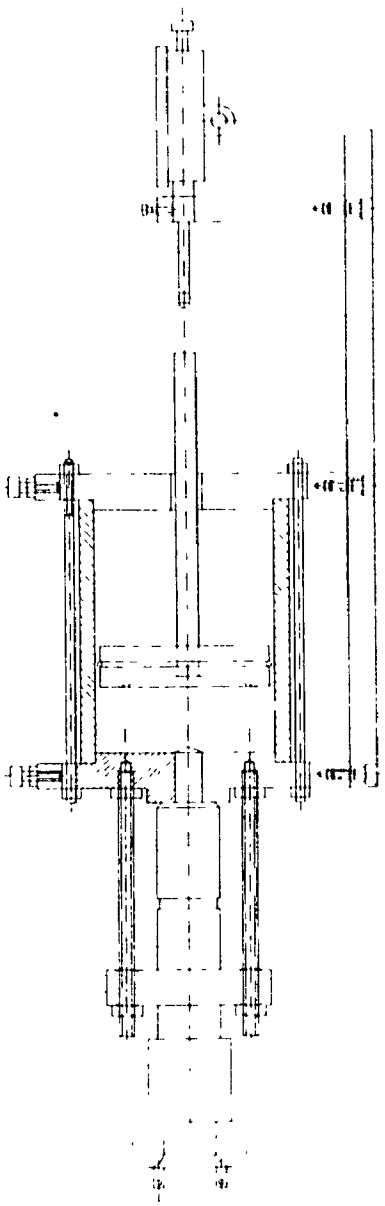

Figure 5.11 Sectional view of the device used for measuring the fuel dose from the injector

Since the engine was not running, during the injector calibration, the microcontroller had to receive a signal to trigger the injector from another source. To replace the optical switch triggered by the engine, a function generator was used to send a square wave signal of 5 volts, similar to the signal used on the engine. This signal then triggers the two external interrupts which in turn, causes the program to be executed by the Intel MCS-96 Microcontroller. Figure 5.12 shows the complete setup used for the injector calibration.

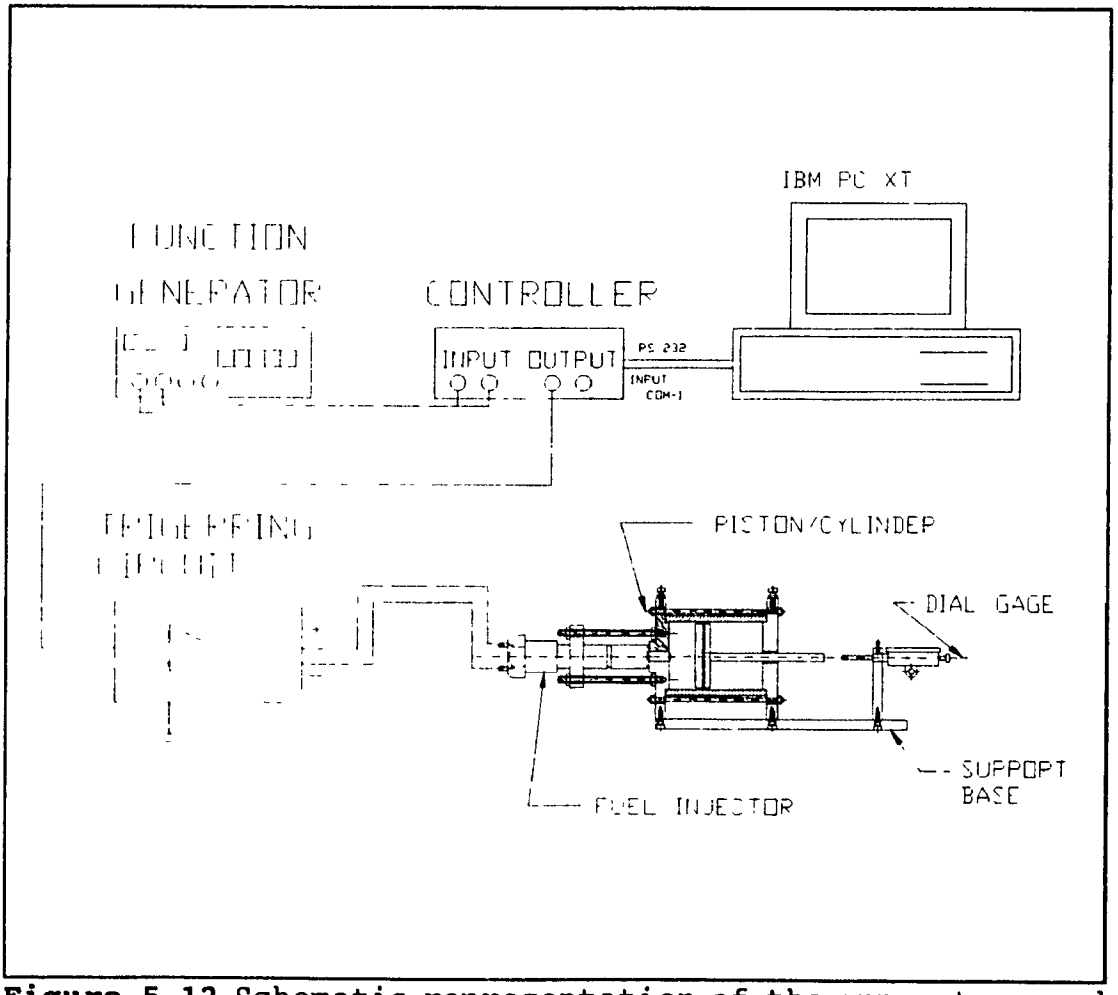

Figure 5.12 Schematic representation of the apparatus used for the fuel dose calibration of the injector

5.3.3 Calibration Methodology

The objective here is to simulate as accurately as possible the conditions which prevail in a diesel engine, including the back pressure caused by the compression of the air in the combustion chamber. This is simulated here by using the shop air to pressurize one side of the piston. Because of design consideration, as well as safety reasons, the back pressure has been limited to only 6.5 [bar]; it is important to point out that the shop air is acting as a spring when injection occurs. Viscous damping is present as well, provided by the small clearance gap which allows the piston to slide in the cylinder. The two parameters mentioned above should be considered before any results are recorded.

It is important to trigger the injector a few times before the test to fill-up the methane compartment, and to release it through the relief valve so that only pure methane will remain in that portion of the cylinder. At that point the injector pressure can be kept at around 14.6 [bar]. Then, an initial volume of methane has to be present in the fuel part of the cylinder, at least 50 times larger than the fuel dose, so that the piston does not move violently, potentially damaging the instrument. Following this procedure, the injector pressure is raised to the working pressure of 70 [bar]. The instrument is now ready for operation.

Since the software is used to regulate the fuel dose to the engine, this variable is considered as the independent variable. The hexadecimal number will be incremented from 250 to 1000 Hex in steps of 100 Hex (see Table 5.1). To record the time of opening of the injector, a pressure transducer placed in the body of the injector is used to record the pressure variations. Upon the triggering of the injector, the pressure transducer indicates the time of injector opening, and the dial indicator gives the relative piston displacement. Two curves are produced from this experiment. Figure 5.13 shows the software delay versus the injector opening in milliseconds, and the other curve, Figure 5.14 shows the time of opening versus the fuel dose in milligrams of CH_4. These two plots will later be used to determine the fuel dose delivered to the engine.

Table 5.1 Conversion table from decimal to hexadecimal

Delay [decimal]	Delay [hexadecimal]
592	250
848	350
1024	400
1280	500
1536	600
1792	700
2048	800
2304	900
2560	1000

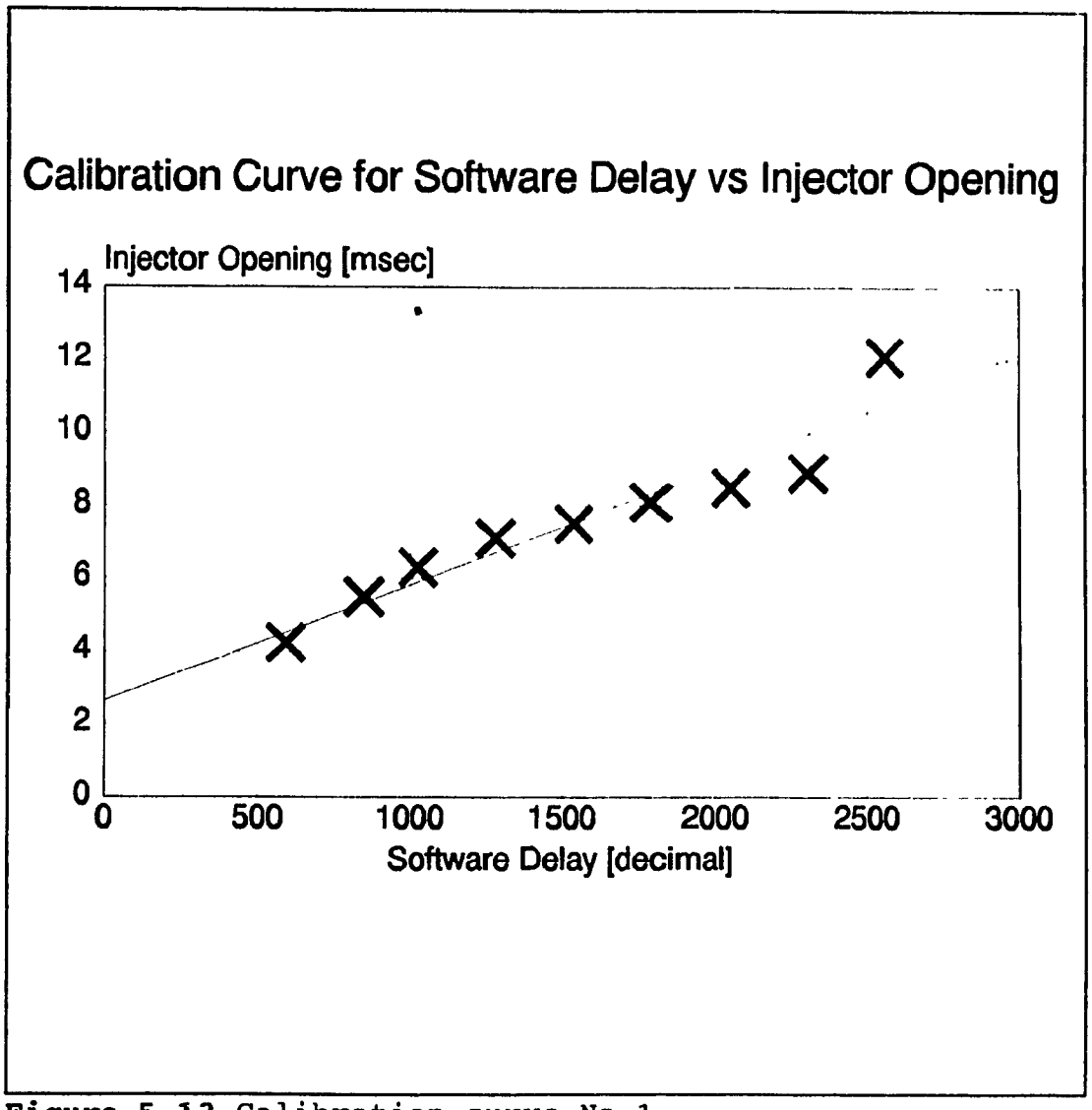

Figure 5.13 Calibration curve No.1

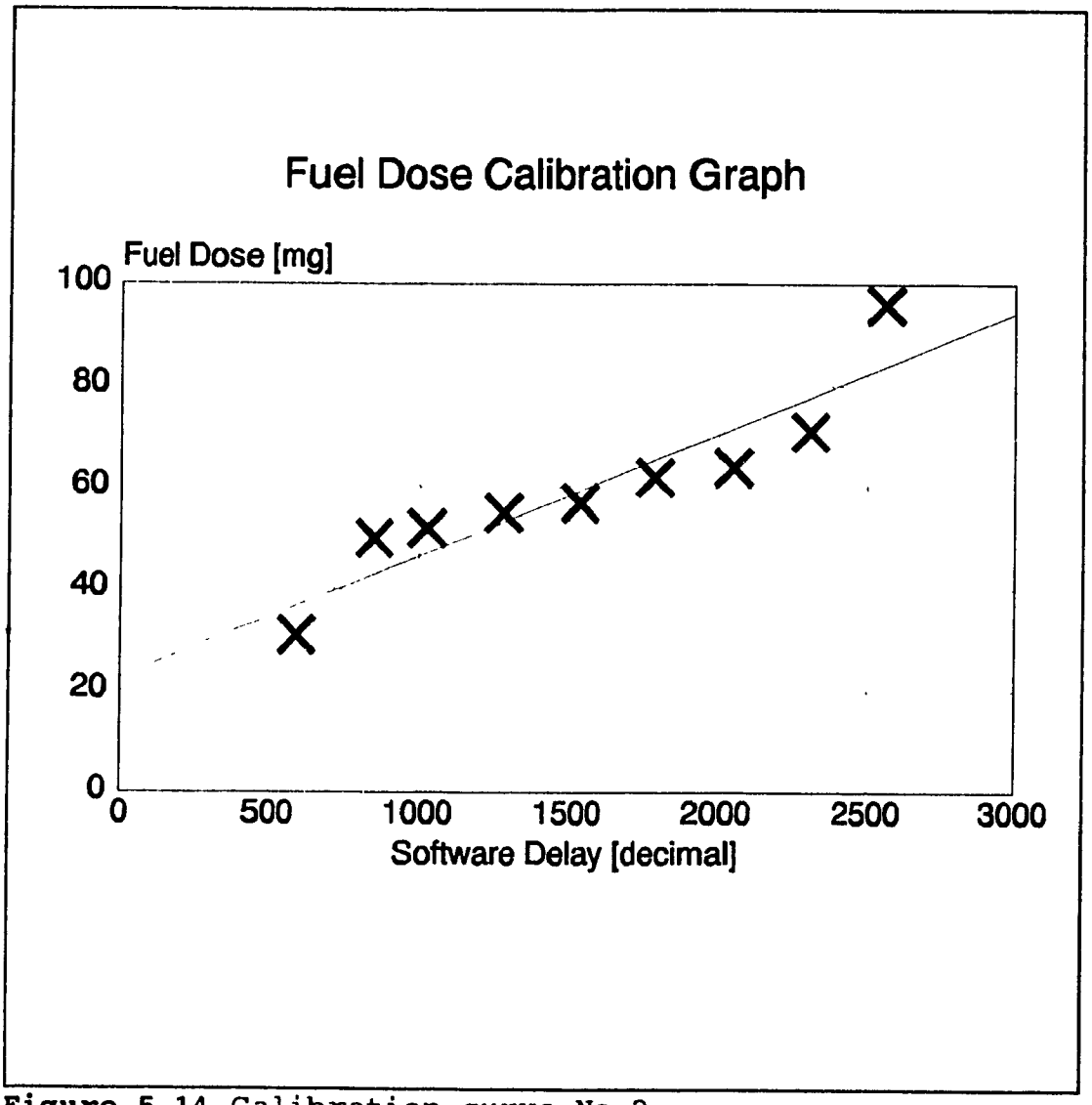

Figure 5.14 Calibration curve No.2

5.3.4 Calibration Results and Discussion

The experimental results shown in Figure 5.14 exhibit a linear increase of the gas dose in the range of 35 to 70 [mg] of CH_4. This range is more than what is required for the fuel delivery schedule of the engine. The engine range should not exceed 45 [mg] of fuel. It was established in section 5.3.1 that for 30% excess air the fuel dose required should be 30 [mg] of fuel. This calibration curve however indicates that the injector orifice may have to be reduced in order to increase the range of operation for this injector. A reduction in the order of 30% of the flow area may be sufficient. However, it is important to point out that the amount of fuel going into the ignition chamber is not only a function of the total dose of fuel going into the engine. The amount of fuel is also varied by the injector position, which allows more or less fuel to remain in the ignition chamber.

It can be concluded that for the initial testing of the engine the following starting values would be required. The software setting at 250 HEX would yield a fuel dose of about 31 [mg] of CH_4 which is close to the calculated value of 30 [mg] from the analysis. The difference resides in the fact that the injector opening required here is 4.0 [msec] instead of the 3.0 [msec], as previously calculated. The fact that the mass flow rate is slightly lower for the experimental case as compared with the theoretical case, is attributed to the fact that, for a viscous flow the boundary layer growth in the orifice causes a

reduction in effective flow area. The general term used for such case is referred to as vena contracta.

5.3.5 Determination of the Gas Jet Angle

The last step before installing the injector on the test engine, is to find an initial position for the injector, using the spacers to locate it with respect to the ignition chamber. The method described here is very simple however, it should be sufficient for the initial engine tests.

It consists of triggering the injector onto a metallic screen impregnated with grease. Figure 5.15 shows how the set-up is mounted. The injector is placed at a distance L from the metallic screen and mounted firmly on a surface. The metallic screen is sufficiently large so that the injector, when triggered, leaves a print of the jet on the screen. The resulting circle is used along with the distance L to determine the gas jet cone angle. By simple geometry we get the equation:

$$\alpha = ARCTAN\ (\frac{D}{2L})$$

Where 2 times the angle α is equal the cone angle.

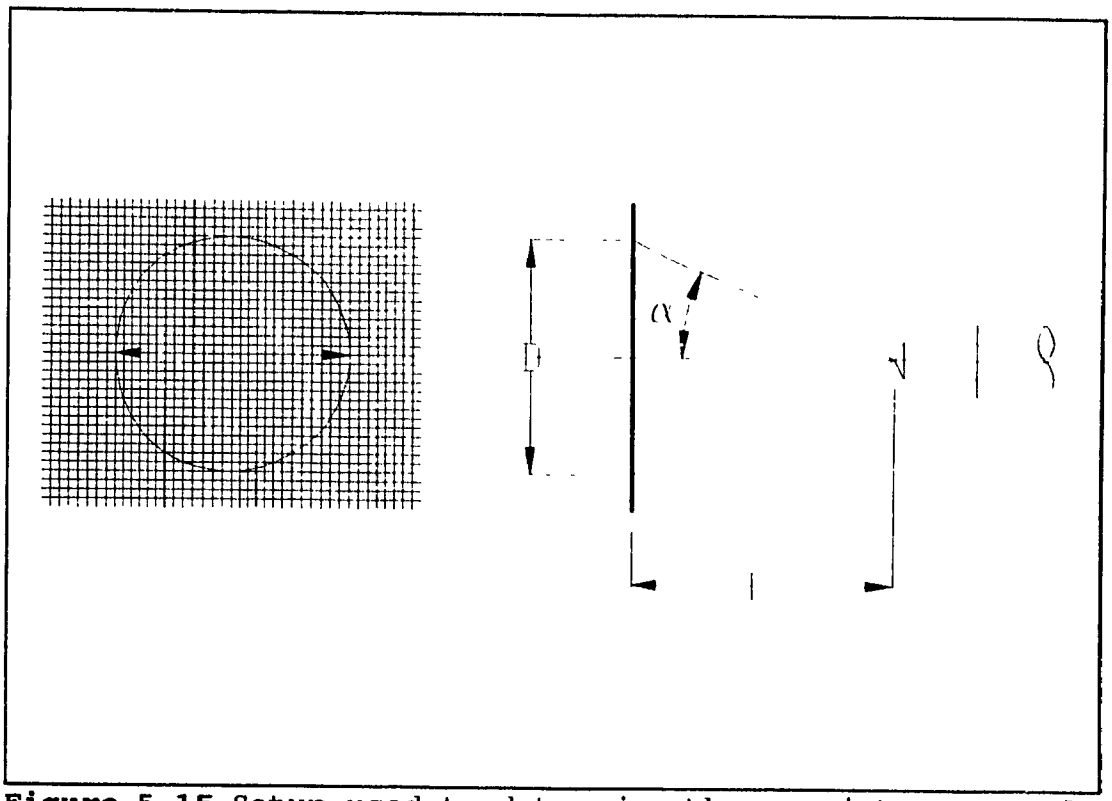

Figure 5.15 Setup used to determine the gas jet cone angle

5.4 Injector Control Circuit

The control of the electronic fuel injector is accomplished via an amplification circuit, which uses the low input current signal from the microcontroller and outputs a high current signal sufficient to unseat the injector needle. For this experimental setup two test circuits have been tried, namely, an H-bridge circuit and a boost circuit, for which each circuit has particular output characteristic.

As previously noted, both circuits use a forward signal as well as a reverse signal. The reverse signal is used to demagnetize the solenoid hence, insuring a faster closing of the injector. However, both circuits have different current and voltage output feature. The H-bridge circuit (see Figure 5.16) used by T.Krepec et al. [21], has a constant output voltage of 12 volts, as shown in Figure 5.17 where the current rises in the solenoid slowly, and peaks toward the end of the signal. Since the force generated by a solenoid is proportional to the current passing through it, the maximum force for this solenoid is only available toward the end of the input pulse. The force generated by the current passing through the solenoid has to overcome the spring preload, as well as the high gas pressure present in the injector body. As a result, a substantial delay exists between the beginning of the input pulse and the injector needle lifting of its seat (see Figure 5.17). This is where the design of the boost circuit becomes more advantageous. The initial circuit design was developed by Green et al. [22], and subsequently modified by Hong et al. [23, 24].

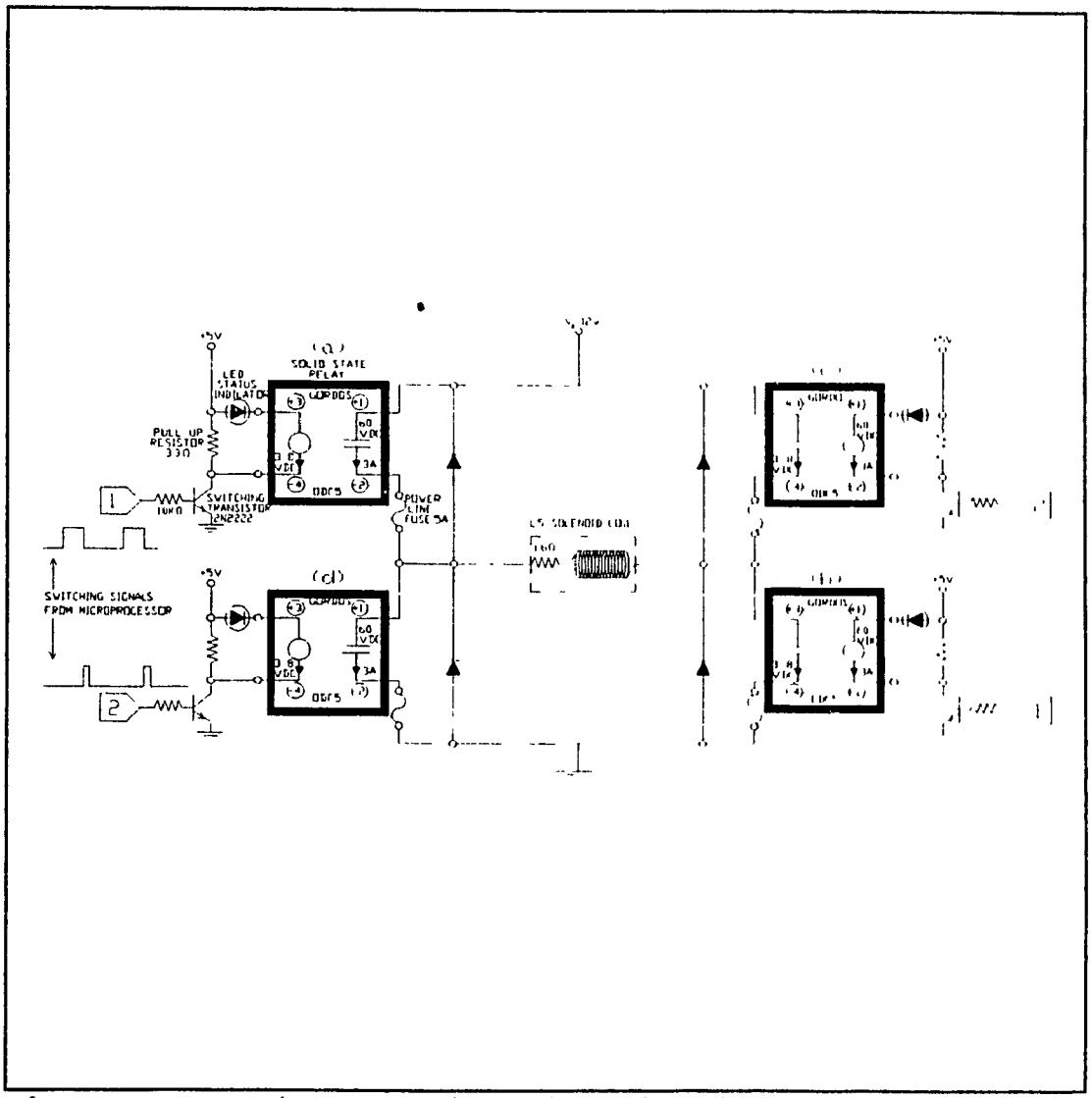

Figure 5.16 Injector triggering circuit, H-bridge type

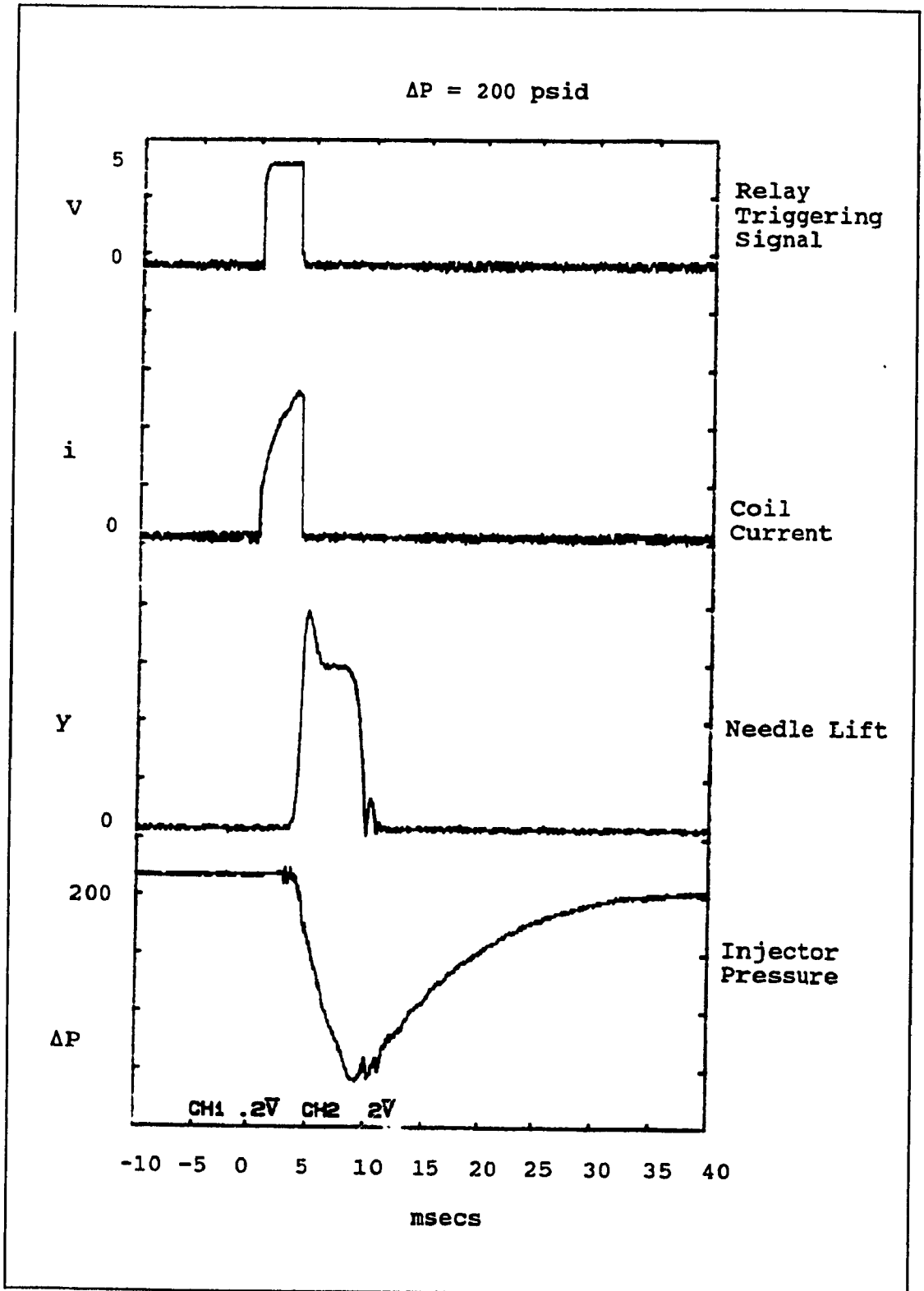

Figure 5.17 H-bridge circuit performance for ΔP of 14.6 [bar]

This circuit allows to change the transient characteristics of the current in the solenoid. There is a maximum mean current that the solenoid can tolerate without damaging it. Thereby, using this parameter, one can change the transient current characteristics, without exceeding this value, such that the maximum current is available at the early stage of the input signal. Instead of using a constant 12 [V] supply to the injector, a capacitor previously charged to 100 [V] is discharged through the solenoid, so that a maximum current is available closer to the beginning of the signal. As a result, the maximum force applied to the injector needle is obtained in the early part of the input signal. This boost signal allows to unseat the needle and balance the pressure across the injector in a faster manner than the H-bridge could have accomplished. After balancing of the pressure forces on the needle, the remaining part of the signal is maintained at 12[V] across the solenoid. The 100[V] signal is used to overcome the spring preload, the viscous damping and the needle inertia.

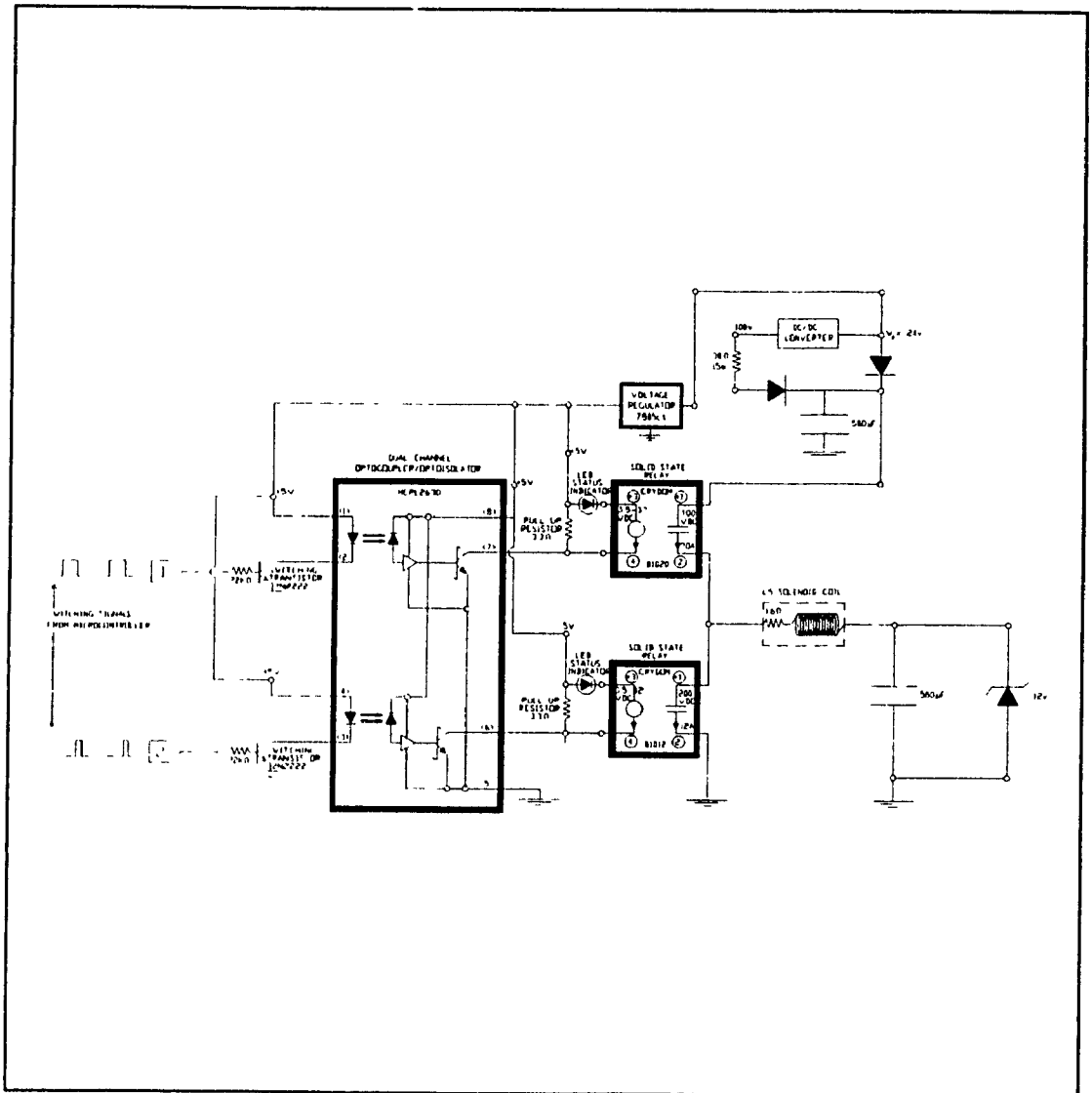

Figure 5.18 Injector triggering circuit (boost circuit)

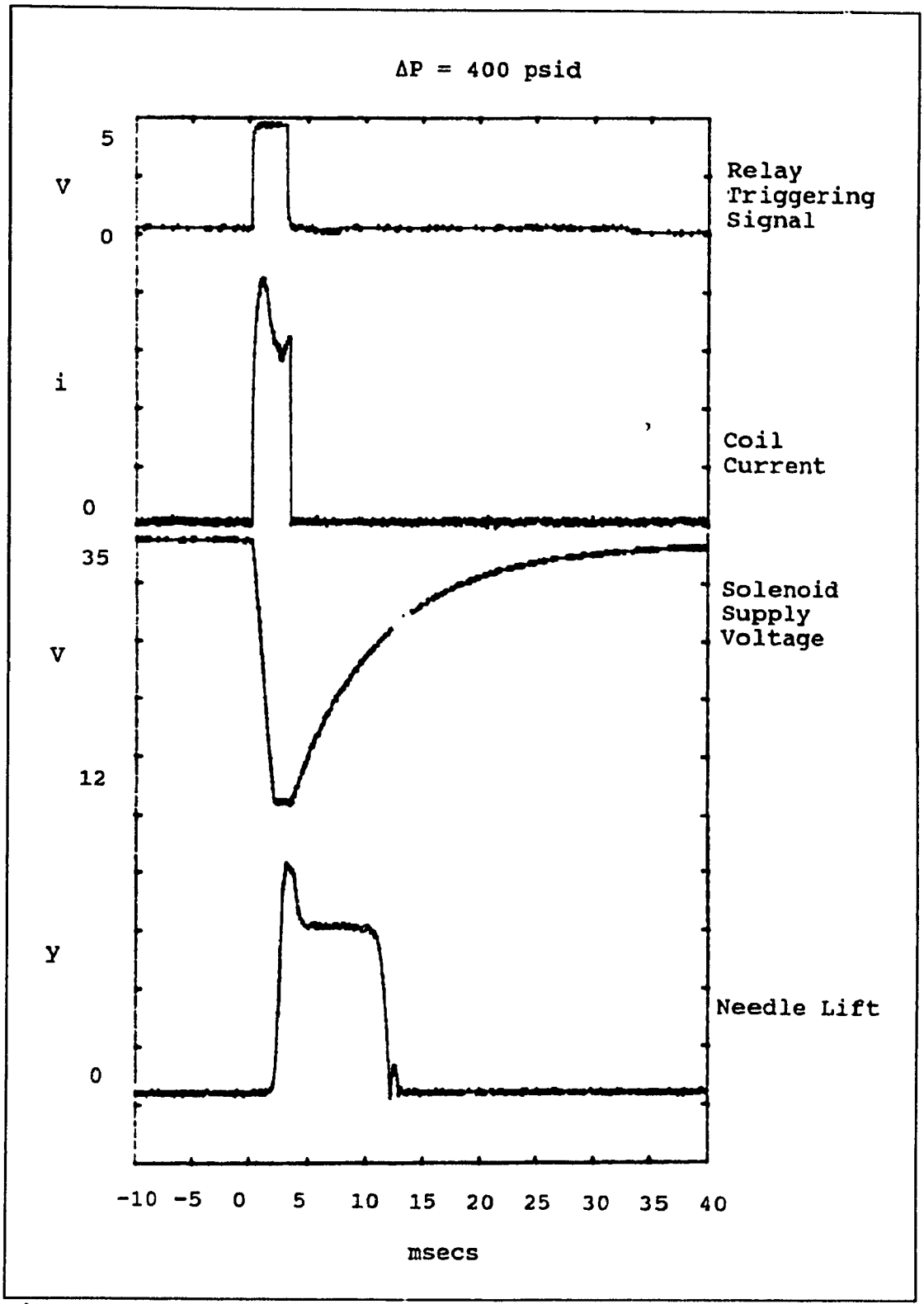

Figure 5.19 Boost circuit performance for a ΔP of 28.2 [bar]

The boost circuit of Figure 5.18 shows the protective diodes used to shield the 24 [V] source and the boost capacitor which provides the large current input to the solenoid (see Figure 5.19). The other feature which render this circuit more advantageous to use over the H-bridge configuration is the use of two relays instead of four. These solid state relays substantially increase the cost of the amplification circuit. In turn, this circuit requires two supply voltages of 24 and 100 [V] as compared to 12 [V] for the H-bridge configuration. The circuit simplification is in part due to the use of a zener diode and a 35 [V] 560 [μF] capacitor placed along side of it. Once the forward signal has been sent via the relay A, that relay is then closed and relay B opens for the reverse signal. This reverse signal is accomplished by discharging the capacitor to the ground through relay B. The zener diode is used to limit the voltage to only 12 [V] across the capacitor during the entire forward signal.

Another feature that is found in both circuits, is the protective device used to insulate the microcontroller from the amplifier. The HCPL2630 optocoupler consists of light emitting diodes that upon switching to ground, send light to a phototransistor that output a signal to the relays. This device is used as a protection against possible back emf that occurs when switching large current.

The boost circuit advantage is the possibility of varying the capacitor value (100 [V] side) and the 15 [W]

resistor, thus allowing control of the transient current characteristics of the circuit. This possibility is not available with the H-bridge.

After testing both circuits under working conditions, i.e. an injector pressure of 70 [bar], it was found that the H-bridge circuit could not open the injector, even with the high air pressure present in the engine cylinder during compression. Therefore, the circuit which will be used on the test rig will be the boost circuit configuration.

5.5 Signal Conditioning Circuit for Measuring the Crankshaft Position

A diesel engine, unlike an spark ignition engine, requires the fuel dose to be injected near TDC. To achieve this, the proper timing between the piston position and the opening of the fuel injector is of paramount importance. For an engine using an electronic control, the monitoring of the piston position can be accomplished by using electronic switches. There exist other electronic means for finding a piston position, such as magnetic pick-up which is often used in automotive application, however, the opto-switch was retained for this experimental setup. Initially it was assumed that the signal coming out from the opto-switch could be sent directly to the microcontroller. Because of the electric motor used to turn the diesel engine, electromagnetic interference generated by the motor was present and picked-up by the cable that links the opto-

switch to the controller and other system components. After shielding every component of the system namely, the microcontroller, the ignition control box, and the injector amplification circuit, there was still some electromagnetic interference coming into the system.

A second order low pass active filter of the type Butterworth, was used here to filter out the unwanted electromagnetic disturbance between the opto-switch and the controller. The cutoff frequency was initially set at 20Hz (by setting the resistors labelled 8K and the capacitor labelled 0.001 mF one get a cutoff frequency of 20Hz, as shown in Figure 5.20), and varied until the desired response was achieved. Because the second order filter decays at 40db/decade, this feature allows for better performance from the point of view of removing large amplitude spikes that may occur at frequencies above, but closer to the cutoff point. By using an operational amplifier (op-amp) this provides a high impedance with respect to the opto-switch and a low impedance with respect to the two Schmitt triggers placed after the filter. For the Butterworth filter (some times referred to as a equal-component-value Sallen-Key filter) [25] the ratio between the resistor labelled R_a and R_b has to be such that it is equal to 0.586; this is to ensure that the op-amp does not go into an inverting mode.

However, further signal conditioning is required after the low pass filter. As shown in Figure 5.20, the shape of the signal is not compatible for the microcontroller. By passing the signal through two inverting Schmitt triggers, the signal is transformed to a standard TTL signal. The Schmitt triggers are acting as a large gain amplifier, that upon passing a threshold value, the large gain saturate the amplifier at 5 or 0 volts. However, when using a SN7414 Schmitt trigger the threshold value is fixed. The second inverter is needed only to bring back the signal to its initial setting.

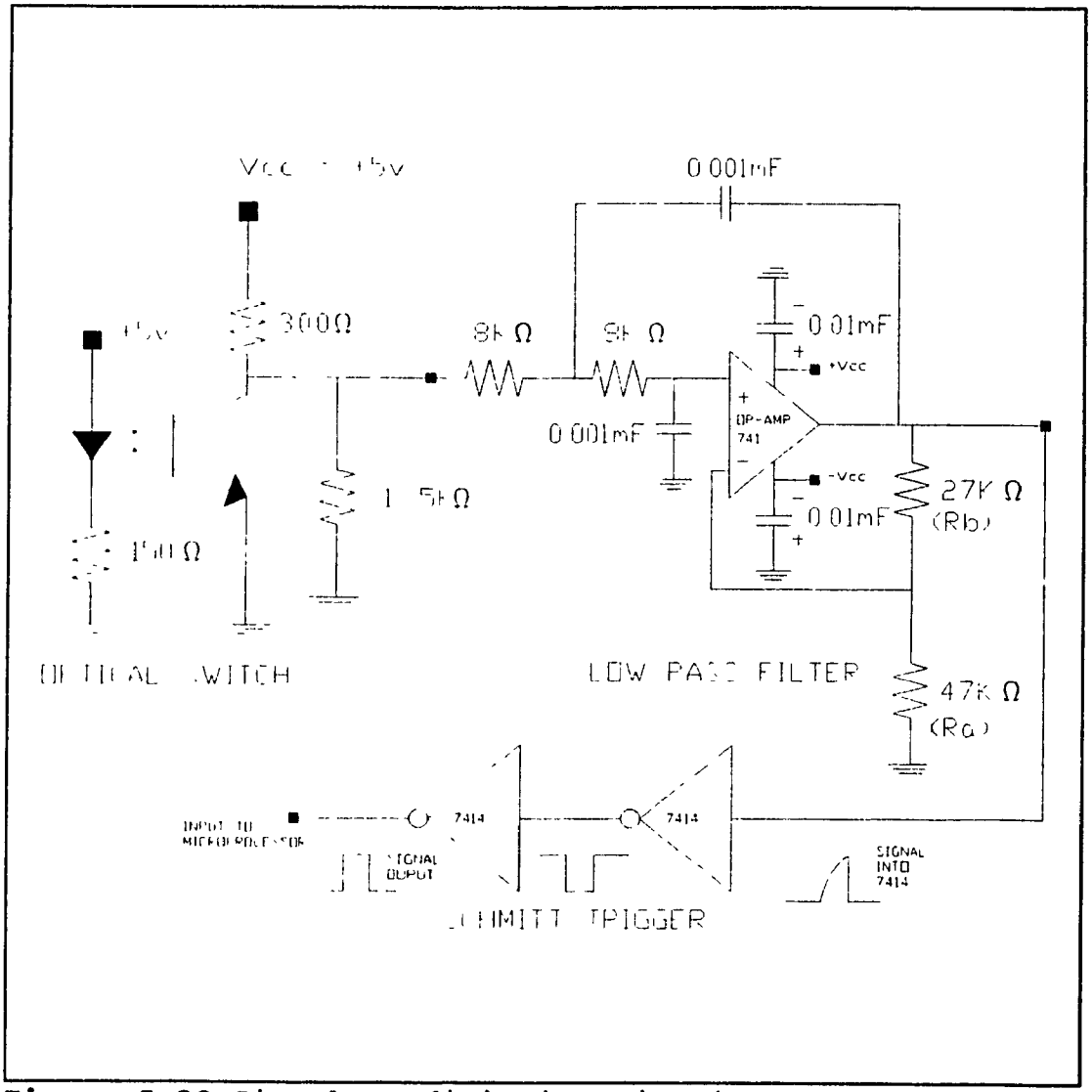

Figure 5.20 Signal conditioning circuit

5.6 Spark Ignition System Evaluation

The goal of this investigation is to evaluate different ignition systems, and suitably select one which can be used on the gaseous fuel engine prototype.

A spark comparator was built in order to verify the strength of the spark generated by the ignition systems. This tool along with a properly designed triggering system, constitute the test setup necessary to carry out the experiment.

5.6.1 Spark Ignition Theory

The theory behind the spark mechanism was briefly covered in the chapter 2 (Literature Study) however, more detail should be presented at this point to better understand the justification for this experiment. The various phases occurring during a spark discharge are summarized as follows.

A large potential difference across the gap is necessary to overcome the resistance of the air volume contained in this gap, which acts as an insulator (see Figure 5.21). The critical magnitude of the potential gradient (to obtain a flow of electrons) depends on the charge density of the mixture, as well as the homogeneity of the gases contained in that volume. In this present case, the mixture is formed with air and methane mixture. Initially, the gas acts as an insulator between the two electrodes.

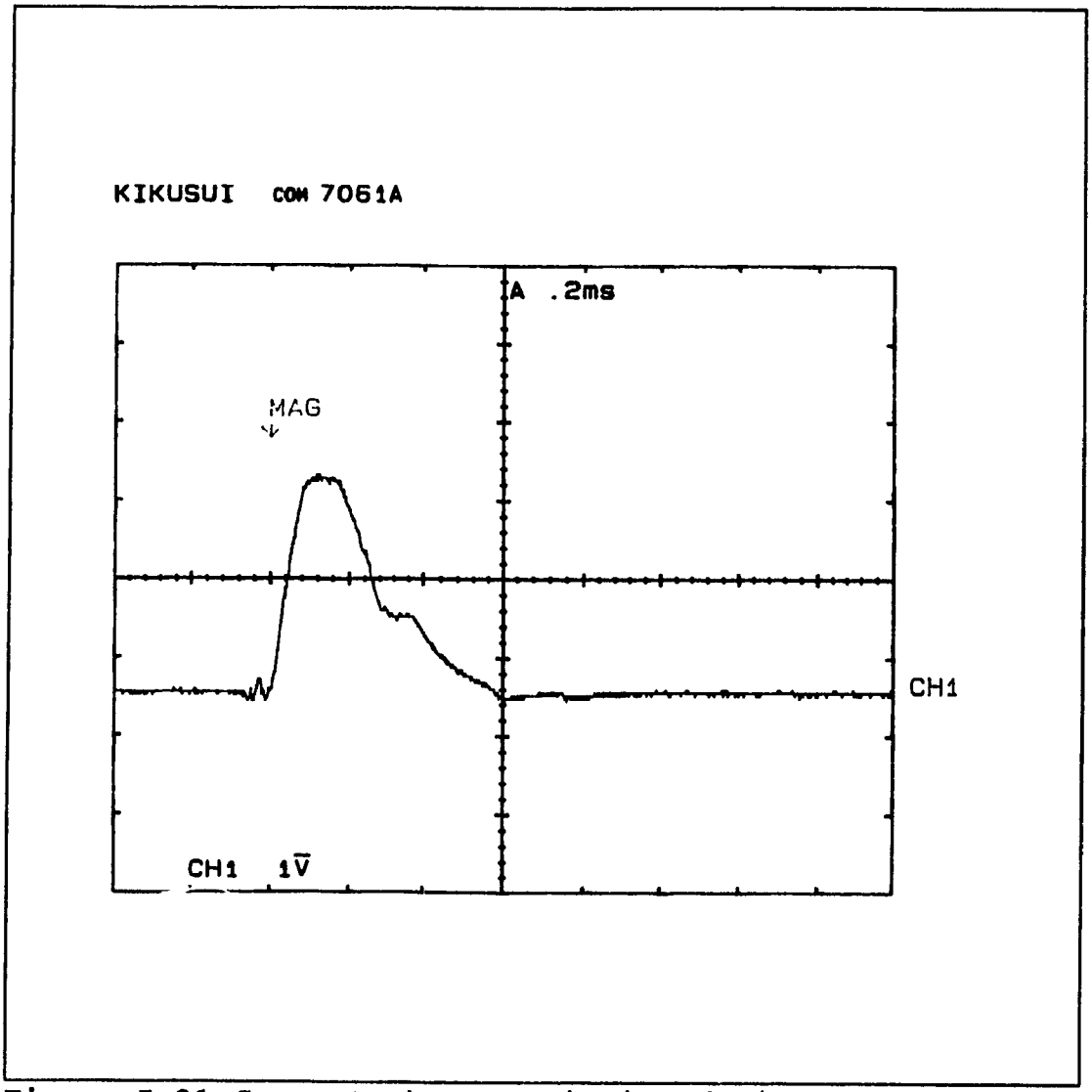

Figure 5.21 Current characteristics during sparking, the current probe setting is 100 mV/amp

It is only after reaching a potential gradient large enough (20 to 30kV) across the two electrodes that an ion can reach a critical velocity so that collision between other gas molecules form other ions and as a result, causes the air gap to become a conductor. The mean distance or mean free path between the electrodes plays an important role in providing sufficient distance for the ion to attain the so called critical velocity [26]. Once the gap is ionized, the electrons start flowing rapidly thus, large current rise (in excess of 100 [amp]), see Figure 5.21, can be obtained. Similarly, the voltage drops just as rapidly. During this period an intense light occur, and energy is transferred to the air-methane mixture which causes ignition of the gas. Knowing these facts about the ignition mechanism helps to make a right decision on the type of ignition system to be selected for the engine test setup.

The other component of the system often overlooked for obtaining a good ignition, is the triggering circuit placed on the primary circuit of the ignition coil. This circuit should be designed with the intent of minimizing the energy loss, so that a maximum of energy is transferred to the ignition coil. The energy loss in a transistorized system is due to the heating of the transistor. This results in a substantially decreased effective energy available for ignition at the spark plug electrodes. For utilizing maximum energy, a MOSFET transistor has been chosen over a bi-polar type transistor because of its energy efficiency characteristic.

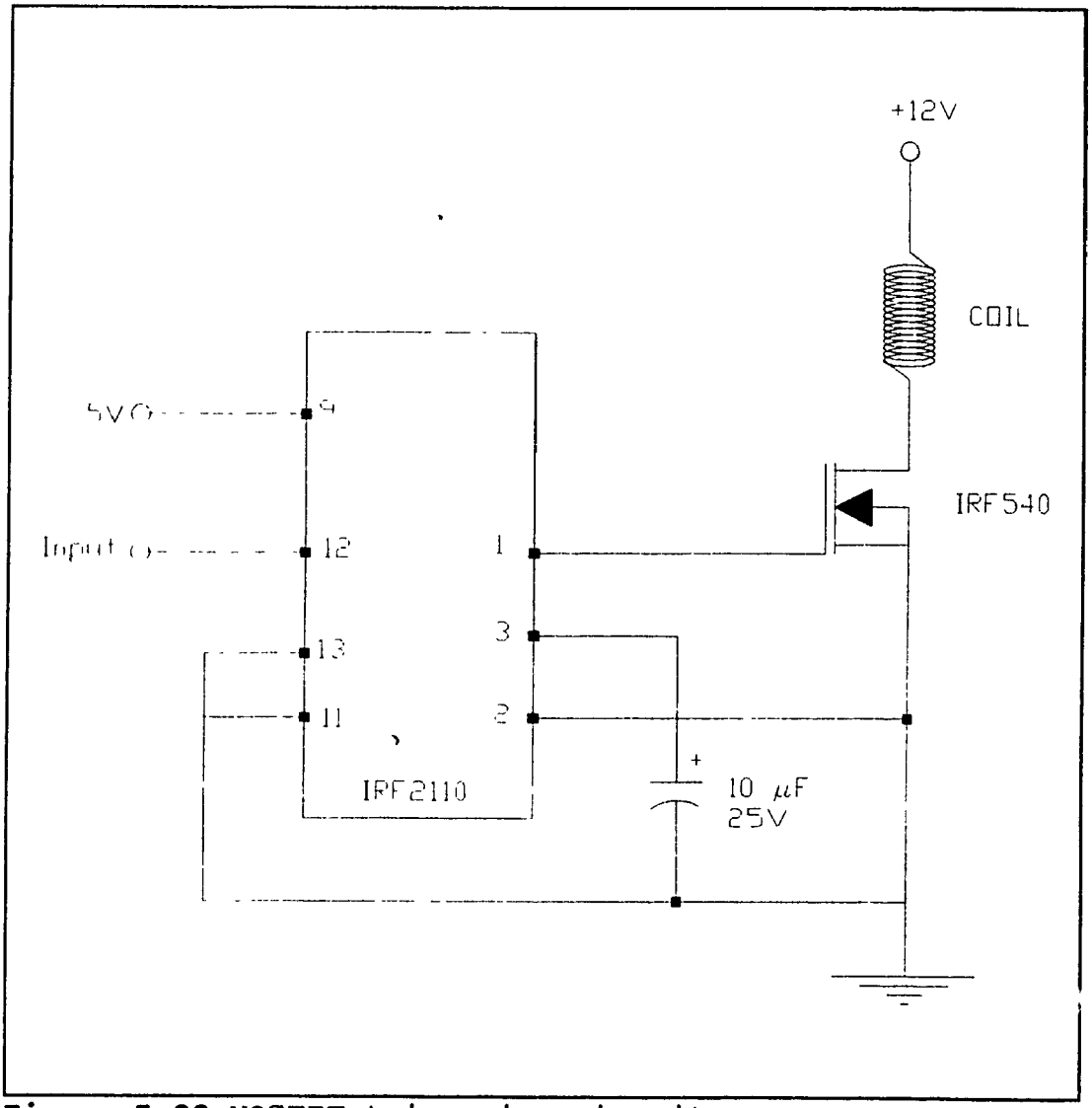

Figure 5.22 MOSFET triggering circuit

5.6.2 Spark Ignition Selection

The purpose of this investigation is to select an ignition system suitable for ignition of gaseous fuel operating in a diesel engine. For this purpose, several ignition systems comprising of the ignition coil and the triggering circuit will be tested on a special instrument referred to as a spark comparator (see Figure 5.23). For different system configuration, this instrument will help to determine the best combination of coil and circuit for the test engine.

Two triggering systems will be used namely, a MOSFET circuit and a circuit which is readily available from MSD ignition system company. Both circuits will be evaluated with different ignition coils. In selecting an ignition coil to obtain the best spark performance, it is necessary for the primary circuit of the coil to have a low primary resistance so that a maximum current can be drawn.

The testing of the system cannot be done in an environment where the pressure and temperature corresponds to the diesel cylinder conditions. Therefore, the system being tested will be compared to a standard General Motors system which will serve as a basis of comparison. The experiments will be carried under ambient conditions.

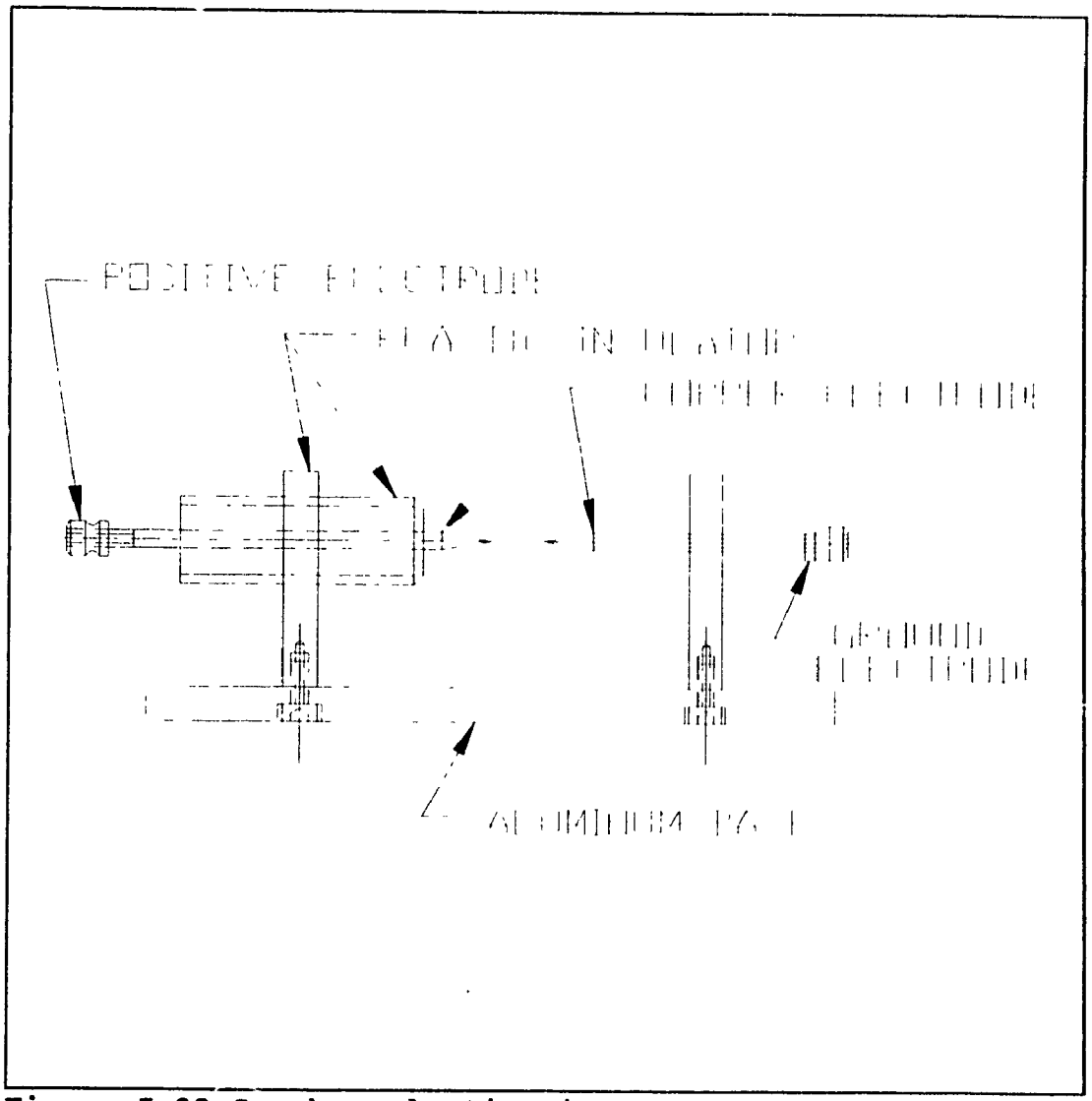

Figure 5.23 Spark evaluation instrument

5.6.3 Description of the Apparatus and Testing Methodology

The spark comparator is an instrument which consist of a fixed needle tip and a micrometer head which can be used to vary the gap between the two tips (see Figure 5.23). However, the fixed tip can be pre-adjusted in order to accommodate different spark lengths. The mounting plate on which the fixed tip is assembled, is made of plexiglass. This material is used to ensure that the spark jumps only to the other electrode tip. The micrometer head can be positioned between 0 to 25 [mm]. Finally, a standard ignition coil wire will be mounted directly on this instrument in place of a spark plug.

The other aspect of this experiment is the use of an efficient triggering circuit to generate the spark. The selection criteria for the system are based on the heat dissipated by the device and on the performance characteristic. After testing different systems, it was found that a triggering circuit using a MOSFET unit would offer the best compromise (see Figure 5.22), due to the high gate impedance of the MOSFET, and its low ON resistance. Therefore, a minimum heat is generated, which could alter the switching performance of the circuit. After completion of this circuit and testing it with the spark comparator, it will be implemented on the engine prototype.

The testing approach used for testing different systems is fairly simple. It consists of connecting the ignition system to the spark comparator as previously mentioned. A ground wire is attached to the structure of the spark comparator to

complete the current flow path (see Figure 5.24). The ignition system is supplied by a 12 [V] battery, rather than a power supply because of the high current requirement. The switching circuit is placed on one of the supply wires to the coil. To generate a signal to the switching unit, a function generator is used to simulate the TTL microcontroller signal.

Once the whole circuit is operational, an initial gap is set on the spark comparator. The function generator will pulse a signal varying between 10 to 60 hz, to simulate the engine speed. Before taking any data, a certain amount of time is allowed for the system to reach a steady state temperature. Once that condition is achieved, proper testing can begin. The micrometer head setting is increased gradually until misfiring occurs. This distance is recorded. The above testing procedure is performed on different systems, and the results are used as a basis of comparison.

5.6.4 Ignition Triggering Circuit

For this evaluation experiment, two triggering systems have been tested namely, a standard MSD ignition box, and a transistorized circuit using a MOSFET transistor. The MSD system provides multiple signals to the primary coil thus, generating multiple sparks, whereas the MOSFET circuit produces a single signal to the coil.

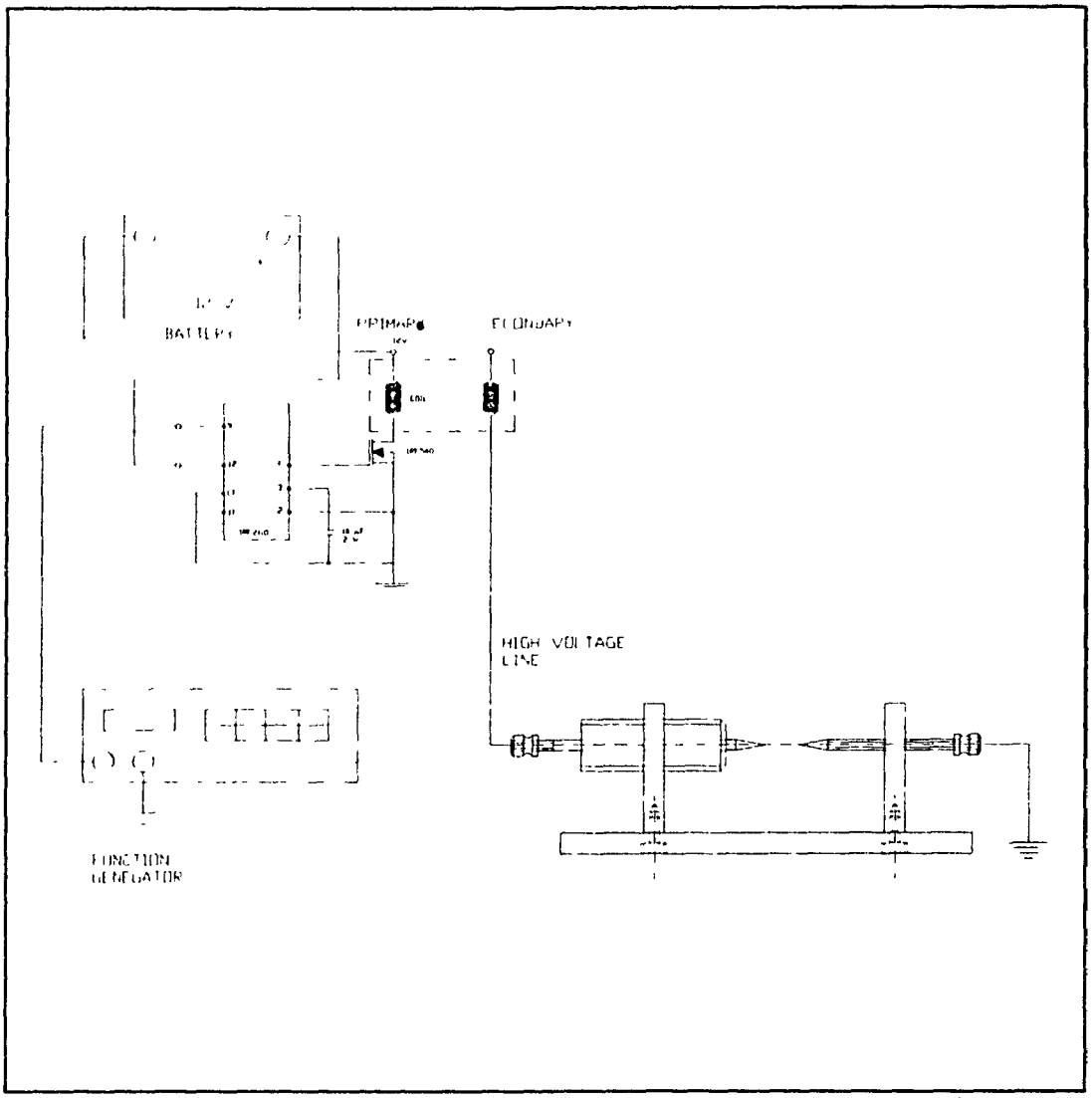

Figure 5.24 Schematic diagram of the apparatus using the MOSFET triggering circuit

The MSD series six multiple spark discharge ignition circuit serves as replacement for the standard ignition system on most american car. This system used with the recommended MSD Blaster coil can produce secondary voltage in excess of 40kV. However, the ignition box can be used, as well with the standard coil or other after-market coils. The key feature here is to use a coil with a primary input impedance as low as possible in order to obtain the best possible performance. Since most cars are using distributor style switching box for generating the proper firing sequence, the MSD system is designed such that it can be incorporated without modification to a standard ignition system. The advantages of using a multiple discharge ignition box can be summarized as follows. The effect of heating up the two electrodes of the spark plug improves the ionization characteristics of the air gap. By the same method, the multiple discharge permits augmentation of the spark plug gap. Therefore, by increasing the spark plug gap, the net area for energy transfer is also increased. Furthermore, by increasing the time for this energy transfer, the total rate of energy transfer to the mixture will be increased by several folds. The problem encountered with this device is that it is difficult to tell at which instance the ignition has occurred in the cylinder and which spark is responsible for the ignition of the mixture. This disadvantage only hinders the ability to pin point the exact moment of ignition. It is disadvantageous only from an experimental point of view.

The MOSFET ignition system is simply a power IRF540 transistor with a resistance drain to source of 0.085 (R_{ds}) [ohm] and a rated voltage and current of 100 volts and 27 amps respectively. The R_{ds} resistance has to be as low as possible so that a minimum of energy is dissipated by the transistor. The voltage rating should be in excess of 100 volts, because of the large back emf that occurs when switching large current. However, for very low primary coil impedance one should allow for a rating voltage higher than 200 volts. For switching this transistor, a chip driver of the type IR2110 is used in this design. This design is shown in Figure 5.22. The IR2110 is a gate driver that accepts a logic input signal of the type TTL and outputs a signal to the transistor gate which has the same potential level as the drain voltage. By complete saturation of the transistor gate, it is possible to operate the device as a switch. The advantage of using such a driver is that it provides an optimal switching characteristic as seen from the load, hence it allows for a minimum energy loss.

5.6.5 Ignition System Tested

The following ignition systems have been tested with the spark comparator.

Ignition System 1
GM Standard Ignition Coil with MOSFET Circuit

This coil produces a secondary voltage of about 30 kV, and has a primary resistance of 2 ohms. Therefore, the primary current which can be expected to be drawn is 6 amps, for a 12 [V] primary supply. The result of the test is shown in the Table 5.2.

Ignition System 2
GM HEI Ignition Coil with MOSFET Circuit

This ignition coil, also manufactured by GM produces a secondary voltage of about 40 kV. This coil's primary resistance, at 0.5 ohms is much lower than the previous. The primary current which can be drawn from the coil for a 12 V source is 24 amps. The results are shown in Table 5.2.

Ignition System 3
GM HEI Ignition Coil with MSD High Energy Ignition System

The MSD high energy ignition system is placed on the primary circuit of the ignition coil in order to increase the primary voltage, which in turn significantly increases the voltage output of the coil secondary. This after-market product can be either adapted to a genuine coil, or used along another after-market low resistance coil. The results are shown in Table 5.2.

Ignition System 4
MSD Blaster 2 Ignition Coil with MSD High Energy Ignition System

This system essentially has the same system configuration as the one previously mentioned, except that an ignition coil with low primary resistance, manufactured by the same company, is being used in place of a GM coil. The results are shown in Table 5.2.

Ignition System 5
MSD Ignition Coil with MOSFET Triggering Circuit

This system uses the LOW primary resistance of the MSD ignition coil and uses the MOSFET transistor for switching. The difference between this system and Ignition System 4, is that only one spark occurs here. The results are shown in Table 5.2.

5.6.6 Test Results

The following results have been obtained from the spark comparator experiments.

Table 5.2 Results obtained from the experiments

Ign. System	Std GM Coil with MOS trig. circuit	GM HEI Coil with MOS trig. circuit	GM HEI with MSD Ignition box	MSD Coil with MSD Ignition box	MSD Coil with MOS trig. circuit
Max Gap [mm]	10.3	12.4	24.8	27.3	22.9
App. Volt [V]	12	12	12	12	12
Coil Pri. Imp. Ohm	2.0	0.5	0.5	0.4	0.4

The above results clearly indicates the superiority of the MSD high energy ignition used with an MSD coil. The quantitative results, as well as the qualitative results in terms of spark intensity, indicates that this system should be used for further testing on the gas engine.

5.6.7 Discussion of the Results and Recommendations

Although only five ignition systems have been tested in this experiment, more tests could be performed on different ignition systems, in order to investigate their possibilities toward gaseous fuel ignition. Higher energy systems in excess of 60 KV could be tested and tried on the prototype. However, high performance systems may not be the most suitable for gaseous fuel ignition, because they may lack reliability and cause a fast wearing of the spark plug. The other concerns include the high price of such systems.

During the ignition testing, one problem encountered was the temperature fluctuation of the coil. This effect leads to an increase in the coil primary resistance. Because of this problem, some time is needed for the coil to reach a steady state temperature. Only then, should the results be recorded. This factor has an effect on the outcome of the results and the repeatability of the experiment. For this reason, performing pre-trials at different frequencies, prior to testing, is suggested before recording any final values.

The system selected for the feasibility experiment is the MOSFET circuit along with the MSD coil. This decision was rendered for the reason that only one spark is produced hence exact position of the sparking can be determined. However, ignition could be more easily obtained from the MSD coil with the MSD ignition box, since the results recorded indicates a better performance that the aforementioned system. This results could

have been well predicted based on the spark ignition theory elaborated in section 5.6.1.

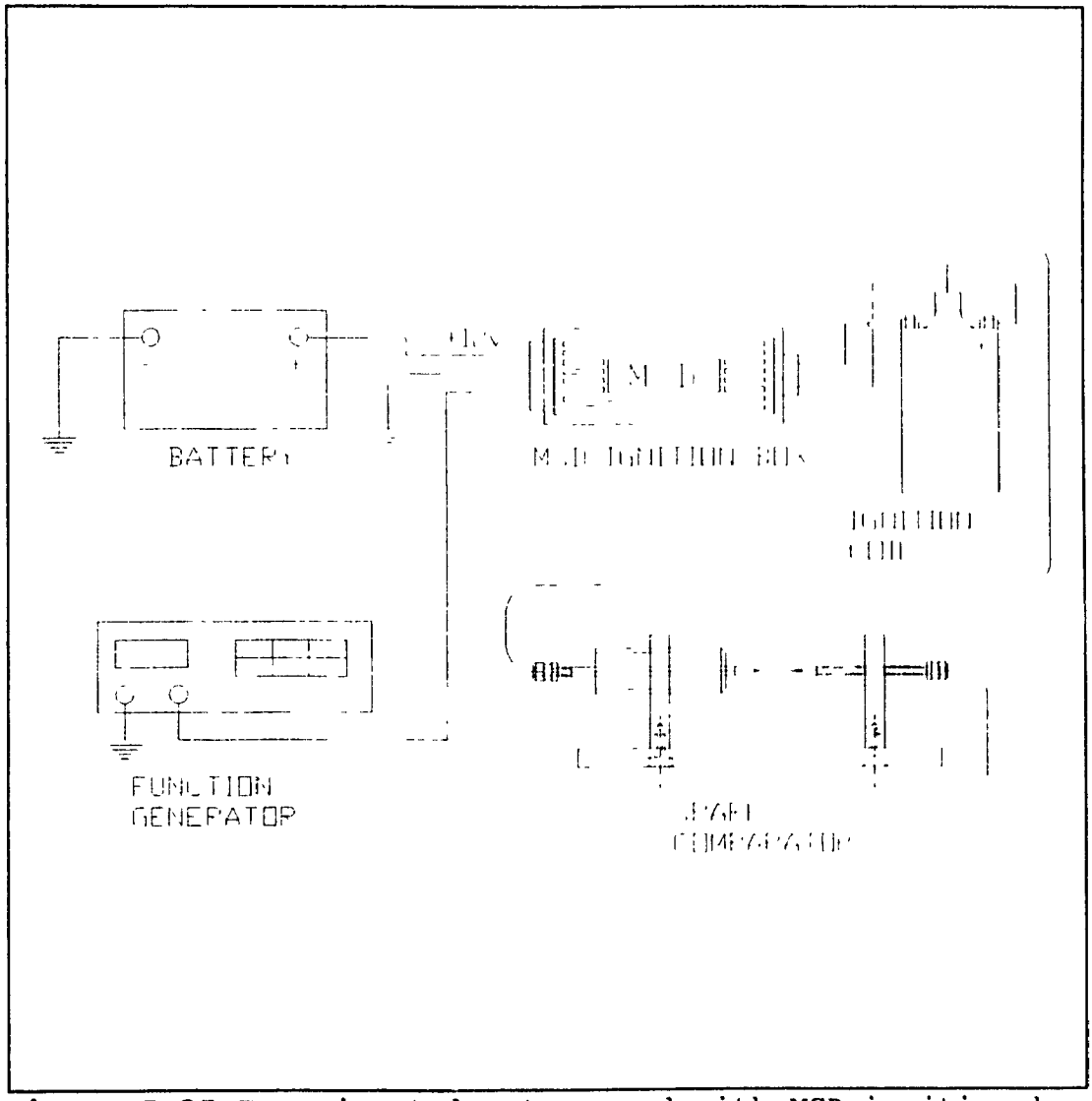

Figure 5.25 Experimental setup used with MSD ignition box

5.7 Software for MCS-96 Controller

For controlling the sequence of operations between the injection, the ignition and the TDC crankshaft position, a 16 bit microcontroller is used on this engine test bed. The MCS-96 microcontroller family offers the flexibility needed for the rapid control of dynamic systems, and also has the capability to rapidly change the operating parameters by modifying the software. The communication with the microcontroller is achieved through the personal computer serial port, which is of the type RS-232, and the host interface port located on the microcontroller. The program is written in assembler language and compiled in the host interface. For the engine test setup an 8088 IBM personal computer is used as the host interface. The ECM-96 interface communication software is utilized for downloading the machine language code into the microcontroller memory. Up to 64K bytes of addressable memory space is available to the user [27].

The key features which prevail a microcontroller over a personal computer (PC) in this kind of operation can be summarized has follows. The microcontroller offers direct access to the microprocessor through the digital I/O port, and the analog input port. The design of a PC is not intended for the external control of dynamic systems. Although it has the capability, it remains a more costly solution. Moreover, a data acquisition card can be used for external communication but is often more expensive than a high end microcontroller.

For this engine an Intel 80C196KB microcontroller evaluation board is used for operating the engine test bed. It features high speed input and output board connection, analog input, external clock, pulse width modulated output and vectored interrupts. For operating the engine test bed, only the high speed I/O port and the vectored interrupts are utilized.

The operation that needs to be performed with the controller is as follows. It is required that the engine undergoes 50 crankshaft revolutions before a sequence of events takes place to ensure that the engine remains cool between every injection. Instead of reading the signal from the crankshaft, the camshaft will be used. Because the camshaft is revolving at half the speed, only twenty five revolutions is then required. The two input signals coming from the optical switch are fed into the microcontroller on pin 22 and 42. Both external pins are used, as external interrupts for the microcontroller. The external interrupts are edge triggered each time that camshaft undergoes a complete turn. Once the counter has reached the count of 25 or 19 hexadecimal (H), the controller outputs a sequence of signals on pin 6, 8 and 10 for triggering the injector and the ignition circuit. Pin 6 and 8 (see Figure 5.26) are responsible for the forward and the reverse signals respectively, while pin 10 is used for controlling the ignition circuit. In summary these are the operational requirements of the software.

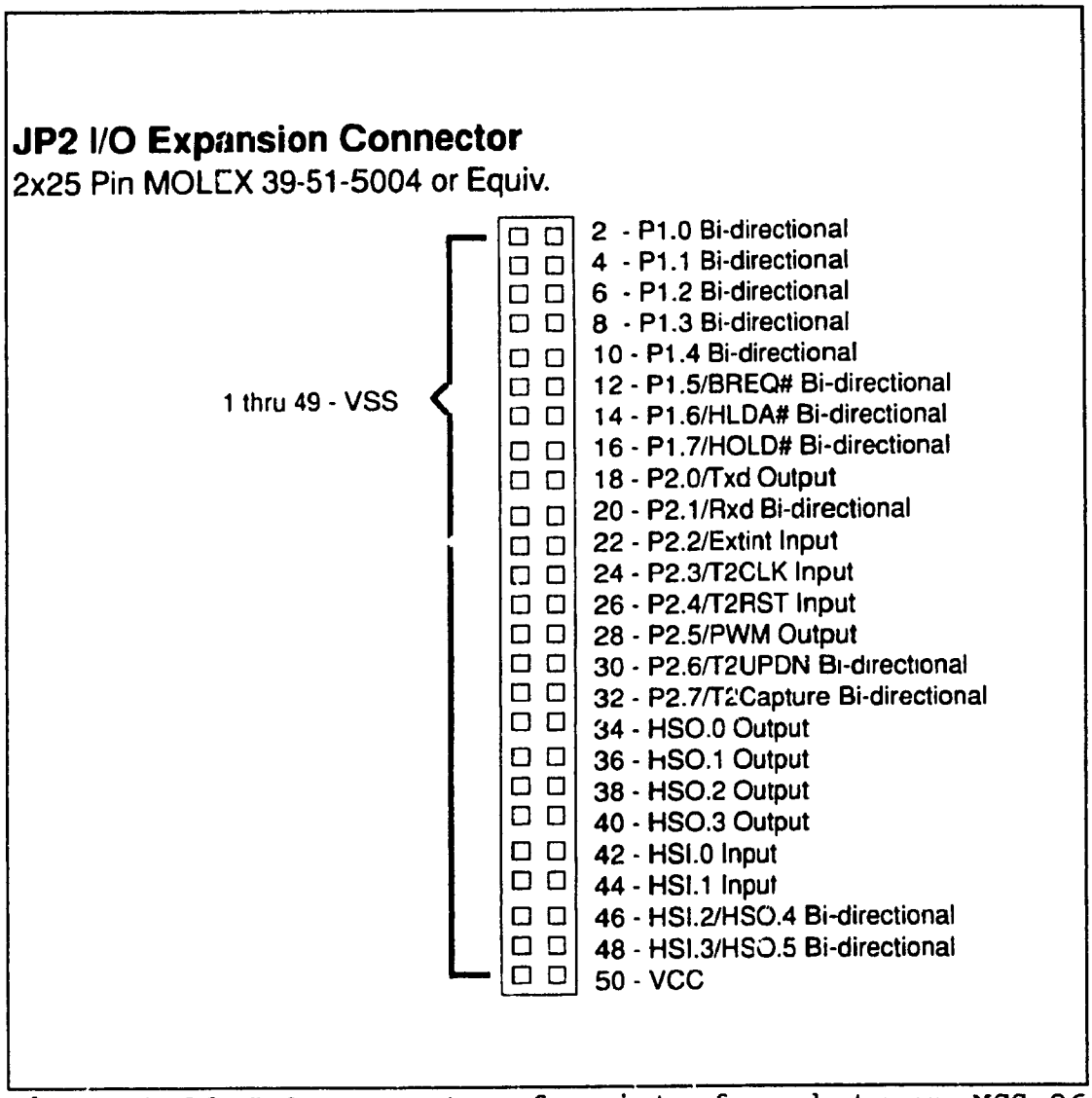

Figure 5.26 JP2 connector for interface between MCS-96 microcontroller and peripheral [28]

The software has been designed as follows. For the reference, the complete software listing is given in Appendix A and a flow chart is available in Figure 5.27. The program core begins at address 2080 and ends at address 2099. The code consists of clearing registers ax, bx, cx, and dx, then loads the stack pointer with #100H and enables the external interrupts. The external interrupts are edge triggered pins that are programmed to cause a counter to increment, for example, *EXTINT_PIN* on line 49 (pin 22 on the board, see 92), or *HSIO_PIN* on line 53 (pin 42 on the board). Also, the I/O port1 (*ioport1*) is loaded with the value 00H so that all output pins are now LOW. Once all variables have been initialized, the instruction *EI* enables the interrupts. Lastly, a loop is placed at the end of the programm core so that it is always waiting until interrupts are generated. This feature ensures that the programm is executed in a loop.

The first interrupt is serviced at address 209B, this subroutine is used to trigger the fuel injector with a forward and a reverse pulse for a set duration. Before the *rev* loop is executed the instruction *PUSHF* ensures that all interrupts are disabled, therefore the subroutines can be executed atomically. Initially, the loop labelled *rev* is counting the camshaft revolution by incrementing the ax register. When ax equals 0018H it branches out of the loop to execute *skipit2*. At that point the value 10H is loaded in *ioport1*. This causes the output pin #10 (10 has no relation to 10H) to go HIGH. This signal allows the

current to flow through the ignition coil.

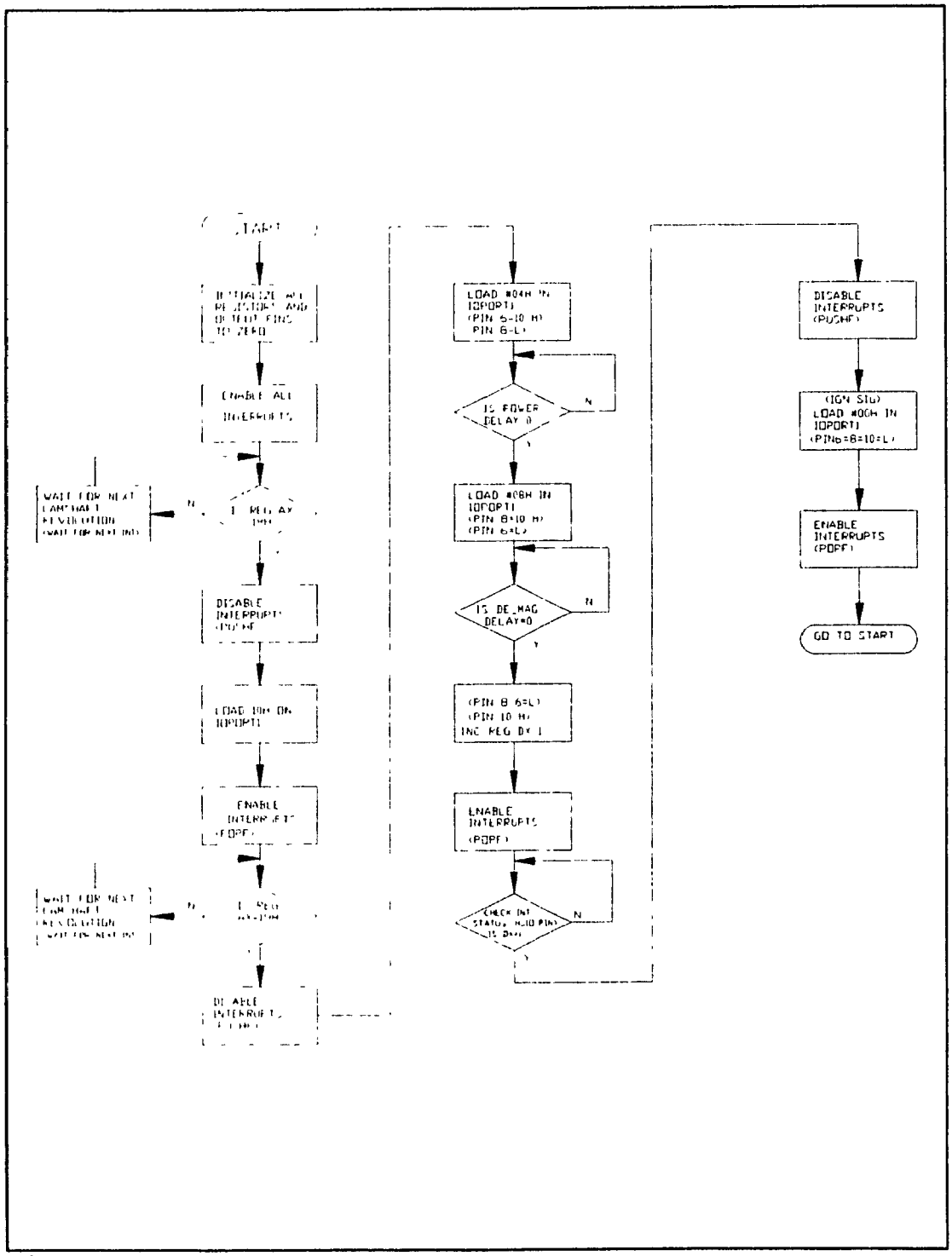

Figure 5.27 Flow chart for ENGINE program

To produce a spark at the spark plug, the current must be cut suddenly so that the collapsing of the magnetic field in the coil primary occurs: this way, a high voltage can be produced in the secondary. When the ax register reaches the value 19H, the *rev* loop continues and goes through the loops labelled *power* (forward signal) and *de_mag* (reverse signal). The loops *power* and *de_mag* represents the ON time duration of each signal (200H represents approximately 1.2 [msec]). Under all other conditions, where ax is between 0 to 17H, it branches to *skipit* which re-enables the interrupt by the instruction *POPF* and returns to the program core. At that point it waits for another positive edge from the *EXTINT_PIN* to increment register ax. The signalling duration for the forward and reverse pulse signals are on lines 59 and 60 of the program listing.

To obtain a spark, the *HSI0_pin* (which is acting as an interrupt) sends a count to address 20D3 to verify the content of register dx. If dx is equal to 0001H, then the program can proceed with the ignition, otherwise it branches to *skipit1*, which re-enables the interrupt, and will wait for the next count and verify it again. The ignition occurs at the spark plug when pin 10 goes LOW. This is caused by loading *ioport1* with the number #00H, which brings all the pins back to a LOW.

This software design implies that both, the power pulse as well as the damaged pulse have to be executed before the ignition can occur. The code is designed such that register dx has to be incremented to 1 before the ignition sequence can happen. The increment of register dx is done during the *power* and *demagt* interrupt service routine. However, this time delay is less than 2.0 [msec] if the *power* and *demagt* is no more than 300H. To facilitate the understanding of this program, a flow chart is supplied in Figure 5.28.

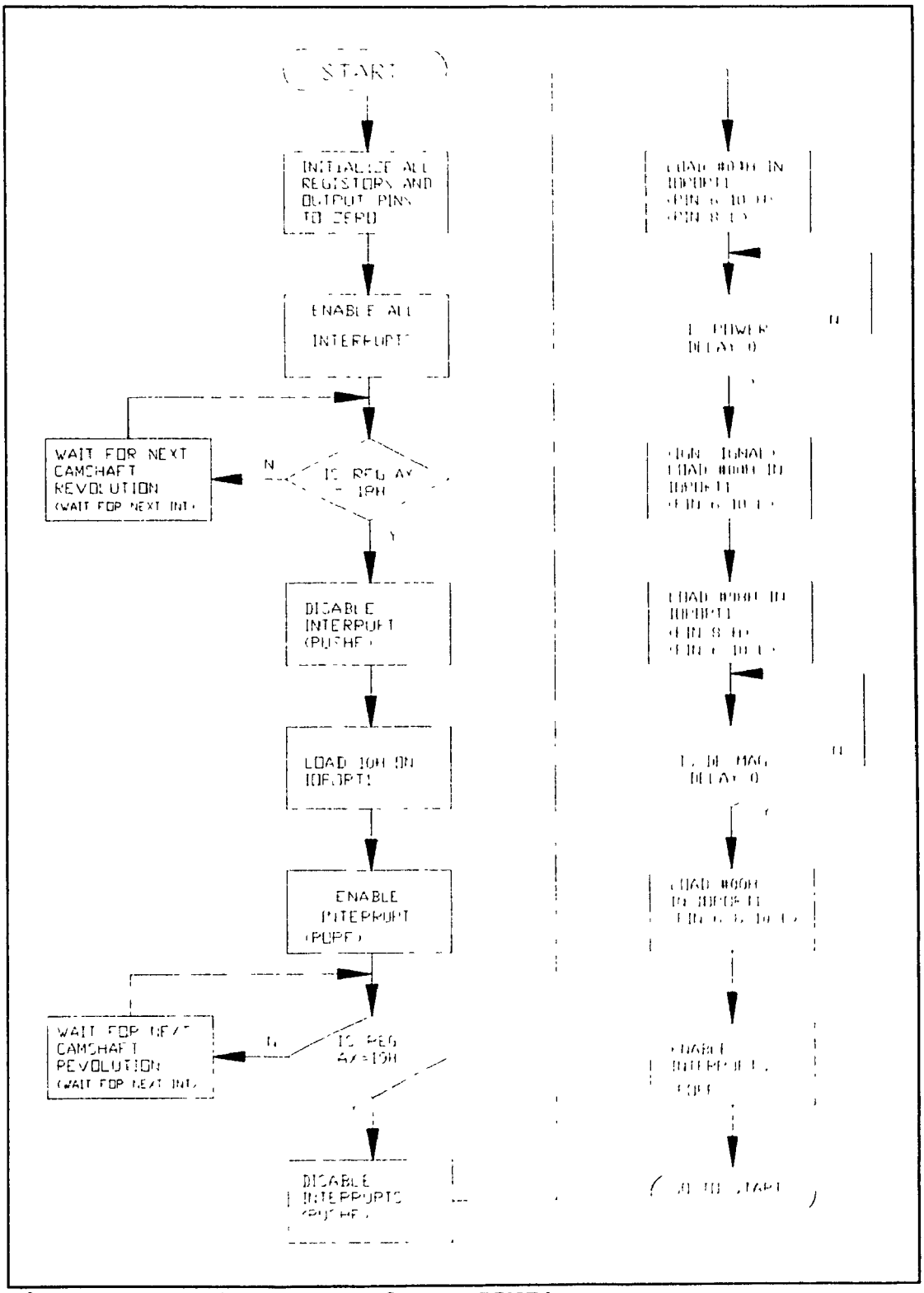

Figure 5.28 Flow chart for ENGINE1 program

CHAPTER 6

6.0 PRELIMINARY ENGINE IGNITION TESTS

The objectives of this experiment is to ignite a fuel dose delivered by a high pressure gas injector and to find the mechanism which causes ignition. The previous chapters discussed the Gas Ignition Concepts (chapter 3), the Methodology (chapter 4) of experimentation, and the Test Setup for Ignition Investigation (chapter 5). After performing the experiment, the following results have been obtained from the ignition tests.

For clarity certain details should be addressed before discussing the experimental results. Firstly, since all the engine tests are performed at 300 [rpm], the injection advance as well as the spark advance are listed in units of time i.e. [msec], instead of degrees. This is to facilitate the cross referencing between the results table and the oscillogram for the reader. Also, to indicate the position of the injector against the ignition chamber inter-passage, Table 6.1 shows the distances for the different spacer used. To better visualize that distance, see Appendix C and Figure 6.1.

Table 6.1 Injector Position

Injector Position	**Equivalent Distance L [mm]** (Refer to App. C)
1	0.50
2	2.0
3	3.5
4	5.0
5	8.0
6	12.0
7	15.0

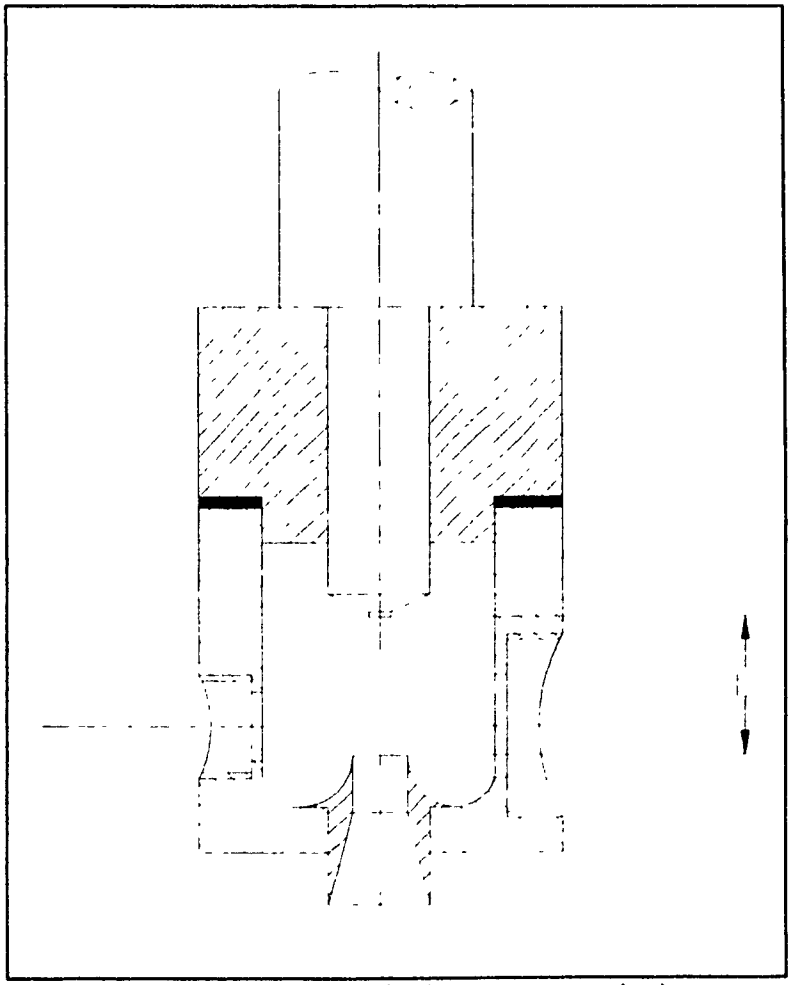

Figure 6.1 Various injector position

Before starting the testing, initial parameters had to be selected namely, the injection advance, the spark advance and the injector position. As a starting point, the injector has been set to the farthest position no.6, the injection advance to 3.3 [msec] BTDC and the spark advance to TDC. The TDC spark advance position has been chosen, because at that point, the temperature and pressure is at its highest in the cylinder. Therefore, it is offering a more favourable condition for ignition. Concerning the ignition system, because of the high compression ratio of this engine, the MSD multi-spark ignition system has been preferred for the preliminary tests over the MOSFET single spark system. However, after obtaining satisfactory results, the MSD system would by replaced with the MOSFET single spark system.

The initial sets of tests have been performed with the spark signal at TDC, and the only two parameters varied have been the injection advance and the injector position. For one injection advance setting the injector was moved from its highest position to its lowest. After being unsuccessful in obtaining ignition at a broad range of positions, it was decided that the fuel dose should be reduced. To achieve the dose reduction in a simple way, the bottle pressure was reduced from 70 [bar] to 55 [bar]. During the trial no.41 (see Table 6.2b), with the injector at position number 2 and an injection advance of 2.0 [msec], ignition occurred.

Table 6.2a Initial ignition test results

Trial	Ign Adv	Inj Pos	Inj Adv [msec]	Inj Dur [msec]	Ign	Plot No.
Bottle pressure 70 [bar]						
1	TDC	7	3.3	6.0	No	
2	TDC	6	3.3	6.0	No	
3	TDC	5	3.3	6.0	No	
4	TDC	4	3.3	6.0	No	
5	TDC	3	3.3	6.0	No	
6	TDC	2	3.3	6.0	No	
7	TDC	1	3.3	6.0	No	
8	TDC	7	5.5	6.0	No	
9	TDC	6	5.5	6.0	No	
10	TDC	5	5.5	6.0	No	
11	TDC	4	5.5	6.0	No	
12	TDC	3	5.5	6.0	No	
13	TDC	2	5.5	6.0	No	
14	TDC	1	5.5	6.0	No	
15	TDC	7	5.5	6.0	No	
16	TDC	6	5.5	6.0	No	
17	TDC	7	2.4	6.0	No	
18	TDC	6	2.4	6.0	No	
19	TDC	6	1.5	6.0	No	
20	TDC	3	1.5	6.0	No	
21	TDC	3	2.5	6.0	No	
22	TDC	3	5.5	6.0	No	

Table 6.2b Initial ignition test results

Trial	Ign Adv	Inj Pos	Inj Adv [msec]	Inj Dur [msec]	Ign	Plot No.
Bottle pressure 70 [bar]						
23	TDC	7	2.0	6.0	No	
24	TDC	7	6.0	6.0	No	
25	TDC	7	4.0	6.0	No	
26	TDC	6	4.0	6.0	No	
27	TDC	6	2.0	6.0	No	
28	TDC	6	6.0	6.0	No	
29	TDC	1	6.0	6.0	No	
30	TDC	1	4.0	6.0	No	
31	TDC	1	2.0	6.0	No	
32	TDC	1	2.0	6.0	No	
33	TDC	1	4.0	6.0	No	
34	TDC	1	6.0	6.0	No	
35	TDC	2	6.0	6.0	No	
36	TDC	2	4.0	6.0	No	
37	TDC	2	2.0	6.0	No	
Bottle pressure 55 [bar]						
38	TDC	2	2.0	6.0	Yes	1a & 1b
39	TDC	2	4.0	6.0	Yes	N.R.*
40	TDC	2	6.0	6.0	No	
41	TDC	1	2.0	6.0	Yes	2a & 2b
42	TDC	1	4.0	6.0	No	
43	TDC	1	6.0	6.0	No	
44	TDC	1	1.5	6.0	Yes	3a & 3b

* Result not recorded

Table 6.2c Initial ignition test results

Trial	Ign Adv	Inj Pos	Inj Adv [msec]	Inj Dur [msec]	Ign	Plot No.
Bottle pressure 55 [bar]						
45	TDC	7	1.5	6.0	No	
46	TDC	6	1.5	6.0	No	
47	TDC	5	1.5	6.0	No	
48	TDC	4	1.5	6.0	Yes	4a & 4b
49	TDC	3	1.5	6.0	No	5a & 5b
Bottle pressure 50 [bar]						
50	TDC	7	1.5	6.0	No	
51	TDC	6	1.5	6.0	No	
52	TDC	5	1.5	6.0	Yes	6a & 6b
53	TDC	4	1.5	6.0	Yes	7a & 7b
Bottle pressure 40 [bar]						
54	TDC	7	1.5	6.0	Yes	8a & 8b
55	TDC	6	1.5	6.0	No	
56	TDC	5	1.5	6.0	No	
Bottle pressure 70 [bar]						
57	TDC	7	1.5	7.0	Yes	9
58	TDC	6	1.5	7.0	Yes	10
59	TDC	5	1.5	7.0	Yes	11
60	TDC	4	1.5	7.0	Yes	12 & 13
61	TDC	3	1.5	7.0	Yes	14
62	TDC	2	1.5	7.0	No	
63	TDC	1	1.5	7.0	No	
64	6.4 ATDC	5	1.5	6.0	Yes	15
65	3.8 ATDC	5	1.5	6.0	Yes	16
66	1.2 ATDC	5	1.5	6.0	Yes	17
67	TDC	5	1.5	6.0	Yes	18
68	2.0 BTDC	5	6.0	6.0	Yes	19

In order to assert that the higher initial fuel dose was the cause for not obtaining the ignition, more tests have been carried starting from trial no.52 (see Table 6.2c), with further reduction of gas pressure from the bottle, and also, with further increase of the injector distance. At that time it was decided to reduce the injector nozzle orifice size to decrease the fuel flow rate, and consequently, the fuel dose being injected.

Beginning at trial no.60 (see Table 6.2c), with an injector orifice of 0.7 [mm] diameter, a bottle pressure of 70 [bar], ignition has been recorded. To confirm that a fuel dose reduction was appropriate with an injection advance of 1.5 [msec], the injector position was varied from its highest to its lowest position.

Another task performed early in the experiment, was to check if the spark plug orientation was linked to the lack of ignition. Figure 6.2 shows the two different spark plug orientations used during the tests. For trials no.1 to 14 (see Table 6.2a), the orientation of Figure 6.2,top was used, and during trials no.15 to 31, orientation of Figure 6.2,bottom was used.

For the last few trials namely, no.69 to 73 (see Table 6.2c), it was decided to replace the MSD ignition system with the MOSFET single spark circuit. This modification was necessary to locate the exact timing of ignition. Furthermore, to verify that the spark was in fact responsible for the ignition, the spark plug was disconnected. Indeed, no ignition occurred. This

confirmed that the ignition was the result of the presence of a spark, and not auto-ignition because of the high gas temperature that exists near TDC.

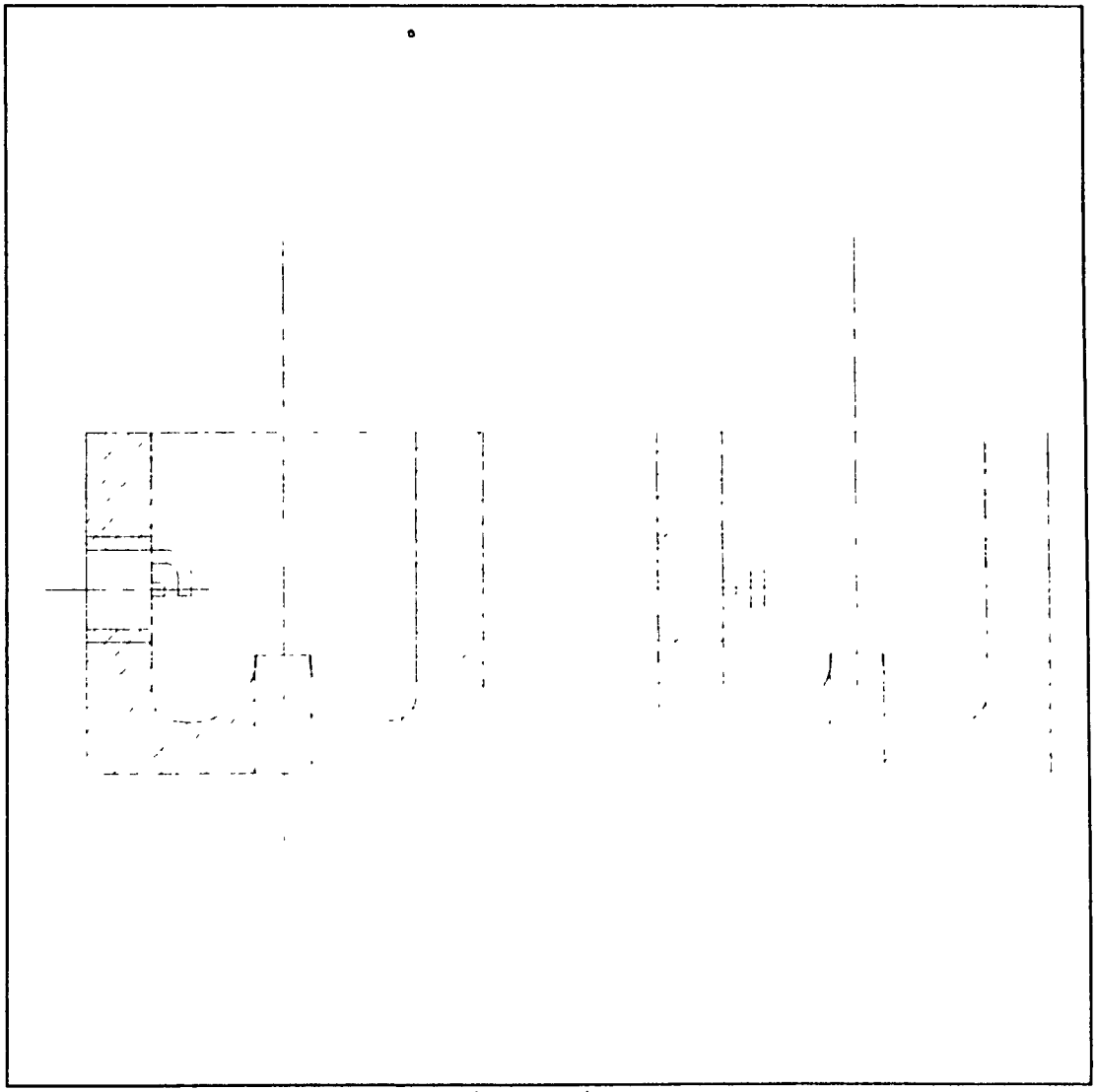

Figure 6.2 Spark plug orientation

6.1 Test Results and Discussion

The objective of this experiment, to achieve the ignition of a charge of methane, has been successfully attained. However, the optimization of the ignition chamber prototype would require some further work. During the initial phase of the testing, several problems had to be solved in order to have the test rig performing as needed. Problems dealing from electromagnetic interference to the selection of the proper injector, circuit design and equipment for testing the ignition chamber prototype had to be addressed.

Concerning electromagnetic interference, two measures had to be taken to eliminate it. First, the replacement of the standard spark plug with an R type plug from NGK did help to suppress the interference. The R spark plug is especially designed to suppress electromagnetic disturbances generated from high voltage ignition systems. Secondly, shielding of all wires carrying a signal to the microprocessor and insuring that all the equipment is properly connected to a common ground, did eliminate the interference.

During the evaluation of the amplification circuits, a constant gas leak along the gas injector solenoid wire necessitated the modification of the solenoid housing. The redesigning of the solenoid housing consisted of installing two terminals imbedded in an insulation material. The terminal ends allowed to hold the wires in place with screws.

After properly sealing the gas injector, the testing

of the H-bridge circuit revealed that the circuit was unable to open the gas injector at pressures above 55 [bar]. After extensive testing of the H-bridge circuit and not being able to operate the injector at pressures above 70 [bar], it was decided to switch to the boost circuit configuration. The initial testing of the boost circuit showed very good results. From the first tests, the injector was operated successfully at 70 [bar]. It was possible to operate the gas injector at pressures up to 83 [bar], and obtain reliable gas injection.

While completing the assembly of the engine test rig, a question arised concerning the capability of the spark ignition to properly operate in a diesel engine, because of the high compression ratio. To solve this problem, a spark comparator has been used to determine the efficiency of each spark ignition system. The results obtained from this experiment showed that the multi-spark MSD coil and triggering system was more suitable for the engine test setup. The MSD system has been used only for the initial engine testing since it offered the most energetic sparks. However, in spite of this advantage, it was difficult to indicate the exact moment where ignition has occurred. It was then decided that for a lost part of the experiments the MSD coil with the MOSFET single spark ignition system would be used. The reason was that a single spark system shows precisely the timing whereas, a multispark system does not offer this possibility (see Figure 6.3 and Figure 6.4).

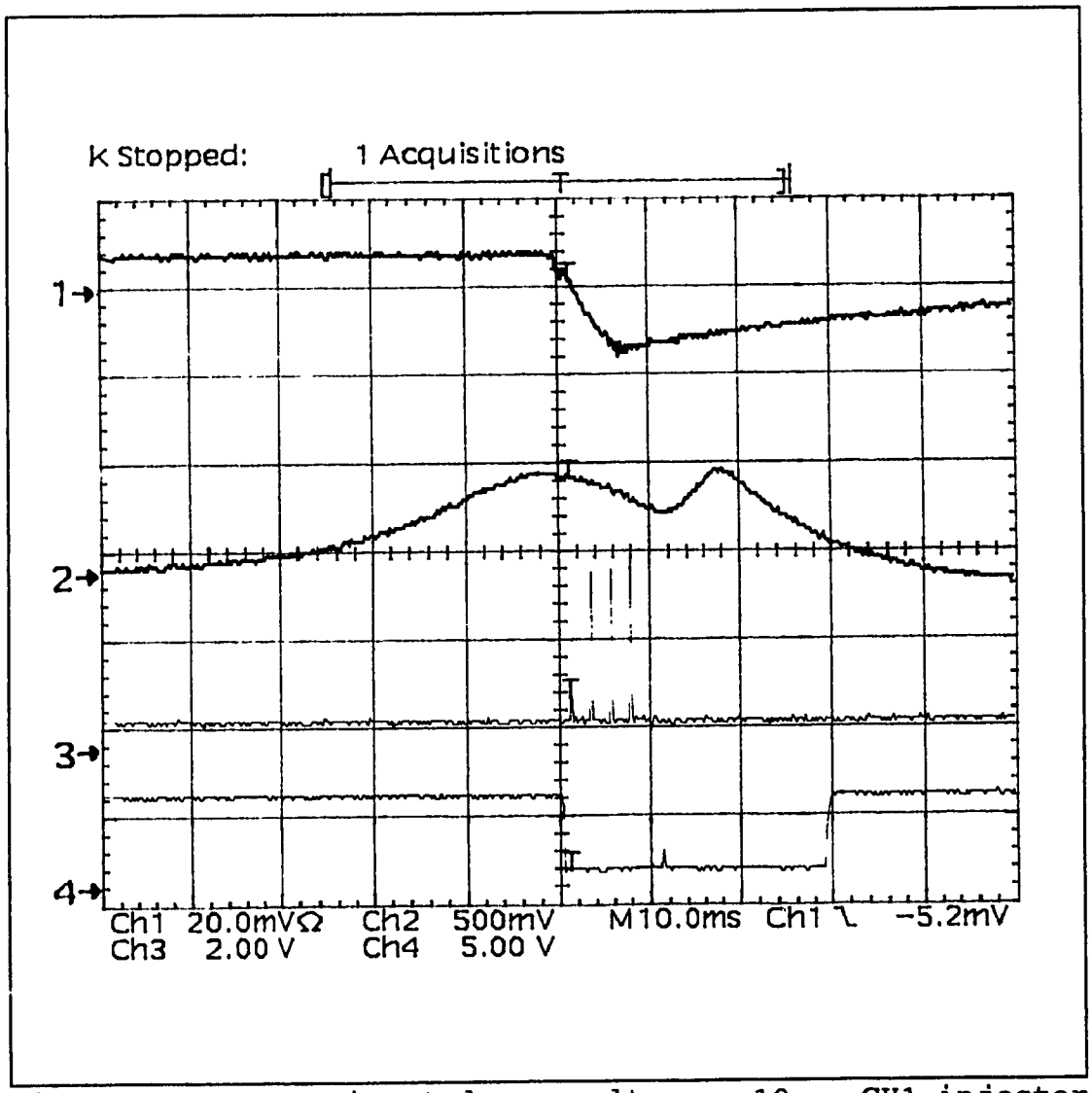

Figure 6.3 Experimental result no.10, CH1-injector pressure, CH2-ignition chamber pressure, CH3-spark plug current, CH4-TDC on falling edge

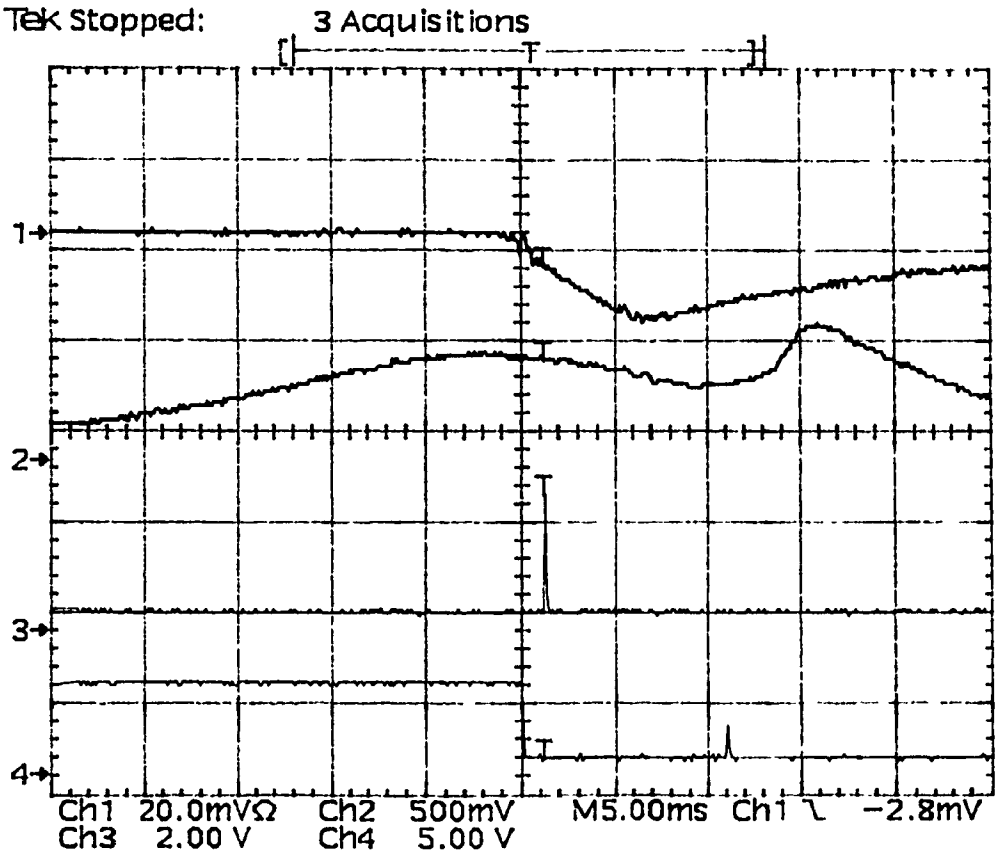

Figure 6.4 Experimental result no.17

After completing the preparation of the engine test setup and drafting the testing schedule, the engine was ready for testing of the ignition chamber prototype. The initial conditions have been determined to be; the spark advance set at TDC and the injection advance set to 3.3 [msec], with the only parameter changed being the injector position.

The injector has been positioned from the highest position (position no.7) and moved down to reduce the amount of fuel distributed to the ignition chamber. At this point, no ignition has been recorded. In spite of the fact that the quantity of fuel remaining in the ignition chamber has been varied by changing the injector spacer, it was no ignition upon sparking. To obtain ignition, the injection advance has been varied to increase or decrease the mass of fuel present in the ignition chamber upon sparking. In other words, the sparking signal was kept at the TDC position, and the injection advance was varied as it can be seen from table 6.1a and 6.1b (tests no.15 to 37).

After exhausting all the possibilities, it was decided to reduce the fuel flow rate by decreasing the bottle pressure. This was to further decrease the fuel amount present in the ignition chamber upon sparking. On trial no.38 in table 6.1b, the ignition was recorded with the injector at position no.2. Therefore, the direction to take was to reduce the fuel flow rate. Note, that the injector was almost at its lowest position (position no.2) and the spark was produced at the beginning of

injection. For the same injector position, however, with the spark at the end of injection, no ignition was recorded. Therefore it seemed logical to further reduce the fuel flow rate.

Starting at test 50, the bottle pressure was further reduced to 50 [bar], with the injector distance increased. With the injection advance at 1.5 [msec], a bottle pressure at 41.8 [bar] and the injector position no.7 on trial no.54, ignition was obtained again. This confirmed that the fuel mass flow rate should be reduced.

To reduce the injector flow rate, the injector nozzle orifice was decreased from the 1 [mm] diameter, as calculated in section 5.3.1, to 0.7 [mm] diameter. This modification should allow to operate the gas injector at pressure above 70 [bar]. The other modification performed on the injector nozzle was to change the orifice geometry. The nozzle geometry was changed from a diverging nozzle to a cylindrical hole. This was to allow more gas expansion to take place outside the injector orifice, thus increasing the jet cone angle. However, the impact of this modification will require further explanation.

On trial no.57, the bottle pressure was raised back to 69 [bar], and ignition was successfully obtained with the injector placed at position no.7 and the injector advance set at 1.5 [msec] (see Figure 6.5). The injector position was set closer, keeping the other parameters fixed (see Figure 6.3). Ignition was obtained for all the position numbers, except at injector position no.2.

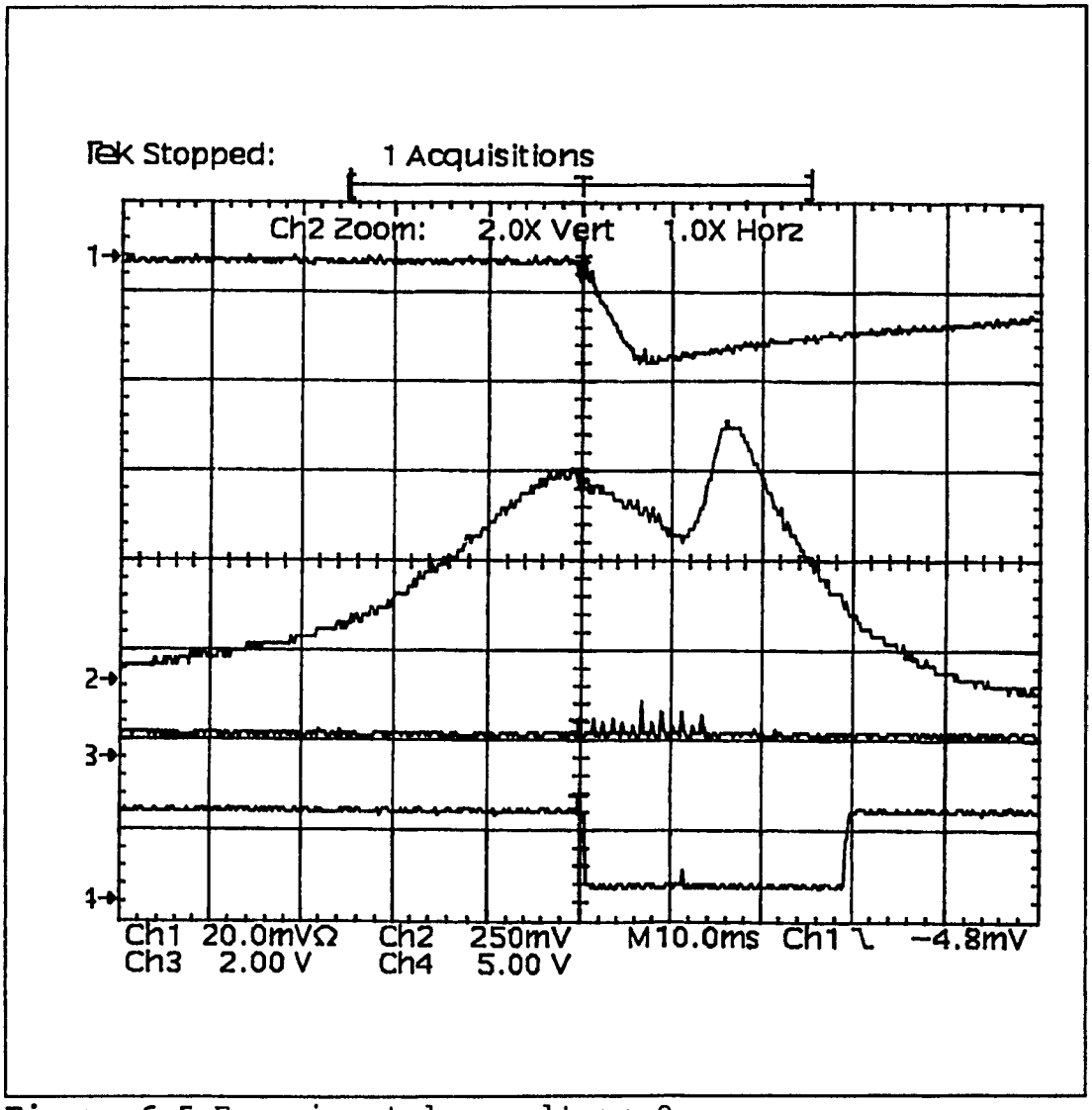

Figure 6.5 Experimental result no.9

At this stage of the experiment, consistent ignition was obtained, with the best result at position no.5 with an spark advance of 1.5 [msec], and ignition signal at TDC. However, one question arises from the fact that a long time delay between the spark occurrence in the ignition chamber, and an increase in pressure is recorded in the cylinder. This can be observed in Figure 6.4, where the time delay measured on the graph is approximately 10 [msec]. To reduce this delay, it was decided to change the position of the spark advance to 4.0 [msec] after TDC and see if the time delay would increase or decrease. With the spark at 2 or 4 [msec] after TDC, the time delay did not change significantly. On the other hand, when the injection was completed before TDC and sparking occurred just before TDC a significant reduction in time delay was observed. Figure 6.6 shows this result with the injection beginning 6 [msec] before TDC and the spark signal sent 2 [msec] before TDC; the ignition delay for this case was about 6 to 7 [msec].

The long ignition delay recorded on the oscillogram, and the unclear mixing mechanism in the ignition chamber required more, in depth, investigations. A better understanding of the flow process taking place inside the ignition chamber would provide the necessary tools for optimizing the new pre-ignition chamber prototype. To achieve this, the schlieren visualization method was used.

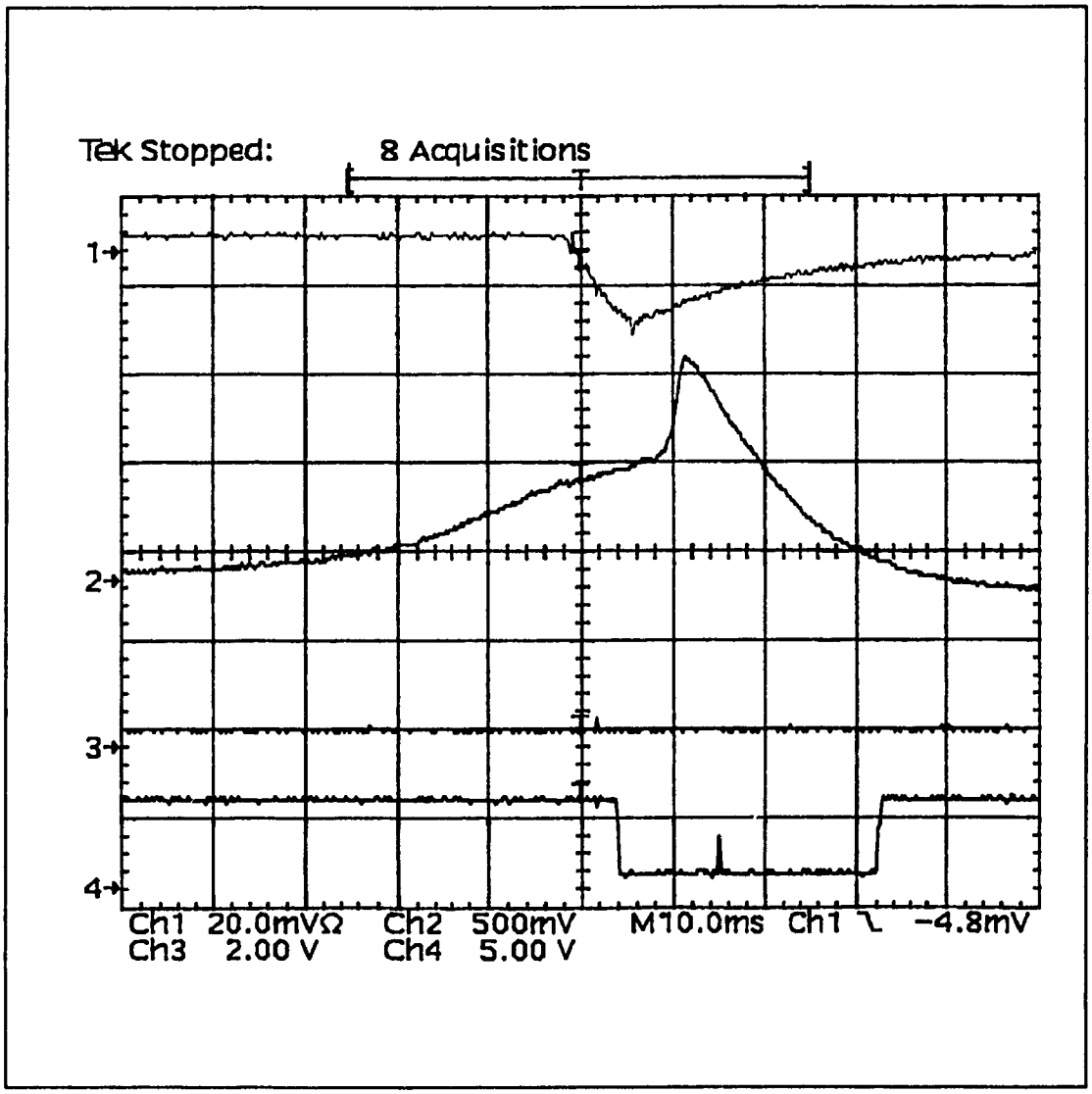

Figure 6.6 Experimental result no.19

CHAPTER 7

7.0 VISUALIZATION OF THE GAS FLOW PATH USING SCHLIEREN PHOTOGRAPHY

The results obtained in chapter 6 suggested that a better understanding of the gas flow mechanism inside the ignition chamber is necessary, prior to further ignition testing. Several gas flow visualization methods are available such as shadowgraph and schlieren photography. Because of the availability of the equipment, schlieren photography is used. The advantage of schlieren photography is that the equipment required, as well as the skill needed for building the experimental setup, was available.

Schlieren photography helps in understanding the ignition process taking place in the ignition chamber because the gas flow path can be made visible with this method. To simplify the test setup, it was decided that the visualization of the gas flow in the chamber will be performed on a chamber model dedicated for the schlieren photography use, instead of mounting all the schlieren apparatus around the engine and modifying the existing ignition chamber by installing quartz windows; this would be very difficult on such a small chamber and the relocation of the spark plug and the pressure transducer would make it even more difficult. To overcome this problem, an ignition chamber model which had the same dimensions as the original chamber was mounted in a special pressurized chamber, where large quartz windows were installed on either side of the

chamber to allow the light to pass through the test section.

7.1 Experimental Apparatus

Schlieren photography is a method which consists of capturing on film a gas or a liquid flow path that occurs in a time span no less than 0.1 [msec]. Its limiting variable is the spark duration, which is of the order of 1 [μsec]. For a good and clear picture, the duration of the event should not be less than the time limitation aforementioned. Additional explanation on the theory surrounding schlieren photography is provided in section 7.5.

As previously mentioned in section 7.0, the ignition chamber flow visualisation will not be performed on the test engine itself but rather on a special model of the chamber installed in a pressure chamber. The schlieren photography method requires passing a straight column of parallel light through a test section. To achieve this, the test section will be placed between two concave mirrors where the light is allowed to penetrate the test section via the quartz windows placed on both sides of the pressure vessel (see Figure 7.1 and Figure 7.2). The schlieren setup shown in Figure 7.1 is referred to as the Z configuration. The light leaves the point source to reach the first mirror, then passes through the test section to reach the second mirror then goes through the knife edge and finally reaches the photographic plate. This passage forms the letter Z, hence term the Z configuration. Other configurations

are also available, however, this configuration is most often used for flow visualisation.

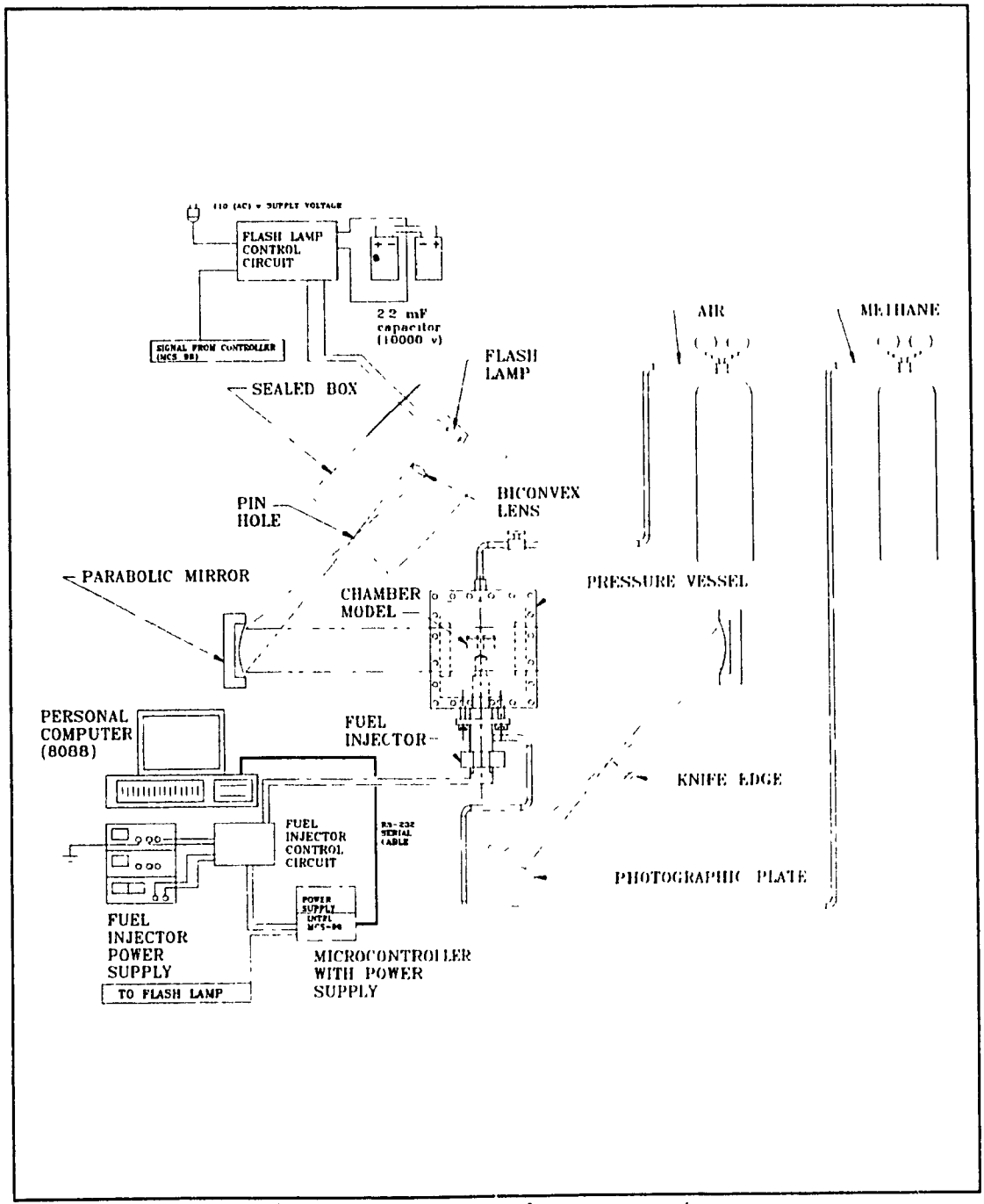

Figure 7.1 Schlieren photography apparatus

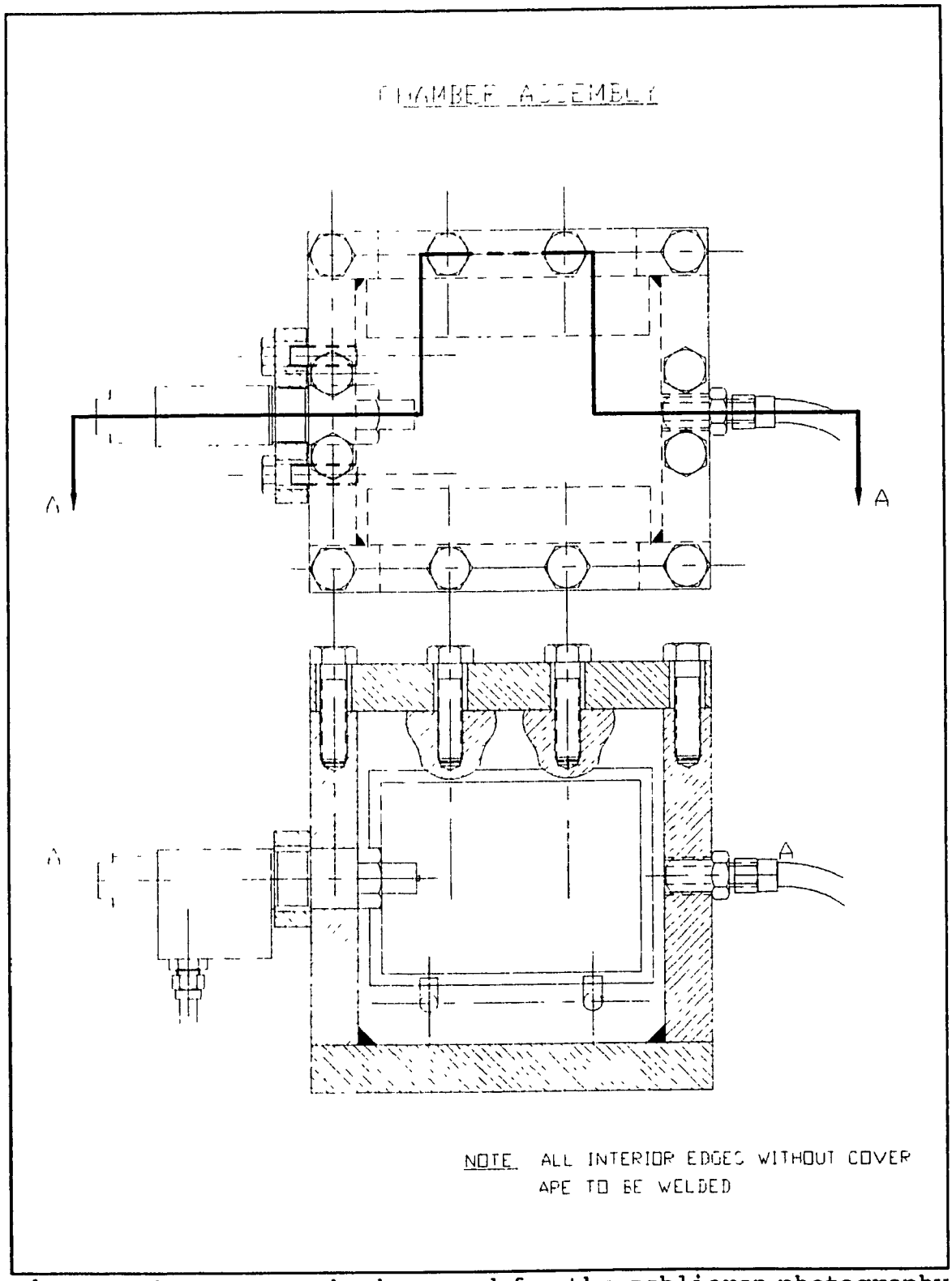

Figure 7.2 Pressure chamber used for the schlieren photography experiment

The purpose of each component in a schlieren setup can be summarized as follows. The flash lamp is used to generate the amount of light required to expose the test section. A 1000 volts power supply provides the necessary energy to produce a spark, from the flash lamp. The energy available for sparking can be controlled by varying the size of the capacitors placed before the flash lamp. The triggering unit for the flash lamp is also incorporated in the power supply. The only other connection to the power block is the external signal, to cause the lamp to flash. A standard TTL signal is required to trigger the flash lamp. The TTL signal is provided by an Intel MCS-96 microcontroller. The same controller also provides the triggering signal to the fuel injector.

Once a spark has occurred, part of the light is passed through the first of two lenses which is used to focus the light on a pin hole. The location of the pin hole is at the focal point. The size of the pin hole is determine by the object which is being observed. In general, the pin hole should be ten times smaller than the object which we want to focus on, at the test section. In the present situation, the fuel injector nozzle orifice being less than 1 [mm] diameter suggests a pin hole of 0.1 [mm] diameter. Practically speaking, a pin hole diameter of this size is too small, since it would require a very large amount of light to be produced by the flash lamp. To find a compromise, several hole sizes will be tried on the setup until satisfactory results are achieved. The flash lamp as well as the

pin hole and the lens are enclosed in a sealed box so that no light can escape from the box.

The light leaving the pinhole diverges into a parabolic mirror with a focal length of 1.21 [m]. This highly polished silver plated mirror sends a beam of parallel light through the test section enclosed in a pressure vessel. The light is then received by another parabolic mirror with the same focal length. The converging light cone is focused on a knife edge placed at the second mirror focal length. The knife edge is used to control the light intensity. It is controlled with micrometric screws placed perpendicularly, so that the position in the x and y axis can be accurately set. The intensity of light sent to the photographic plate can be controlled by two means namely, the capacitor size in the flash lamp power supply and the position of the knife edge. Once the right contrast is achieved, the light beam is diverging to the photographic plate. There is no need to have a lens on the camera because the focusing used with this method is achieved with a pin hole and a proper positioning of the knife edge. Since flashing of the light occurs in approximately 1 [μsec], a highly sensitive film, a 3000 ASA Polaroid film is used. It is important to emphasize here that the setup is operated in pitch dark room and the light source is triggered by the microprocessor.

7.2 Design of a High Pressure Vessel with Quartz Windows

This pressure vessel has been developed to simulate the pressure effects after the air compression in a diesel engine (see Figure 7.3). In the present case, the maximum pressure recorded in the modified engine, without ignition, has been 28.2 [bar]. This maximum pressure has been measured with the piezo-electric pressure transducer located in the ignition chamber.

An important consideration of this design was the wall rigidity. With this consideration, the deflection of the pressure chamber wall where the quartz windows are located, have been designed for a minimal deflection. If a large deflection of the wall would be allowed, the windows could possibly crack because of stresses produced in the quartz blocks. The windows thickness is 25 [mm] and they are made of top grade quartz. The quality of the quartz windows is of paramount importance because they can cause a substantial deformation of the image observed at the test section.

In order to access the ignition chamber model, the top plate of the pressure chamber was made removable. It is screwed into place with 12 3/8 NC bolts. To ensure proper sealing between the cover and the chamber, a copper gasket is used on this design.

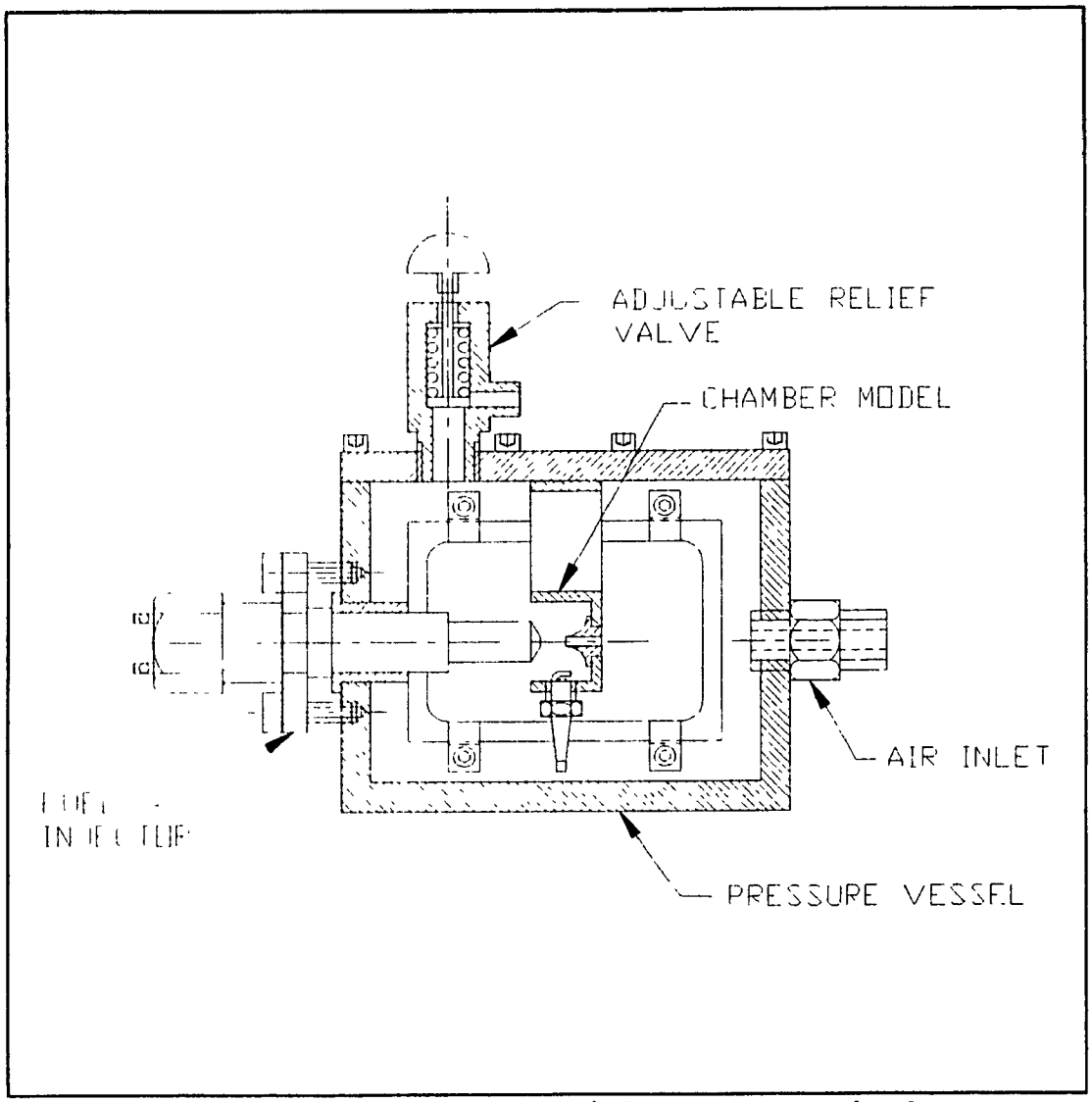

Figure 7.3 Relief valve used with pressure chamber

The ignition chamber model (shown in Figure 7.5) is bolted onto the cover plate of the pressure chamber. Because it is not possible to vary the injector position in the chamber, the model is able to move back and forth via slotted holes, which are also used to attach the model to the cover plate.

For security reasons, a pressure relief valve has been installed on the cover plate as well, and it has been set to break open at 28.2 [bar] (see Figure 7.3). This feature is necessary in case when the injector may remain in the open position or in the worst case, when the ignition of the fuel dose would occur; however, the later possibility is very unlikely. Furthermore, the pressure chamber is grounded. Note that this pressure chamber simulates only the impact of pressure in the engine chamber; the temperature remains at room conditions. An actual picture of the pressurized chamber, before modifications, is shown in Figure 7.4.

The other flow component not simulated with this apparatus, is the reverse flow, where upon compression, some air is flowing from the main chamber into the ignition chamber. It has been determined, by measuring the pressure in both chambers that the reverse flow is minimal at TDC piston position and may be discarded in order to simplify the apparatus. The important goal to be achieved with this chamber is to gain some knowledge about the flow path inside the ignition chamber, as well as, the conditions modifying the fuel jet shape after leaving the injector. Nonetheless, this setup may be used as a first

strategy for optimizing the ignition chamber.

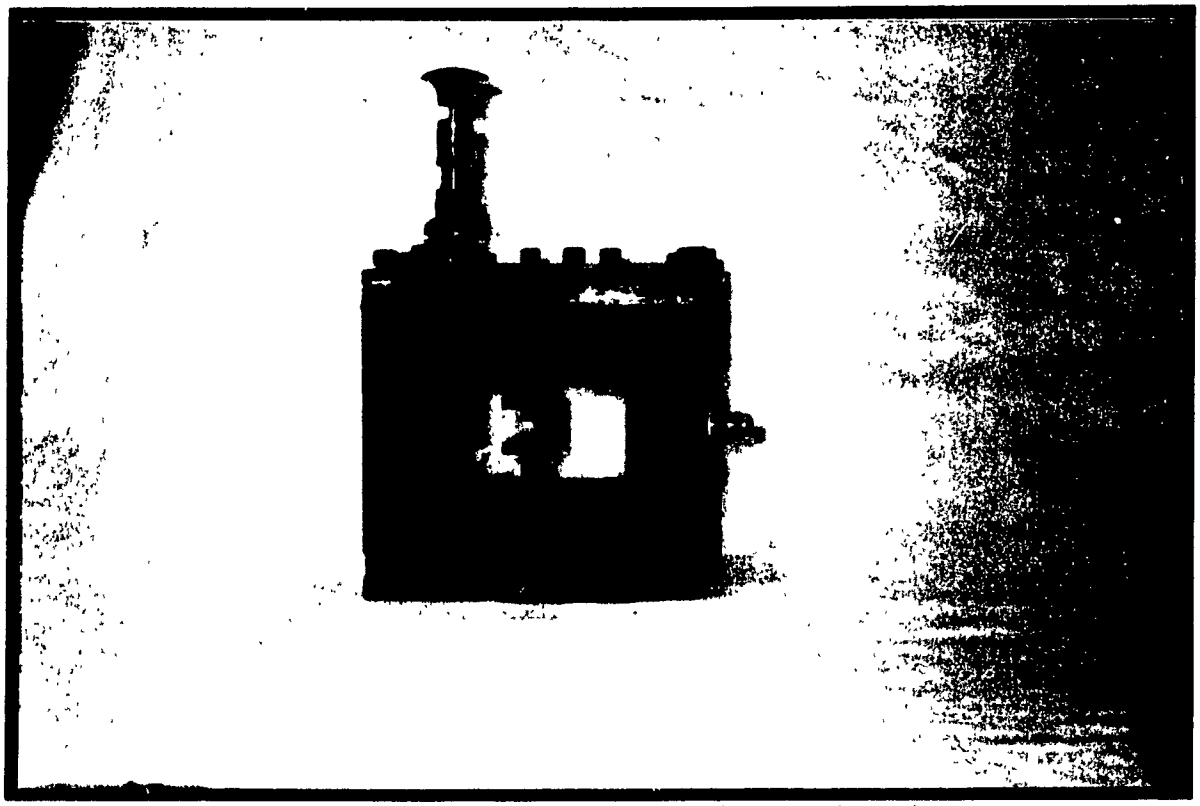

Figure 7.4 Pressurized chamber for investigation of gaseous jets

7.3 Ignition Chamber Model Used for the Experiment

Since the testing of the actual ignition chamber presented many problems, mainly because of the poor accessibility to the interior of the chamber, a simple model has been designed to replace the original one. The approach used was to completely open the sides of the chamber, so that the chamber profile could be uncovered, thereby allowing to see the gas flow path circulating around the spark plug. The main simplification made here was to take a 3-dimensional chamber and reduce it to a 2-dimensional shape. However, our interest in this problem was to identify the gas flow from the injector until it reaches the spark plug. The spark plug has been placed at the original position so that the model can be geometrically correct as compared to the actual chamber. The only component missing in this model was the pressure transducer which is present in the original ignition chamber. The material used to produce the model was aluminum because it is easy to machine. However, a problem of a highly reflective surface arised which resulted from machining. To overcome this problem, the model was painted with a flat black paint so that no light was reflected from the surface. The effect of a bright area on a schlieren photography indicates a low gas density and therefore it was important to pay attention to such detail. A detail drawing in Figure 7.5 shows the shape of the ignition chamber model.

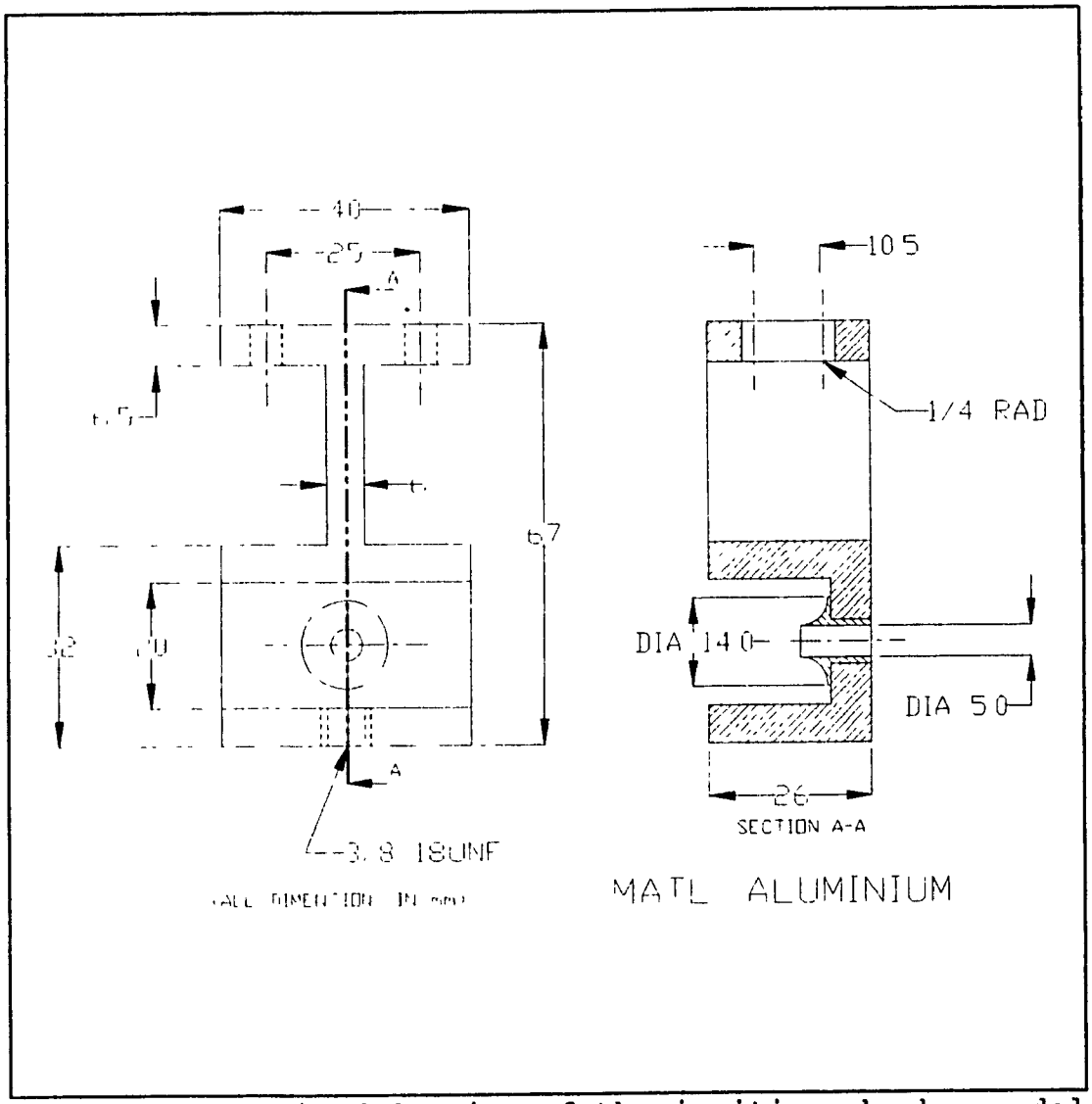

Figure 7.5 Detailed drawing of the ignition chamber model

7.4 Software for the MCS-96 Controller

This software was used to control the timing between the injector opening signal, the signal sent to flash the lamp and the reverse signal to close the injector. All the signals are generated in the aforementioned sequence. The main difference between this computer program and the previous computer program used for operating the ignition system on the engine is that no external interrupts are used. In essence, the ignition signal is replaced by the lamp flashing signal.

To have sufficient time to operate the equipment i.e. to close the room light and open the camera shutter, a time delay is required in initiating the process. By nesting counting loops in the software, a 15 second delay can be easily generated, which is sufficient for the operator to accomplish his task.

To better explain the software, a flow chart is provided in Figure 7.6. Also, the software listing for this program is located in Appendix A for reference.

The first instruction that the program executes is to load #00H in the *ioport1*. This causes all the output pins to be LOW. As soon as this instruction has been performed, a 15 second loop is generated. For simplicity on the flow chart, only one loop is shown, however, in actual facts two nested loops are necessary. Once the delay is over, the number #04H is loaded in *ioport1*, and this causes output pin number 6 to go HIGH for a duration determined by the *power* loop.

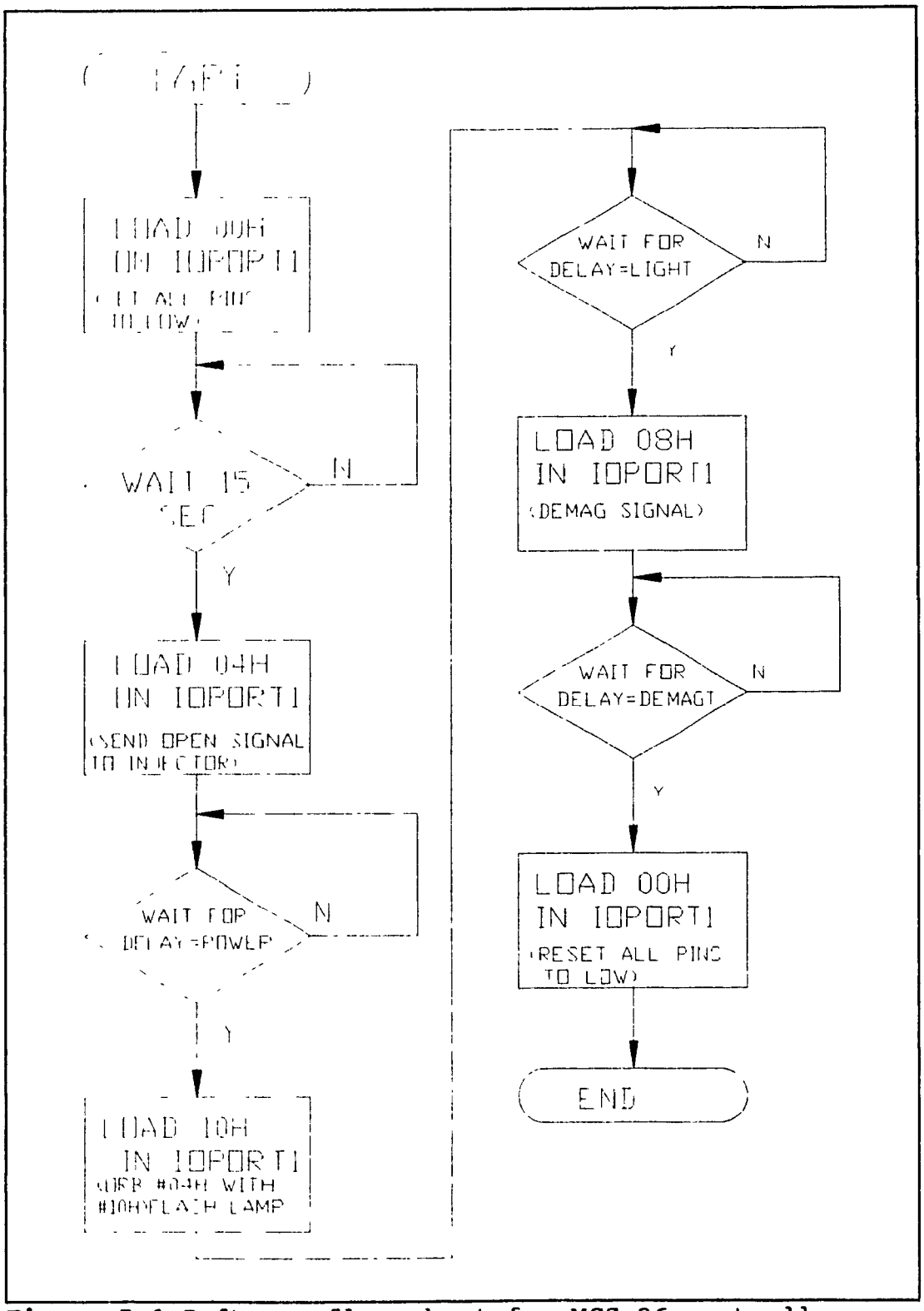

Figure 7.6 Software flow chart for MCS-96 controller

Again, upon completion of this loop, which is used to trigger the injector opening, the previous value loaded in *ioport1* is *OR*ed with the number #10H. As a result, two pins are now HIGH namely, pins 6 and 10. When pin 10 goes HIGH, the light source is triggered. In turn, this causes the event taking place in the pressure chamber to be recorded on the photographic plate. Since the light is triggered only on a positive edge, the pulse duration is not important. However, for this case the pulse duration is kept fixed for a count of 200H, representing a pulse duration of about 1.0 [msec]. Note that the value of the other two loops *energy* and *demagt*, have values that are varied depending on the injector opening duration. When the second loop is completed, the reverse signal is generated for closing the injector. The only purpose of this signal is to reduce the total time opening of the injector thus, to reduce the accumulation of methane in the pressure chamber. To achieve this, the pins 6 and 10 are *AND*ed with the value #08H in *ioport1*, as a result, pin number 8 goes from LOW to HIGH and pin 6 and 10 are now LOW. The duration of the reverse signal is less than 0.5 [msec]. The last operation to be performed is the reset of all the pins to a LOW state. This is achieved by loading #00H in *ioport1*. At this point all the pins are now LOW. The important feature of this program is the timing sequence between the injector and the light triggering. The total opening duration of the injector is irrelevant since the element of interest here is the flow characteristic at full opening of the injector.

Table 7.1 shows the software duration versus the time delay in seconds. This is measured with an oscilloscope from a reference point. The delay value is the loop duration value loaded in the software.

Table 7.1 Software delay for triggering the light source

Software delay in Hexadecimal	Delay for trig. light [sec]
180	0.28
190	0.36
200	0.46
220	0.67
300	1.1
400	1.6
500	2.1

7.5 Schlieren Photography Operation

This method is widely used in the field of compressible fluid mechanics to visualize discontinuity of a flow path or density gradient in a fluid. The word "schlieren" is a German term which refers to a local inhomogeneity in a medium, that is caused by the bending of the light, as it is passing through different density gradient. As a result, bright and dark area's represent different fluid densities. This method is often used in the discipline of gas dynamics to visualize shock waves. [29]

The schlieren visualization method can be utilized to quantify a density field since the different shades of grey can represent a particular density at each point of that flow field. However, for a quantitative analysis it is required to have a reference schlieren head indicating a known density. For the present experiment the main interest here is not to obtain a qualitative measure but rather see how the flow path develops in the ignition chamber.

The most utilized schlieren setup is the Z configuration [30]. It uses parabolic mirrors with the test section placed in between. The light is emitted from a point source and is placed at the focal point of the first parabolic mirror. The column of parallel light leaving the mirror reaches the test section where a density field bends the light. As a result, dark and bright areas are produced at the test section. The light beam will eventually reach the second mirror and converge to a knife edge. The purpose of the knife edge is to

remove some of the light by diverging it away from the photographic plate. This allows to vary the light intensity on the photographic plate thereby, controlling the amount of light reaching the film. In spite of this, the light is still evenly distributed on the photographic plate.

Several factors pertaining to this method should be emphasised. As mentioned in section 7.1, the light source should be smaller than the object observed at the test plane by a ratio of 10:1. Also, specially designed parabolic mirrors are used for schlieren photography, with their silver coated and highly polished surface.

7.6 Visualization Methodology

The objective of this experiment is to visualize the gas jet leaving the injector under different conditions. Among the cases studied, is the impact of the variation of the injector backpressure by changing the pressure inside the pressure chamber, and the effect of the injector nozzle orifice geometry. The interest of this experiment is to see how it is possible to vary the cone angle of the gas jet discharged from the injector. As the result of the cone angle change, more or less fuel can be allowed to circulate around the spark plug, thus changing the conditions for ignition.

The design of the ignition chamber model allows for the variation of the distance between the injector and the shaving edge of the ignition chamber. This injector position change

corresponds to the different spacers used on the test diesel engine. However, this experiment will focus mainly on injector positions number 5 and 7. The reason for using spacer number 5 is because the best ignition results have been obtained so far with this distance. Spacer number 7 is used here to see what is the maximum fuel jet position distribution allowing the injected gas to remain in the ignition chamber. Once the initial distance is selected, either with spacer no.5 or 7, the chamber will be closed and sealed with silicone to prevent any possible leak.

Next, the pressure relief valve has to be adjusted for a maximum pressure. For this purpose, a known air pressure will be applied in the pressure chamber using the air bottle pressure gage. It has been decided that 28.2 [bar] would be the maximum safe pressure to use with this pressure chamber. At this point, the spring of the relief valve is adjusted, until the air starts leaking out of the valve. It is important to purge the chamber and refill it with fresh air after several injections.

As previously mentioned, the main interest here is to test several nozzle orifice configurations by visualizing the jet formation. Because the flow taking place in this nozzle orifice is unsteady, the prediction of the jet angle using analytical methods is considered as not feasible.

A cylindrical nozzle orifice geometry will be tested first because most of the gas expansion would take place outside the injector orifice. This was the original injector nozzle orifice configuration which has been used on the diesel test

engine, after the reduction in the flow area. Next, a 30° conical orifice nozzle will be tested. In this case, some expansion will take place inside the nozzle orifice and the remaining of the expansion will take place outside the injector. Lastly, a modified gas injector with a grooved needle tip will be used to induce a swirling effect to the gas flow, which should cause the gas jet leaving the injector to increase in angle. This test will still be made with the 30° nozzle orifice angle. All these tests will be performed with a chamber pressure of 21.4 [bar]. The Figure 7.7 below shows the different injector nozzle orifice configurations tested with the schlieren photography setup.

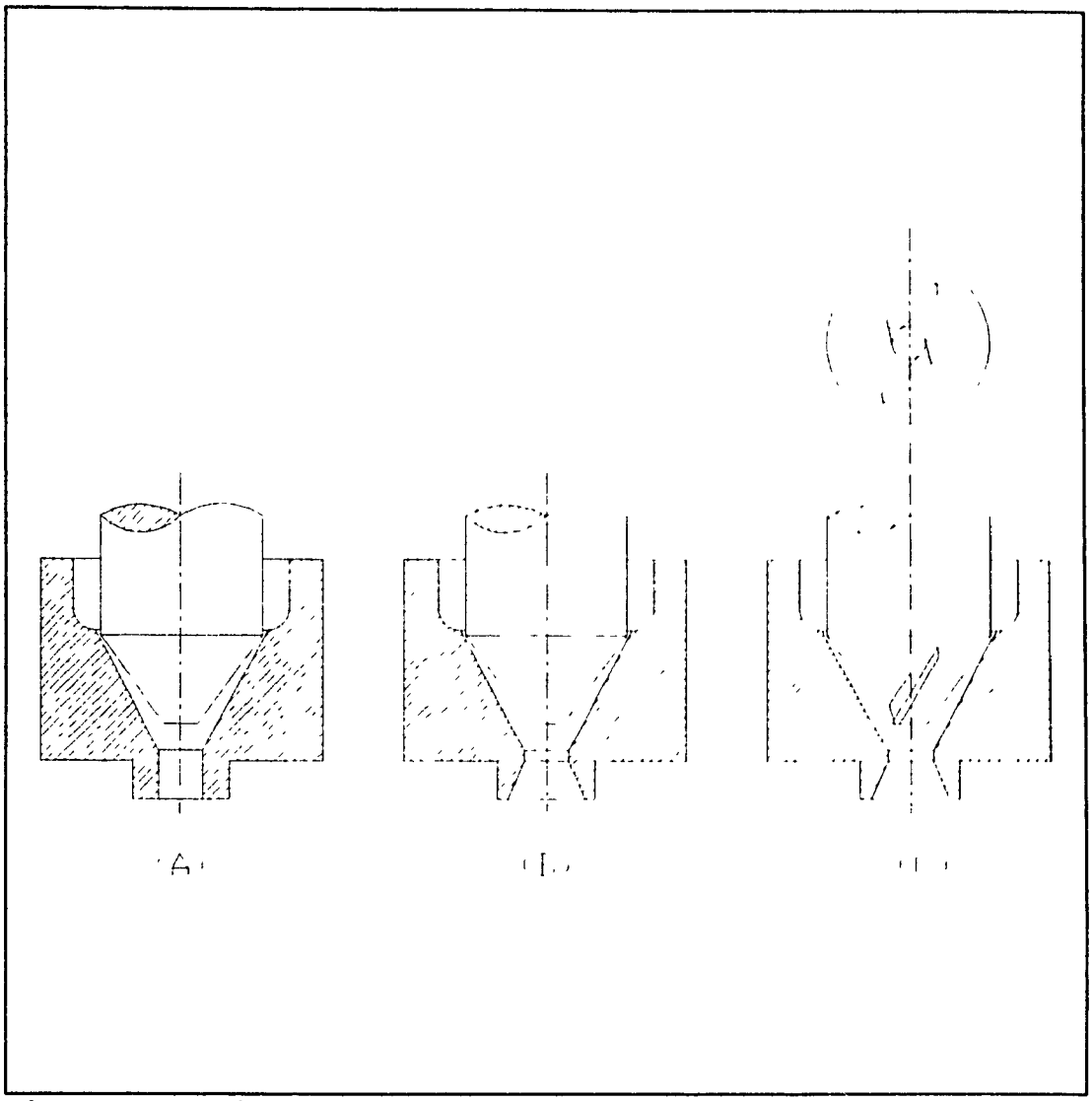

Figure 7.7 Different injector nozzle configuration (A) cylindrical nozzle orifice (B) 30° nozzle orifice angle (C) 30° nozzle orifice angle with modified injector pintle

7.7 Visualization Results

During the initial phase of the testing, which was used to find a working pressure for the pressurized chamber, different trials have been performed at several chamber pressures. It was found that if the chamber pressure is exceeding 15 [bar] with an injector pressure of 70 [bar], the injector would be leaking so that the quality of the schlieren picture would turn out to be poor. However, at a pressure below 15 [bar] that problem was found as not existent. Once a suitable chamber pressure was found (10 [bar]), four sets of tests have been performed namely, the injector at position no.7 with cylindrical nozzle orifice, then the injector at position no.5 again with a cylindrical nozzle orifice, next the injector at position no.5 with a 30° nozzle orifice angle, and finally the injector at position no.5 again, with a 30° nozzle orifice and a modified tip cone to induce a swirl.

The first set of schlieren pictures presented in Figure 7.8, Figure 7.9, and Figure 7.10, clearly showed that the type of gas jet development corresponds to an underexpanded gas jet. The expansion waves present at the jet boundary surrounding the core are typical of what is expected from this type of flow (see Figure 7.9 and Figure 7.10). The other findings not shown on this set of pictures, is the relatively short time needed for the gas stream to reach the spark plug. This time is on average less than 0.5 [msec]. In spite of the fact that with this configuration, ignition has been obtained, the picture does not

clearly reveal that some fuel is coming to the vicinity of the spark plug.

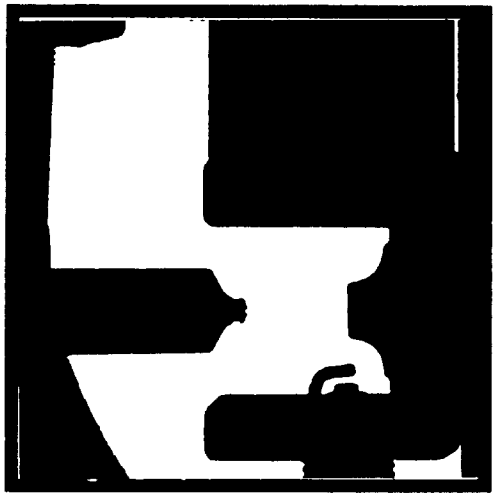

Figure 7.8 Cylindrical nozzle orifice,
Hole diameter: 0.75 [mm],
Distance: position no.7,
Injector opened for 0.36 [msec]

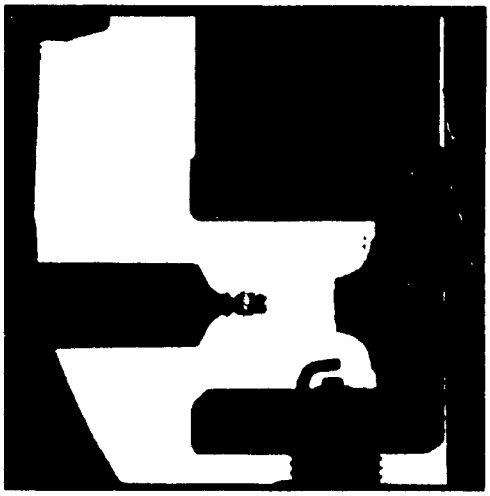

Figure 7.9 Cylindrical nozzle orifice,
Hole diameter: 0.75 [mm],
Distance : position no.7,
Injector opened for 0.67 [msec]

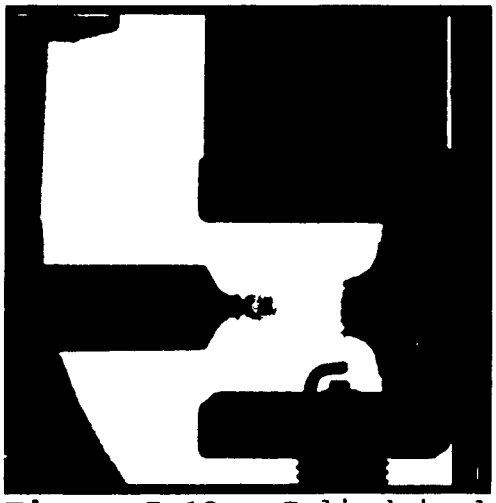

Figure 7.10 Cylindrical nozzle orifice,
Hole diameter: 0.75 [mm],
Distance: position no.7,
Injector opened for 1.60 [msec]

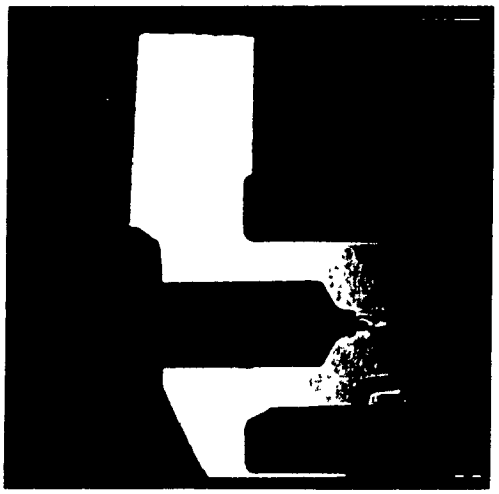

Figure 7.11 Cylindrical nozzle orifice,
Hole diameter: 0.75 [mm],
Distance: position no.5,
Injector opened for 0.28 [msec]

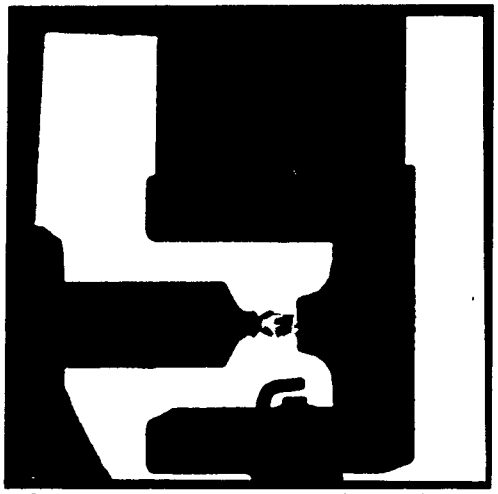

Figure 7.12 Cylindrical nozzle orifice,
Hole diameter: 0.75 [mm],
Distance: position no.5,
Injector opened for 0.46 [msec]

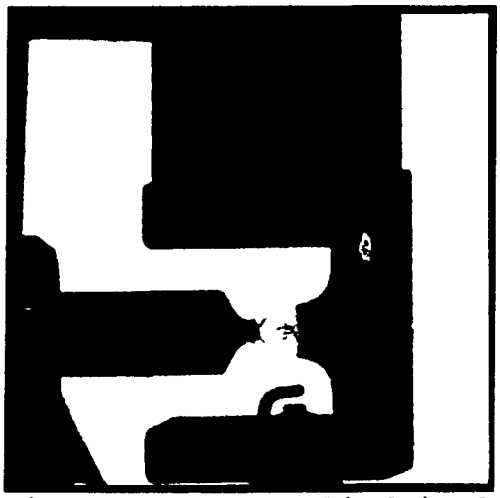

Figure 7.13 Cylindrical nozzle orifice,
Hole diameter: 0.75 [mm],
Distance: position no.5,
Injector opened for 2.10 [msec]

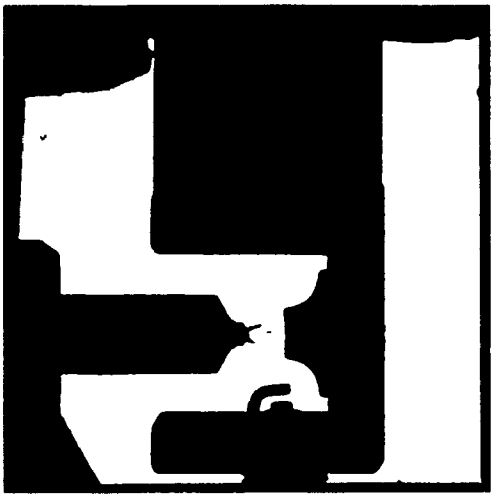

Figure 7.14
30° nozzle orifice angle,
Hole diameter: 0.75 [mm]
Distance: position no.5,
Injector opened for 0.67
[msec]

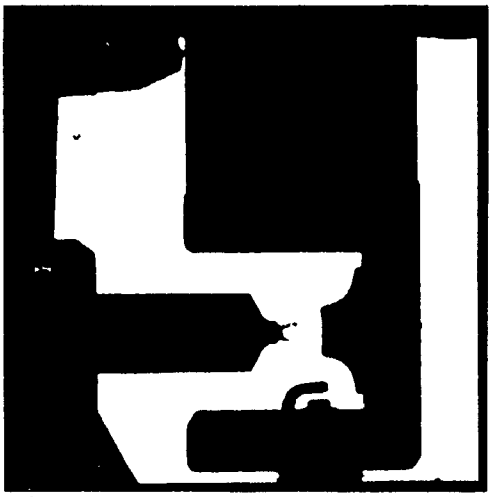

Figure 7.15
30° nozzle orifice angle,
Hole diameter: 0.75 [mm]
Distance: position no.5,
Injector opened for 1.60
[msec]

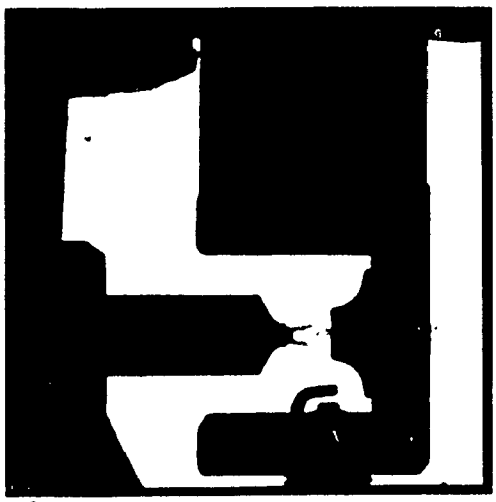

Figure 7.16
30° nozzle orifice angle,
Hole diameter: 0.75 [mm]
Distance: position no.5,
Injector opened for 2.10
[msec]

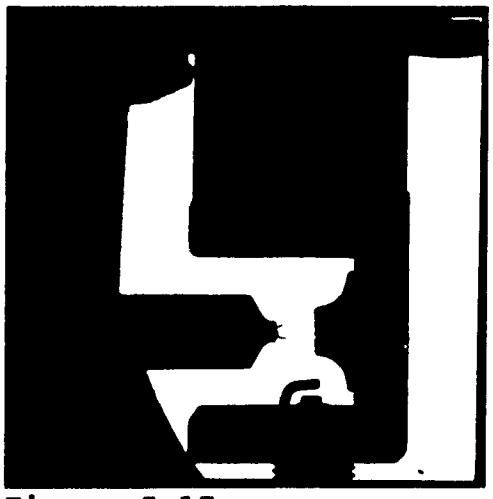

Figure 7.17
30° nozzle orifice angle,
pintle modified to induce swirl,
Hole diameter: 0.75 [mm],
Distance: position no.5,
Injector opened for 0.67 [msec]

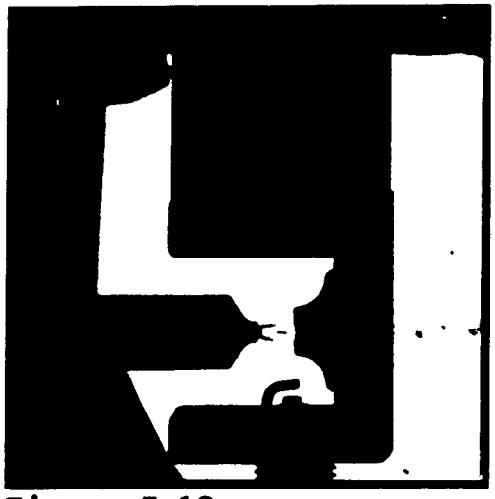

Figure 7.18
30° nozzle orifice angle,
pintle modified to induce swirl,
Hole diameter: 0.75 [mm],
Distance: position no.5,
Injector opened for 0.92 [msec]

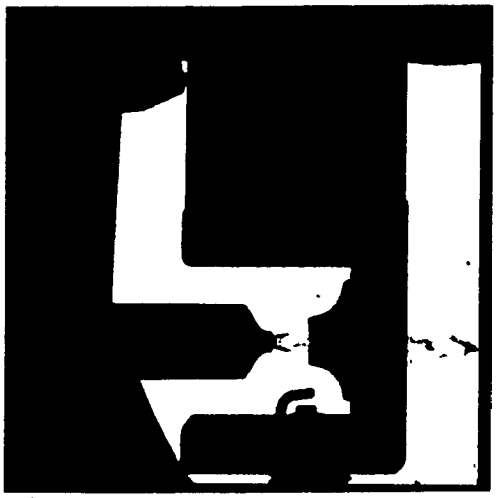

Figure 7.19
30° nozzle orifice angle,
pintle modified to induce swirl,
Hole diameter: 0.75 [mm],
Distance: position no.5,
Injector opened for 1.60 [msec]

However, from measuring the gas jet width at the shaving edge of the chamber, it is evident that some methane should be present at the spark plug. From the engine tests, ignition has been obtained as early as 1.2 [msec] after the beginning of injection. It seems that an even earlier sparking, suitable conditions for ignition could be available as early as 0.5 [msec]. The problem encountered when getting ignition with injector position no.7, was a long ignition delay which is difficult to explain, even though other experiments performed by other researchers have experienced similar ignition delay [31,32]. Refer to Appendix C for scale drawing of injector positions.

The second set of trials has been accomplished with an equivalent distance of injector, position no.5. This distance has provided so far the best ignition results regarding the shortest ignition delay, when tested on the diesel engine. From the schlieren pictures in Figure 7.11, Figure 7.12, and Figure 7.13 the type of gas jet obtained here again is underexpanded. Interestingly enough, it can be seen that no fuel is going into the ignition chamber when observing the jet width near the shaving portion of the ignition chamber (see Figure 7.12 and Figure 7.13). However, it is difficult to distinguish at the corners of the shaving edge the gas flow path. Further observation of the picture in Figure 7.12 reveals that outside the expansion wave boundary some fuel is present. This is shown by the slightly darker shade of grey above the expansion waves.

For the third experiment, a 30° cone orifice has been cut in the insert which was pressed into the nozzle orifice of the injector. The result we were hoping to get, was an increase in the jet opening angle (see Figure 7.14, Figure 7.15, and Figure 7.16). The assumption here was that because the orifice is very short, a minimum amount of expansion would be taking place inside the nozzle orifice, and as a result, the expansion waves would discharge at a greater angle, as compared with the cylindrical hole case. However, the result was not as expected; rather than having an increase in the jet angle, a substantial decrease was the result. Again, looking at the ignition chamber shaving edge, the gas jet diameter when entering the hole is almost half of the size of the cylindrical connecting hole diameter. Lastly, to overcome the problem of the jet angle decrease caused by the opening of the nozzle orifice to a 30° angle, a modification to the nozzle needle tip was proposed by making two small grooves in the sealing surface; this would hopefully induce a swirl of the gas leaving the injector as it is made in gas turbine swirl nozzles. As a result, this modification may lead to an increase in jet angle. Again, the outcome of this modification was negative. It did not lead to the expected result. Instead, the jet cone further decreased in angle, as shown in Figure 7.17, Figure 7.18, and Figure 7.19.

The four tests aforementioned have been performed under the same conditions. The only factor which distinguished them was the fact, that the nozzle orifice seat needed to be

lapped after each modification. However, this had no effect on the diverging part of the nozzle orifice; only the converging part was slightly affected.

7.8 Visualization Results Discussion

The experiments described above show that the schlieren photography method, reveals the exact shape of the jet cone angle.

One problem encountered in this investigation was the pressure level of the pressure chamber; the injector was found to leak when the backpressure was above 15 [bar]. Another factor related to the testing apparatus was the proper sealing of the pressure chamber. Particular attention had to be paid for properly sealing of the quartz windows; to achieve this epoxy glue and a thin rubber gasket was used. Furthermore, for sealing the top cover of the pressure vessel silicone sealant had to be used. Concerning the environment, where the experiment was taking place, because of the 3000 ASA film sensitivity, extra precaution had to be taken to completely seal the room from any possible light.

The experiments revealed that a cylindrical hole provides the largest jet cone angle. This can be explained by the fact that when the gas is entering the nozzle orifice, virtually no expansion is taking place inside the orifice. As a result, most of the gas expansion is taking place outside the orifice i.e. already in the ignition chamber. From basics of the

gas dynamics, the expansion waves resulting from the pressure adjustment are responsible for the enlargement of the jet cone angle; this is referred to as a Prandtl Meyer fan [33]. Furthermore, by increasing the injector pressure, one can obtain a larger gas jet cone. However, the limitation here is that the injector solenoid triggering circuit may not be capable of opening the injector at a pressure in excess of 80 [bar].

The other conclusion that can be drawn from this experiment is that the schlieren photography could have been first used to determine the initial geometry for the ignition chamber. After having obtained the correctly functioning chamber, it could be tested on the engine.

It was decided that another experiment will be repeated on the test engine with a reduced hole size of the fuel shaving edge in the ignition chamber. Instead of using a 5 [mm] hole, the hole will be reduced to 4 [mm]. This is made to allow more of fuel to remain in the pre-chamber using the existing injection.

Further analysis of the test results points toward some controversy, regarding the conclusions being drawn. In the early testing stage of the diesel engine, the test results suggested that an excess of fuel was injected into the ignition chamber. This has been confirmed by the tests showing that ignition could be obtained by sequentially decreasing the injector pressure. However, in these early testing of the engine, a nozzle orifice angle of 30° was used until it was

decided to reduce the flow area. After that modification of the flow area, it was decided to use a cylindrical orifice configuration. Because of this type of geometry (cylindrical instead of a 30° nozzle orifice angle) more fuel was now sent to the ignition chamber. This contradiction of the experimental results gives a strong motivation for performing other tests on the diesel engine setup.

Finally, from combustion theory, some diffusion [34] of the gaseous jet may be also taking place at the jet boundary. This could be a possible explanation for the ignition of a fuel charge in the test engine. In future investigations, using the schlieren method, one could try to focus more on that region and see if some fuel is in fact leaving the jet core, and going toward the spark plug. Moreover, an investigation of the type of flow taking place in the spark plug electrodes vicinity would be an additional and valuable piece of information.

CHAPTER 8

8.0 FINAL ENGINE IGNITION TESTS

A second series of ignition tests was found to be necessary after the schlieren photography experiment. Based on the new findings from the schlieren experiment, the geometry of the ignition chamber insert was redesigned, in such a way, to allow more fuel to remain in the ignition chamber. The testing approach is, in essence, similar to the chapter 6 experimental procedures, where the first ignition tests on the engine have been performed.

During the first tests, the injector nozzle orifice with 1 [mm] diameter was used with a cylindrical hole, as opposed to a diverging orifice used in the first experiment. This new orifice geometry was found to be more suitable, after the schlieren visualization of the jet shape. The other component remachined for this experiment was the ignition chamber insert, which is used to shave some fuel from the gaseous fuel jet and force it toward the spark plug. A drawing of the modified insert is shown in Figure 8.1.

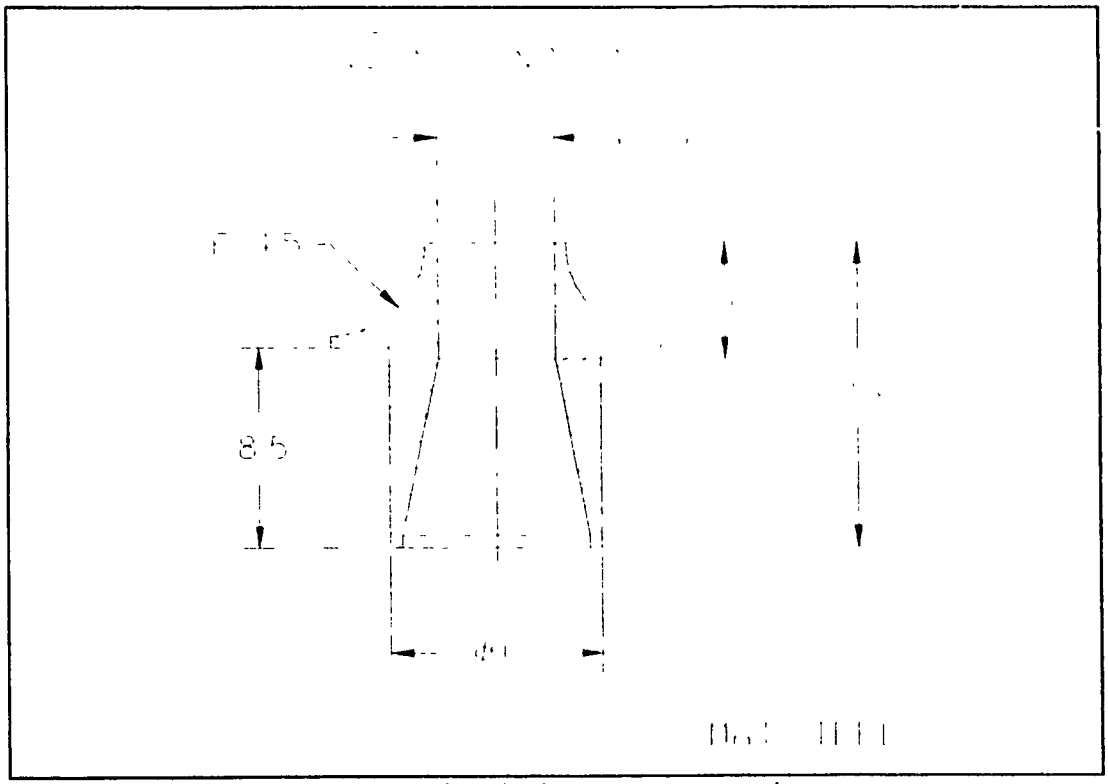

Figure 8.1 Redesigned ignition chamber insert

The new injector nozzle orifice diameter, and the new insert design have been tested in the following sequence. Starting from test no.69 to 78 (see table 8.1), the spark advance was set to 2 [msec] before TDC, the injection advance to 6 [msec], and the injector position has been varied from no.7 to 1. During this testing sequence no ignition was recorded. Then the next sequence, from trial no.76 to 81 (see table 8.1), the spark advance was moved from 2 to 4 [msec] before TDC, the injection advance was retained and the injector position was varied from 7 to 1 again. Ignition was recorded at two injector positions only, namely position no.4 and 5.

For the next experiment sequence, it was decided to reduce the injector flow area once again, from 1 [mm] to 0.8 [mm]; a similar orifice size reduction was found to be necessary during the first ignition experiment described in chapter 6. During this sequence of trials, the spark advance was set to 2 [msec] before TDC, and the injector advance to 7 [msec] before TDC. Beside a reduction in fuel mass flow rate from the injector, the time of injection was increased from 6 to 10 [msec]. The point of interest here was to see if a more gradual fuel introduction would have an impact on the ignition delay. In a similar fashion as in the previous test, the injector position was changed from the highest to the lowest distance. Ignition was recorded on all of the positions , except on injector position nos.7 and 2. It is worth mentioning at this point that a very good ignition repeatability was observed during this testing sequence.

The last test namely, test no.39, was used to identify the origin of ignition. After all the tests performed there was no certitude on the exact provenance of the ignition. By installing a pressure transducer in the main cylinder and recording the pressure increase, it is possible to show the origin of ignition.

Table 8.1 Final ignition test results

Trial	Ign Adv	Inj Pos	Inj Adv	Inj Dur	Ign	Plt No
69	2.0	7	6.0	6.0	No	
70	2.0	6	6.0	6.0	No	
71	2.0	5	6.0	6.0	No	
72	2.0	4	6.0	6.0	No	
73	2.0	3	6.0	6.0	No	
74	2.0	2	6.0	6.0	No	
75	2.0	1	6.0	6.0	No	
76	4.0	7	6.0	6.0	No	
77	4.0	6	6.0	6.0	No	
78	4.0	5	6.0	6.0	Yes	20
79	4.0	4	6.0	6.0	Yes	21
80	4.0	3	6.0	6.0	No	
81	4.0	2	6.0	6.0	No	
82	4.0	1	6.0	6.0	No	
83	2.0	7	7.0	10.0	No	
84	2.0	6	7.0	10.0	Yes	N.R.*
85	2.0	5	7.0	10.0	Yes	21
86	2.0	4	7.0	10.0	Yes	22
87	2.0	3	7.0	10.0	Yes	N.R.
88	2.0	2	7.0	10.0	Yes	N.R.
89	2.0	1	7.0	10.0	No	
90	2.0	5	7.0	10.0	Yes	23

*Result not recorded

8.1 Test Results and Discussion

The first set of trials has been used to investigate if a flow area of 1 [mm] diameter, with a cylindrical orifice geometry, would produce better results. During the first ignition experiment a flow area of 1 [mm] with a diverging orifice geometry was used, but no ignition was recorded. Following the schlieren photography experiment, it has been found that a diverging orifice type is not suitable for this type of chamber geometry, instead a cylindrical geometry is preferable. The main reason for using a larger flow area is because when the engine would be running at high speed, very short injection are required, this implies a time limit for injecting the required fuel dose. Even though this investigation is concerned with only the cold start conditions, this aspect of the short injection problem cannot be neglected.

However, the results of this set of trials revealed that excessive amount of gaseous fuel is still injected upon ignition (see Table 8.1 results no.69 to 75). The results thus far obtained confirmed that the spark should be advanced to 4 [msec] before TDC or closer to the beginning of injection; then less fuel would be present in the ignition chamber upon sparking. During another sets of trials (from trial no.76 to 82), ignition was obtained when the injector was at position no.4 and 5. In spite of the ignition obtained, the repeatability of ignition was very poor. In other words ignition does not always occur at every 50 crank revolution.

For the next set of trials, it was decided to reduce the injector nozzle orifice flow area. It was also decided to use a longer period of injection such, that the total dose would be similar to the fuel dose injected during test no.69 to 82. For this sets of experiment the spark advance was set to 2.0 [msec], the injection advance to 7.0 [msec], and the injection duration was of 10.0 [msec] (see Figure 8.2). During the test no.83 to 89 the injector was moved from position 7 to position 1. Despite the fact that ignition did not occur at position 1 and 7, very good results have been obtained for injector position 4 and 5. Ignition occurred consistently every 50 crank revolution.

The last test has been used to indicate whether the ignition occurs first in the ignition chamber or in the main chamber. The results showed a higher peak pressure in the ignition chamber as compared to the main chamber. Therefore, the ignition must originate from the ignition chamber (see Figure 8.3). Figure 8.4 shows the same pressure rise as in Figure 8.3, but it is on a shorter time scale, so that the small phase lag in pressure is visible in the ignition chamber and the cylinder.

To conclude on this ignition experiment, the schlieren photography method was successful in obtaining information on the flow characteristics inside the ignition chamber thus, suggesting ways which would improve the gas flow in the chamber. The use of a cylindrical injector orifice geometry and the reduction of the diameter of the inter passage hole have been

suggested from the schlieren experiment. It was found during this series of test that the ignition repeatability was very much improved over the first ignition experiment. However, the factors responsible for the long ignition delay recorded in most oscillograms have not been identified.

The pressure measurement in both the ignition chamber and the main chamber are showning well the distinct feature of the concept as presented in Figure 8.3.

Firstly, the pressure difference can be seen between the chambers when the compressed air is being pushed through the connecting channel to the ignition chamber; this difference becomes smaller when the piston speed reduces, i.e. when the piston approaches TDC.

Secondly, the injection of methane is well shown before TDC (see Figure 8.3), as the ignition chamber pressure drops due to the heat transfer from compressed air to the cold methane injected; this maintains the pressure in the ignition chamber below the main chamber pressure until the ignition occurs.

Thirdly, after ignition, the pressure in the ignition chamber becomes higher than the main chamber which allows the remainder of the fuel/air mixture to be injected into the main chamber, thus completing the combustion precess with higher excess air.

The presented graphs are showing a well understood sequence of events, which in general conform to the preliminary

expectation. The only surprising result is that after only methane injection, the impact of lower gas temperature is higher than the impact of the increase mass of gas in the ignition chamber. This leads to the situation that after the gas injection, until ignition, the pressure in the ignition chamber is lower than the main chamber. This may result in limiting the methane flow to the main chamber.

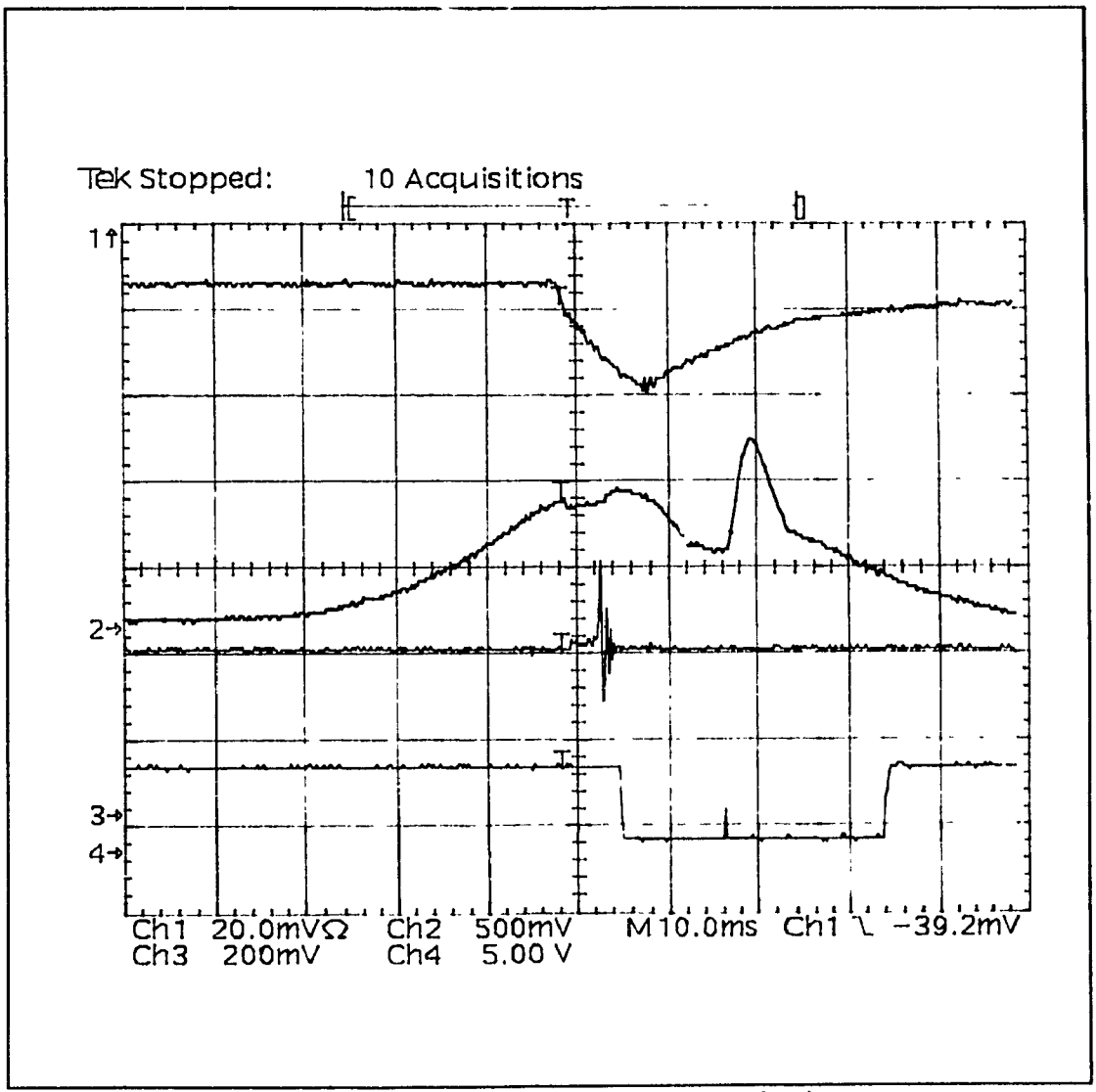

Figure 8.2 Experiment result no.23, CH1-injector pressure, CH2-ignition chamber pressure, CH3-spark plug current, CH4-TDC on falling edge

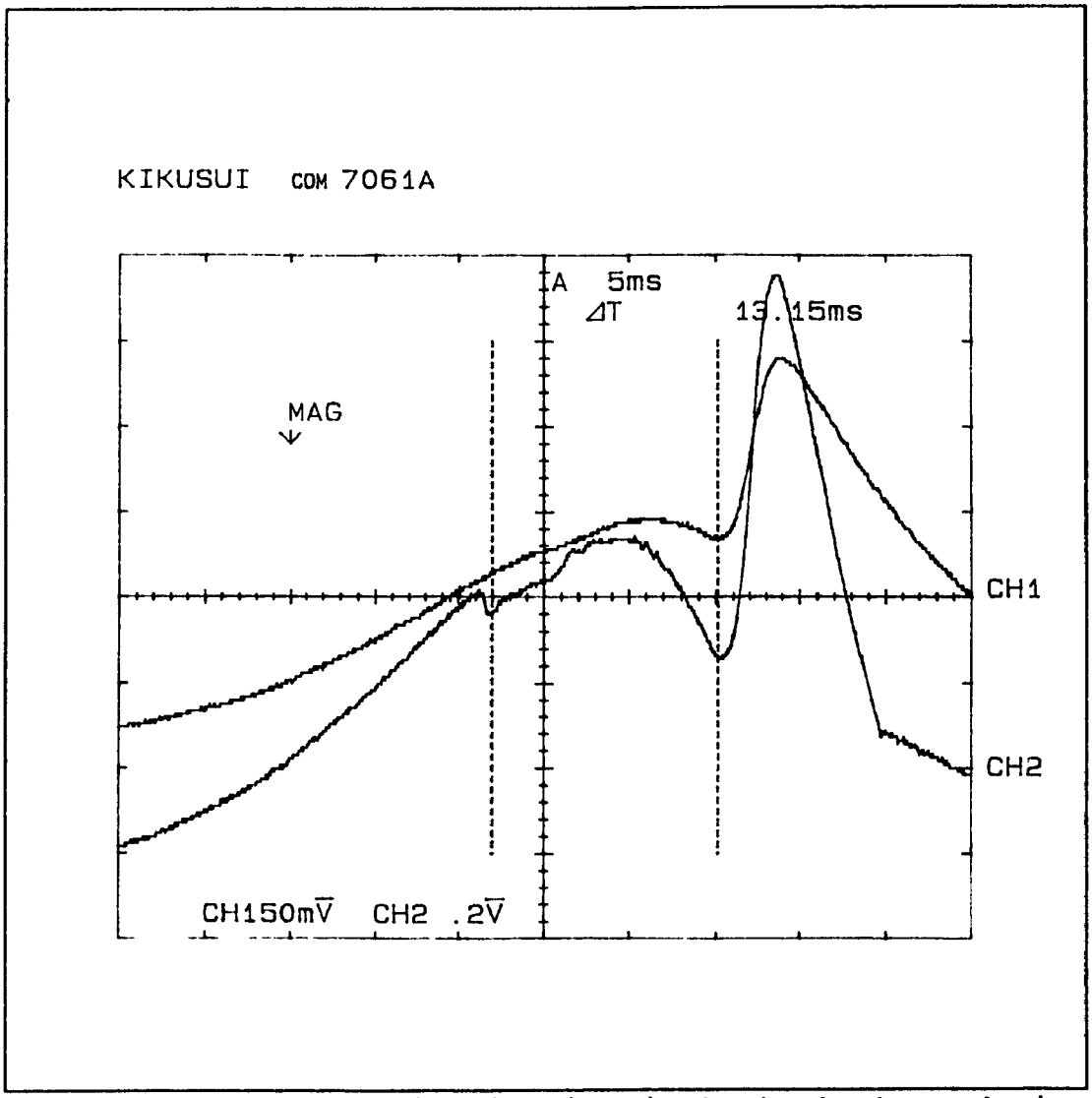

Figure 8.3 Pressure distribution in both chambers during ignition, CH1-cylinder pressure, CH2-ignition chamber pressure

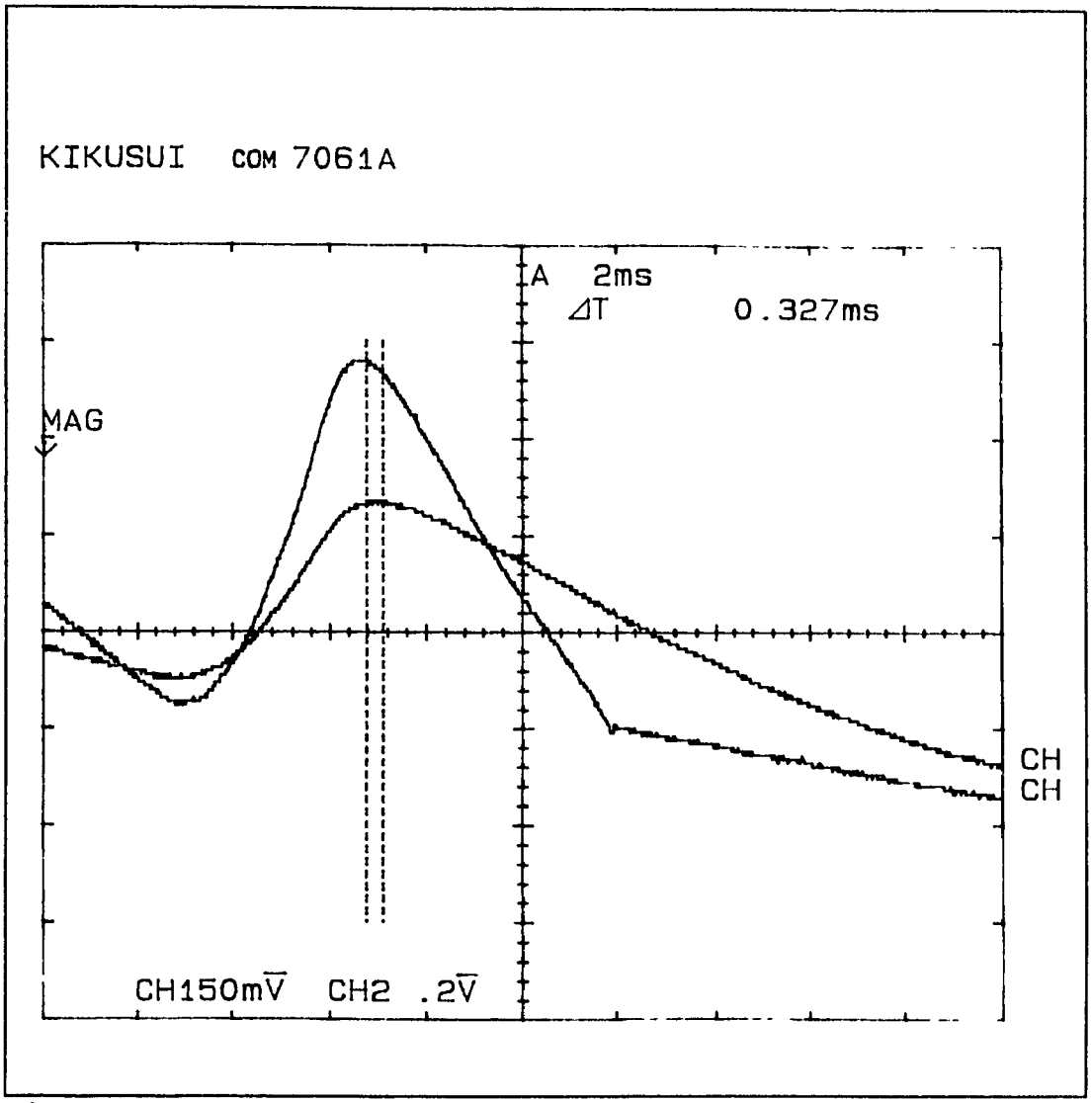

Figure 8.4 Peak pressure registered in both chambers during ignition, CH1-cylinder pressure, CH2-ignition chamber pressure

CHAPTER 9

9.0 SUMMARY, CONCLUSION, AND RECOMMENDATIONS

The objectives of this thesis have been achieved namely, to obtain repeatable ignition from a fuel charge using this newly developed concept of ignition chamber. The engine used for this research also proved to be a valuable tool despite the fact that many problems have been encountered with the electronic part of the engine test setup. The electrical motor used to drive the diesel engine was at the origin of the problem, electromagnetic interference was at the heart of the problem. To overcome this, proper shielding and grounding of the control circuit using Faraday cage and shielded cable for signal transmission have helped to improve the situation; further improvement was achieved by using an antistatic spark plug from NGK. Using this (R) spark plug contributed to eliminate at the source the interference thus, further improving the situation [35]. After those modifications, all the electronics used to control the injector and the spark ignition system, performed well in this environment.

The point of interest during the diesel engine preliminary testing (refer to chapter 6), has been from the fact that an excess of fuel was present in the ignition chamber upon sparking. This problem was believed to be at the origin, for not getting ignition. Following this first series of tests, a reduction of the injector flow area was found to be necessary.

The other modification applied to the injector nozzle orifice was a change in orifice geometry, from a diverging orifice to a cylindrical hole. At first it was believed that if a diverging nozzle was used, the gas would follow the orifice wall, and leave the nozzle approximately at this angle. Although this fact is correct for incompressible fluid, for compressible fluid the gas flow does not adjust itself the same way. For a gas flowing through a diverging orifice, under certain conditions, shock waves may appear in the orifice. This condition is dictated by the pressure ratio across the orifice, namely, the injector internal pressure and the cylinder pressure. As a result from a shock wave, the gas pressure and velocity is substantially decreased as it enters the cylinder. This factor has important consequences on the geometry of the gas jet. However, after modifying the flow area by reducing it, and also by changing the geometry of the orifice from a 30° angle to a cylindrical hole, ignition of the fuel charge occurred.

Although ignition has been obtained using a flow area of 0.8 [mm] diameter, as opposed to 1 [mm] diameter, this orifice size has certain drawbacks. When operating an engine at high speed the time allowed for the fuel dose delivery is relatively short. The typical injection period for a diesel engine is about 2.5 to 3 [msec]. To obtain this characteristic a relatively large flow area is required. For a standard engine the fuel dose required differ, depending on the mode of operation i.e. acceleration, idle, cold start, etc. This is why further

optimization work would require that a flow area of 1 to 1.2 [mm] diameter can be used on this engine, for an injector internal pressure of 69 [bar]. Similarly, an increase of the injector internal pressure can also be used to increase the fuel dose, however, the injector triggering circuit may become less reliable for operating the injector at high internal pressure.

After performing the first sets of test it was then decided to use a method to visualize the gas flow path taking place inside the ignition chamber, in order to reveal the mixing process and point out other possible anomalies with this prototype. It was then decided to use the schlieren photography method to show the flow characteristics inside the ignition chamber.

The schlieren experiment did show that the modifications made on the injector nozzle orifice did in fact, deliver more fuel to the ignition chamber, after the nozzle orifice modification than before (see chapter 6, trial nos.1 to 37). In spite of this result, the previous testing performed on the diesel engine indicated that an excess of fuel may be the cause for not obtaining ignition.

The schlieren photography experiment alsc indicated that a reduction in the size of the passage connecting the ignition chamber with the main chamber could be leading in the proper direction for getting a better ignition. However, an increase of the injector internal pressure would also produce a similar result since it would also increase the jet cone angle.

Although the objectives of this research have been met, obtaining the ignition of a fuel charge, one question still remains unanswered namely, what are the elements responsible for the long ignition delay recorded on the oscillogram.

According to other researchers [25,31,32,36], factors such as fuel property and ignition chamber geometry play important role, with respect to ignition delay. The oxygen concentration in the proximity of the ignition point, and the swirl rate do influence it as well. Of course, for cold start, the fuel property does influence the ignition delay substantially. The fuel octane numbers which are used to indicate how fuels resist ignition, is in part responsible for a variation in ignition delay. The high octane number of natural gas (120 as reported from literature) is probably the most important cause for ignition delay. This factor renders this fuel not only difficult to ignite, but also increases the ignition delay as it was reported by Heywood [25]. Heywood experimentally showed that as the cetane number decreases (fuel more difficult to ignite, inverse of octane number), the ignition delay increases sharply.

Other researchers who studied this phenomena reported similar factors which influence the increase in ignition delay. For instance, H. Hiroyasu et al. [36] , indicate in their research on ignition delay that an ignition delay up to 9.5 [msec] can be recorded at low speeds with diesel fuel in a divided combustion chamber. Furthermore, Heywood and also

Taylor [31,32], indicated that the ignition delay is a function of the compression ratio and engine speed. In the case that concerns us, beside the fact that methane is difficult to ignite, this factor may have played an important role, since the engine was tested at a speed of only 300 [rpm], and after modifying the engine the compression ratio had been lowered from 16.5:1 to about 13:1. Both of these parameters effect directly the ignition delay.

In summary, the ignition of a charge of gaseous methane has been achieved, however, the optimization process for the ignition chamber parameters still require further work. The use of a hole type injector, with this ignition chamber prototype present a problem, because of the difficulty related to the development of the gas jet. Instead, using a pintle type injector may be more appropriate for future work with this type of ignition chamber. The geometry of the pintle is such that it is forcing the gas flow to a certain direction. However, the large flow area required for gaseous fuel may present a problem with a pintle type injector. Further optimization work done in parallel with schlieren photography may lead to a more refined ignition chamber prototype. The possibility to incorporate a schlieren setup on the test engine may prove to be very useful.

For future work the following recommendation can be made to perform more testing on this new prototype;

1 - Using a pintle type injector as opposed to a hole type injector, to force the gas flow in the required direction

2 - Use schlieren photography to further optimize the ignition chamber with the new pintle injector.

3 - Extend the investigation from cold start ignition to higher engine speed range.

4 - Use a second microcontroller to allow the sparking system to be operated independently from the injector, such that ignition investigation can be carried at the very beginning of injection.

REFERENCES

1. T. Krepec, Environmental Impact of Vehicle Design Actual Problems and Prognosis, CSME Forum "Transport 1992+", Vol.II, Concordia University, Montreal, Canada, 1992, pg. 366.

2. H.R. Ricardo, and J.G.G. Hempson, The High-Speed Internal-Combustion Engine. Blackie & Son Limited, Fifth ed., London, 1968, pp. 32-42.

3. M. Alperstein et al., Texaco's Stratified Charge Engine-Multifuel, efficient, clean, and Practical, SAE Technical Paper Series, No. 740563.

4. A.G. Urlaub and F.G. Chmela, High-Speed, Multifuel Engine: L9204 FMV, SAE Technical Paper Series, No. 740122.

5. T. Date and S. Yagi, Research and Development of the Honda CVCC Engine, SAE Technical Paper Series, No. 740605.

6. Colin R. Ferguson, Internal Combustion Engines, Applied Thermosciences, First ed, Purdue University, United States, John Wiley & Sons, 1986, pp. 39.

7. Bosh Co., Swirl-chamber Spark Plugs Improve Combustion Process, Society of Automotive Engineers, Inc., Vol.92, No.7, 1984, pp. 35-39.

8. Carmine Lisio, Experimental Investigation on the Feasibility of Shock Wave Application as a Hydrogen Ignition Source in Diesel Engines, Concordia University Master's Thesis, Montreal, Canada, August 1990, pp. 17-18.

9. E. N. Quiros, and J. W. Adams, Experimental and Theoretical Evaluation of a Toroidal Combustion Chamber for Stratified Charge Engine, SAE Technical Paper Series, No.900606, International Congress and Exposition, Detroit, Michigan, U.S.A., February 26 - March 2, 1990, pp. 1-6.

10. H. Tanabe and G.T. Sato, Experimental Study on Unsteady Wall Impinging Jet, SAE Technical Paper Series, No.900605, 1990, pp. 1-7.

11. S. Furuhama and Y. Kobayashi, Development of a Hot-Surface-Ignition Hydrogen Injection, Two-Stroke Engine, International Journal of Hydrogen Energy, Vol.9, No.3, pp. 205-213.

12. W.L. Mitchell et al., Neat Methanol Combustion in a D.I. Diesel Engine Using Catalytically Coated Glow Plugs, SAE Technical Paper Series, No.912418, pp. 97-104.

13. E. U. Ubong, Development of an Ethanol D.I. Spark Assisted Diesel Engine (SADE), SAE Technical Paper Series, No.901567, 1990, pp. 1-3, 9.

14. Michael A. V. Ward, A New Spark Ignition System for Lean Mixtures Based on a New Approach to Spark Ignition, SAE Technical Paper Series, No.890475, 1989, pp. 1-9.

15. G. T. Kalghatgi, Spark Ignition, Early Flame Development and Cycle Variation in I.C. Engines, SAE Technical Paper Series, No.870163, 1987.

16. T. Krepec et al., Research and Development of a New Concept for On-Board Storage, Direct Injection and Ignition of Gaseous Fuels in Automotive Internal Combustion Engines, Concordia University, Mechanical Engineering Department, Center for Industrial Control, Progress Report No 2, pp. 85-99.

17. T. Fukuma, T. Fujita, P. Pichainarnog, S. Furuhama, Hydrogen Combustion Study in Direct Injection Hot Surface Ignition, SAE Technical Paper Series, 1986, No. 86157.

18. T. Krepec, T. Giannacopoulos, C. Lisio, Preliminary Investigation on a Microprocessor Controlled Gaseous Hydrogen Injector, Hydrogen Energy, 1987, Vol.12, No.12, pp. 855-861.

19. D. Miele, Investigation on a Multi-Point Direct Injection and Control System for Gaseous Fuels in Diesel Engines, Master's Thesis, Concordia University, Department of Mechanical Engineering, pp. 97-134.

20. T. Tebelis et al., A Concept of Electronically Controlled Hydrogen-gas Injector for High Speed Compression Ignition Engines, Proceedings on the Second International Symposium on Hydrogen, Produced for Renewable Energy, 1985, pp. 397-408.

21. T. Krepec et al., Research and Development of a New Concept for On-Board Storage, Direct Injection and Ignition of Gaseous Fuels in Automotive Internal Combustion Engines, Concordia University, Mechanical Engineering Department, Center for Industrial Control, Progress Report No.4, pp. 21-23.

22. C.J. Green et al., Electrically Actuated Injectors for Gaseous Fuels, SAE Technical Paper Series, 1989, No.892143, pp. 135-145.

23. H. Hong et al., Optimization of Electronically Controlled Injectors for Direct Injection of Natural Gas in Diesel Engines, SAE Technical Paper Series, 1993.

24. H. Hong et al., Design Optimization of Solenoid Operated Diesel Injectors for Gaseous Fuels, CSME Forum "Transport 1992+", Vol.II, Concordia University, Montreal, Canada, 1992, pp. 349-354.

25. Jefferson C. Boyce, Operational Amplifier and Linear Integrated Circuit, Second Edition, United States, PWS-Kent Published Company,1988.

26. F.G. Speadbury, Electrical Ignition Equipment, First ed, Great Britain, Constable & Company Ltd, 1954, pg. 29.

27. Intel Corporation, 16-Bit Embedded Controllers Handbook, 1991, pp. 1-13 to 1-27.

28. Intel Corporation, EV80C196KB Microcontroller Evaluation Board, User's Manual, Release 001, Feb., 1989, pg. 17.

29. James E.A. John, Gas Dynamics, Second ed, United States, Allyn and Bacon, 1984, pp. 360-363.

30. Wolfgang Merzkirch, Flow Visualization, Second Edition, Germany, Academic Press Inc, 1987, pp. 134-135.

31. John B. Heywood, Internal Combustion Engine Fundamentals, United States, McGraw-Hill Publishing Company, 1988, pp. 550-551.

32. Charles Fayette Taylor, The Internal-Combustion Engine in Theory and Practice, Volume 2: Combustion, Fuels, Materials, Design, Revised Edition, United States, The M.I.T. Press, 1977, pg. 92.

33. James E.A. John, pp. 139-154.

34. D. Brian Spalding, Combustion and Mass Transfer, First Edition, Pergamon Press, England, 1979, pg. 199.

35. Bosch, Automotive Electric/Electronic Systems, First Edition, Robert Bosch Gmbh, Germany, 1988, pp. 177-179.

36. H. Hiroyasu et al., Supplementary Comments: Fuel spray Characterization in Diesel Engines, in James N. Mattavi and Charles A. Amann (eds.), Combustion Modelling in reciprocating Engines, Plenum Press, 1980, pp. 369-408.

APPENDIX A

The program ENGINE has been designed for the control of the fuel injector and the ignition signal via a signal sent by the camshaft. This software uses two external interrupts which are triggered by optical switches, placed on the engine camshaft so that the crankshaft position can be determined. The details concerning this software are discussed in section 5.1.5.

ENGINE PROGRAM

```
 injector MODULE main
;
;  This file contains a memory test for the EV80C196KB board.
;
rseg
;
zero          equ    00H     ; Zero register
spcon         equ    11H:byte ; Serial port control
spstat        equ    11H:byte ; Serial port status
sbuf          equ    07H:byte ;
watchdog      equ    0aH:byte ; Watchdog timer reset register
baud_reg      equ    0eH:byte ; Baud rate control
ioport1       equ    0fH:byte ; I/O port 1
ioport2       equ    10H:byte ; I/O port 2
ioc1          equ    16H     ; I/O control register (Port2)
ioc0          equ    15H     ; I/O control register (HSIO)
ios0          equ    15H     ; I/O status register 0
ios1          equ    16H     ; I/O status register 1
pwm_control    equ    17H     ; PWM Control register
int_pending    equ    09H     ; Interrupt pend register
int_pend1      equ    12H     ; Interupt pend register 1
int_mask       equ    08H     ; Interupt mask register
int_mask1      equ    13H     ; Interupt mask register 1
timer1         equ    0aH     ; Timer 1
hso_command    equ    06H     ; hso command reg
hso_time       equ    04H     ; hso time reg
hsi_status     equ    06H     ; hsi status reg
hsi_time       equ    04H     ; hsi time reg
hsi_mode       equ    03H     ; hsi mode reg
ad_command     equ    02H     ; A/D command reg
ad_result_lo   equ    02H     ; A/D result reg lo
```

```
ad_result_hi   equ    03H    ; A/D result reg hi
sp             equ    18H    ; The stack pointer
;
;*************************************************************
rseg at 1ch
;
ax:       dsw   1      ; General registers
  al      equ   ax:byte
  ah      equ   (ax+1):byte
bx:       dsw   1
cx:       dsw   1
dx:       dsw   1
;
;*************************************************************
cseg at 203ah
;
EXTINT_pin:  dcw   209BH
;
cseg at 2008h
;
HSI0_Pin:    dcw   20D3H
;
;$eject
;
cseg at 2080h
;
  energy  equ   0300H:word
  de_mag  equ   0300H:word
  ignite  equ   1000H:word
;
reset_vector:
      ld   sp,#100H
      clr  ax
      clr  bx
      clr  cx
      clr  dx
;
      ldb  hso_time,#00H
      ldb  ioport1,#00H
      orb  int_mask1,#00100000B
      orb  int_mask,#00010000B
      EI
;
wait:
      br   wait
;
start_In:
      PUSHF
;
rev:
      inc  ax
;
```

```
      cmp   ax,#0018h
      be    skipit2
;
      cmp   ax,#0019h
      bne   skipit
;
      orb   ioport1,#01H
power: inc   bx
      cmp   bx,#energy
      bne   power
;
      clr   bx
;
      andb  ioport1,#11111110B
      orb   ioport1,#02H
demagt: inc   bx
      cmp   bx,#de_mag
      bne   demagt
;
      clr   bx
      inc   dx
;
      andb  ioport1,#11111101B
      br    skipit
;
skipit2:
      ldb   ioport1,#08H
;
skipit:
;
      POPF
      RET
;
start_Ig:
;
      PUSHF
;
      cmp   dx,#0001h
      bne   skipit1
;
      ldb   ioport1,#00H
ign:   inc   bx
      cmp   bx,#ignite
      bne   ign
;
      clr   bx
      clr   ax
;
      clr   dx
```

```
;
skipit1:
;
        POPF
        RET
;
        end
```

This program called ENGINE1 is designed for the same engine except that it uses only one external interrupt as opposed to two for ENGINE. It is some what similar to the previous program. However, the difference lies in the fact that the ignition is triggered immediately after the injector forward signal. With this program there is no external control for the ignition system whereas the program ENGINE the ignition signal was controlled by an external interrupt.

ENGINE1 PROGRAM

```
 injector MODULE main
;
;  This file contains a memory test for the EV80C196KB board.
;
rseg
;
zero          equ    00H    ; Zero register
spcon         equ    11H:byte ; Serial port control
spstat        equ    11H:byte ; Serial port status
sbuf          equ    07H:byte ;
watchdog      equ    0aH:byte ; Watchdog timer reset register
baud_reg      equ    0eH:byte ; Baud rate control
ioport1       equ    0fH:byte ; I/O port 1
ioport2       equ    10H:byte ; I/O port 2
ioc1          equ    16H    ; I/O control register (Port2)
ioc0          equ    15H    ; I/O control register (HSIO)
ios0          equ    15H    ; I/O status register 0
ios1          equ    16H    ; I/O status register 1
pwm_control    equ    17H    ; PWM Control register
int_pending    equ    09H    ; Interrupt pend register
int_pend1      equ    12H    ; Interupt pend register 1
int_mask       equ    08H    ; Interupt mask register
int_mask1      equ    13H    ; Interupt mask register 1
timer1         equ    0aH    ; Timer 1
hso_command    equ    06H    ; hso command reg
hso_time       equ    04H    ; hso time reg
hsi_status     equ    06H    ; hsi status reg
hsi_time       equ    04H    ; hsi time reg
hsi_mode       equ    03H    ; hsi mode reg
ad_command     equ    02H    ; A/D command reg
ad_result_lo   equ    02H    ; A/D result reg lo
```

```
ad_result_hi   equ    03H    ; A/D result reg hi
sp          equ    18H    ; The stack pointer
;
;*************************************************************
rseg at 1ch
;
ax:       dsw    1      ; General registers
  al      equ    ax:byte
  ah      equ    (ax+1):byte
bx:       dsw    1
cx:       dsw    1
dx:       dsw    1
;
;*************************************************************
cseg at 203ah
;
EXTINT_pin:  dcw   209BH
;
;$eject
;
cseg at 2080h
;
  energy  equ    0100H:word
  de_mag  equ    0300H:word
  ignite  equ    0500H:word
;
reset_vector:
      ld   sp,#100H
      clr  ax
      clr  bx
      clr  cx
      clr  dx
;
      ldb  hso_time,#00H
      ldb  ioport1,#00H
      orb  int_mask1,#00100000B
      orb  int_mask,#00010000B
      EI
;
wait:
      br   wait
;
start_In:
      PUSHF
;
rev:
      inc  ax
;
      cmp  ax,#0018h
      be   skipit2
;
      cmp  ax,#0019h
```

```
      bne   skipit
;
      orb   ioport1,#01H
power: inc   bx
      cmp   bx,#energy
      bne   power
;
      clr   bx
;
      andb  ioport1,#11110110B
      orb   ioport1,#02H
demagt: inc   bx
      cmp   bx,#de_mag
      bne   demagt
;
      clr   bx
      clr   ax
;
      andb  ioport1,#11111101B
      br    skipit
;
skipit2:
      ldb   ioport1,#08H
;
skipit:
;
      POPF
      RET
;
      end
```

This last program has been written for the schlieren photography experiment. It has been used to sequence the injector with the flash lamp and the reverse signal for closing the injector. In this case no external interrupts are used, only a software loop is used to generate a time delay sufficient so that the operator is allowed suficient time to set the equipment.

SP PROGRAM

```
  injector MODULE main
;
;  This file contains a memory test for the EV80C196KB board.
;
rseg
;
zero          equ    00H    ; Zero register
spcon         equ    11H:byte ; Serial port control
spstat        equ    11H:byte ; Serial port status
sbuf          equ    07H:byte ;
watchdog      equ    0aH:byte ; Watchdog timer reset register
baud_reg      equ    0eH:byte ; Baud rate control
ioport1       equ    0fH:byte ; I/O port 1
ioport2       equ    10H:byte ; I/O port 2
ioc1          equ    16H    ; I/O control register (Port2)
ioc0          equ    15H    ; I/O control register (HSIO)
ios0          equ    15H    ; I/O status register 0
ios1          equ    16H    ; I/O status register 1
pwm_control    equ    17H    ; PWM Control register
int_pending    equ    09H    ; Interrupt pend register
int_pend1      equ    12H    ; Interupt pend register 1
int_mask       equ    08H    ; Interupt mask register
int_mask1      equ    13H    ; Interupt mask register 1
timer1         equ    0aH    ; Timer 1
hso_command    equ    06H    ; hso command reg
hso_time       equ    04H    ; hso time reg
hsi_status     equ    06H    ; hsi status reg
hsi_time       equ    04H    ; hsi time reg
hsi_mode       equ    03H    ; hsi mode reg
ad_command     equ    02H    ; A/D command reg
ad_result_lo   equ    02H    ; A/D result reg lo
ad_result_hi   equ    03H    ; A/D result reg hi
sp          equ    18H    ; The stack pointer
```

```
;
;*************************************************************
rseg at 1ch
;
ax:      dsw   1      ; General registers
bx:      dsw   1
cx:      dsw   1
dx:      dsw   1
;
;*************************************************************
cseg at 2080h
;
  energy  equ   0500H:word
  de_mag  equ   0100H:word
  light   equ   0200H:word
;

reset_vector:
      ld   sp,#100H
      clr  ax
      clr  bx
      clr  cx
      clr  dx
;
       ldb  ioport1,#00H

delay1:
     inc ax
     clr bx
   delay2:
        inc bx
        cmp bx,#0150h
        bne delay2
     cmp ax,#5000h
     bne delay1

     clr ax
     clr bx

     ldb  ioport1,#04h
power: inc  bx
    cmp  bx,#energy
    bne power
```

```
start_Light:

      orb  ioport1,#10h
on:    inc  dx
      cmp  dx,#light
      bne  on

      andb ioport1,#00h
      clr  bx
      clr  dx
;
      orb ioport1,#08h
demagt: inc  bx
      cmp  bx,#de_mag
      bne  demagt

      andb  ioport1,#00h
;
wait:
      br wait
      end
```

APPENDIX B

The detail drawings shown in this section, are those of the ignition chamber prototype discused in section 5.2.

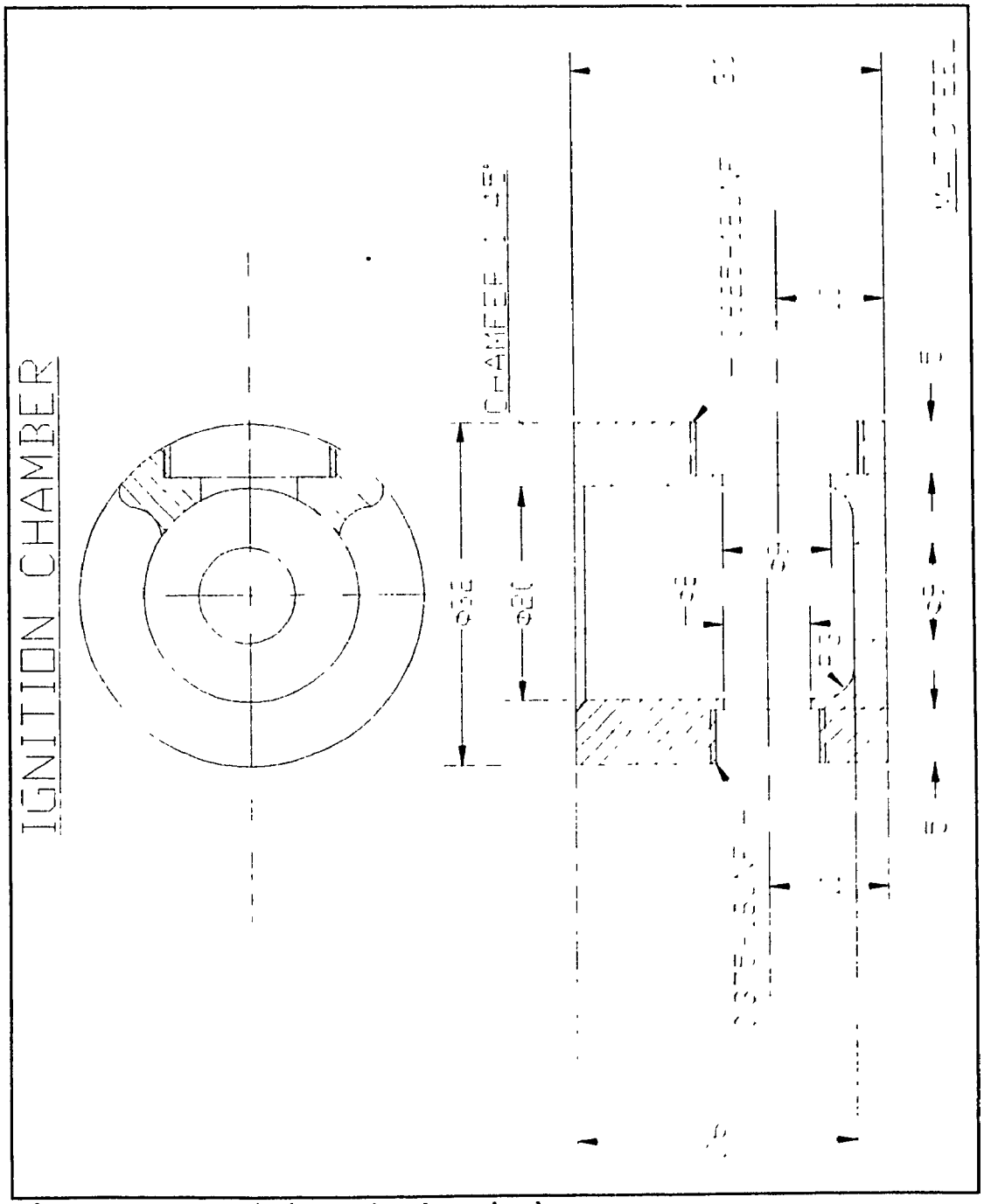

Figure B.1 Ignition chamber body

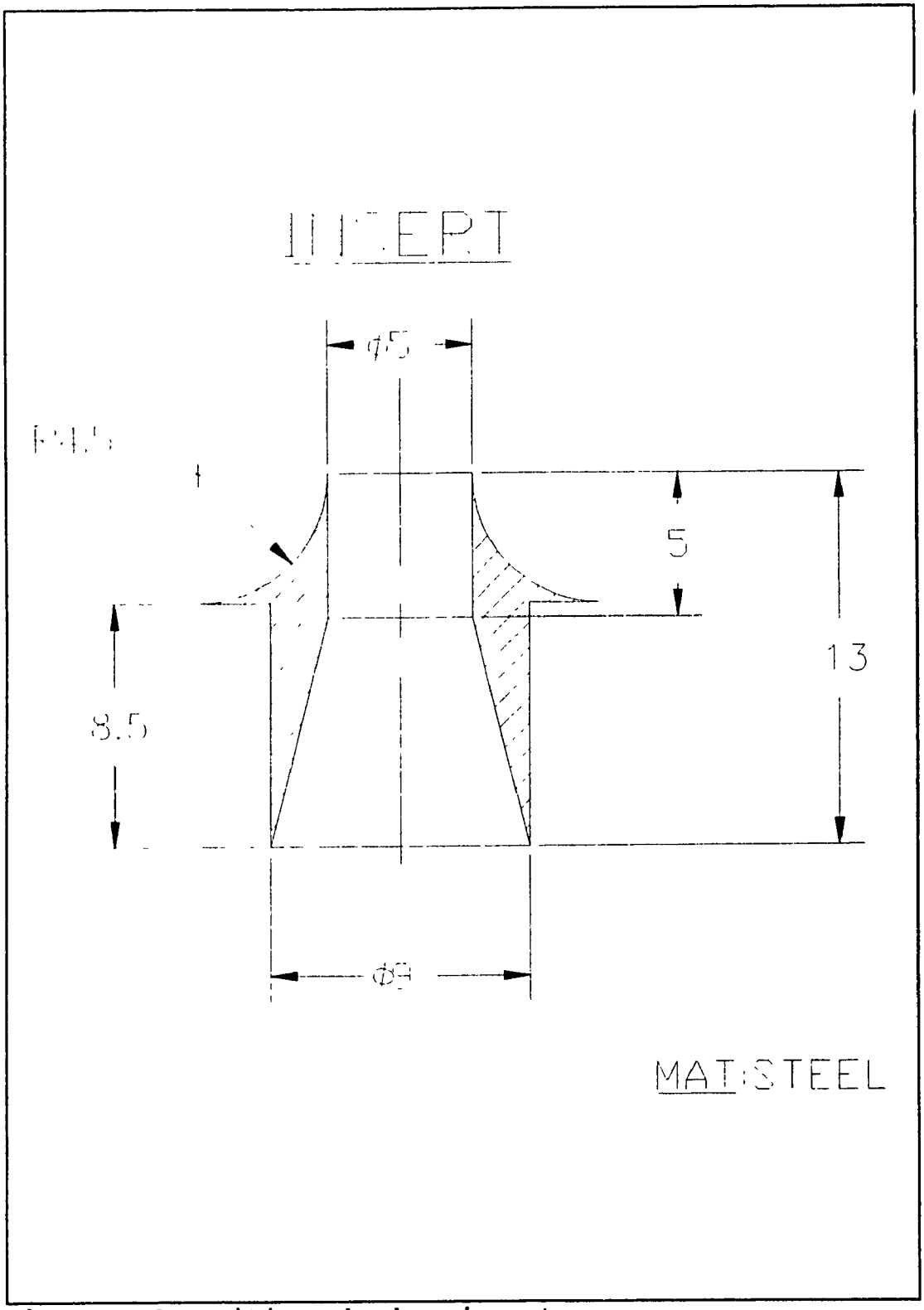

Figure B.2 Ignition chamber insert

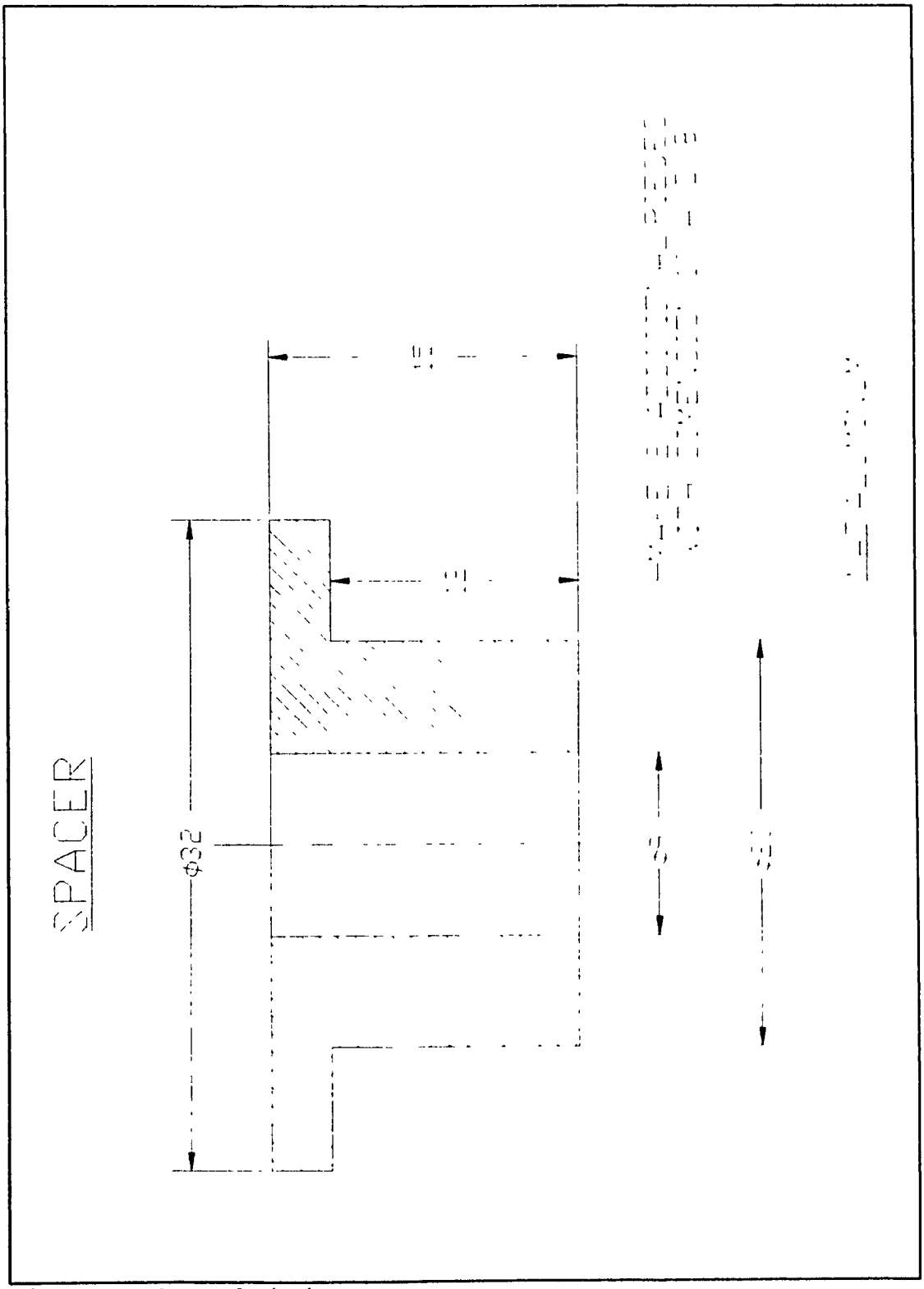

Figure B.3 Fuel injector spacer

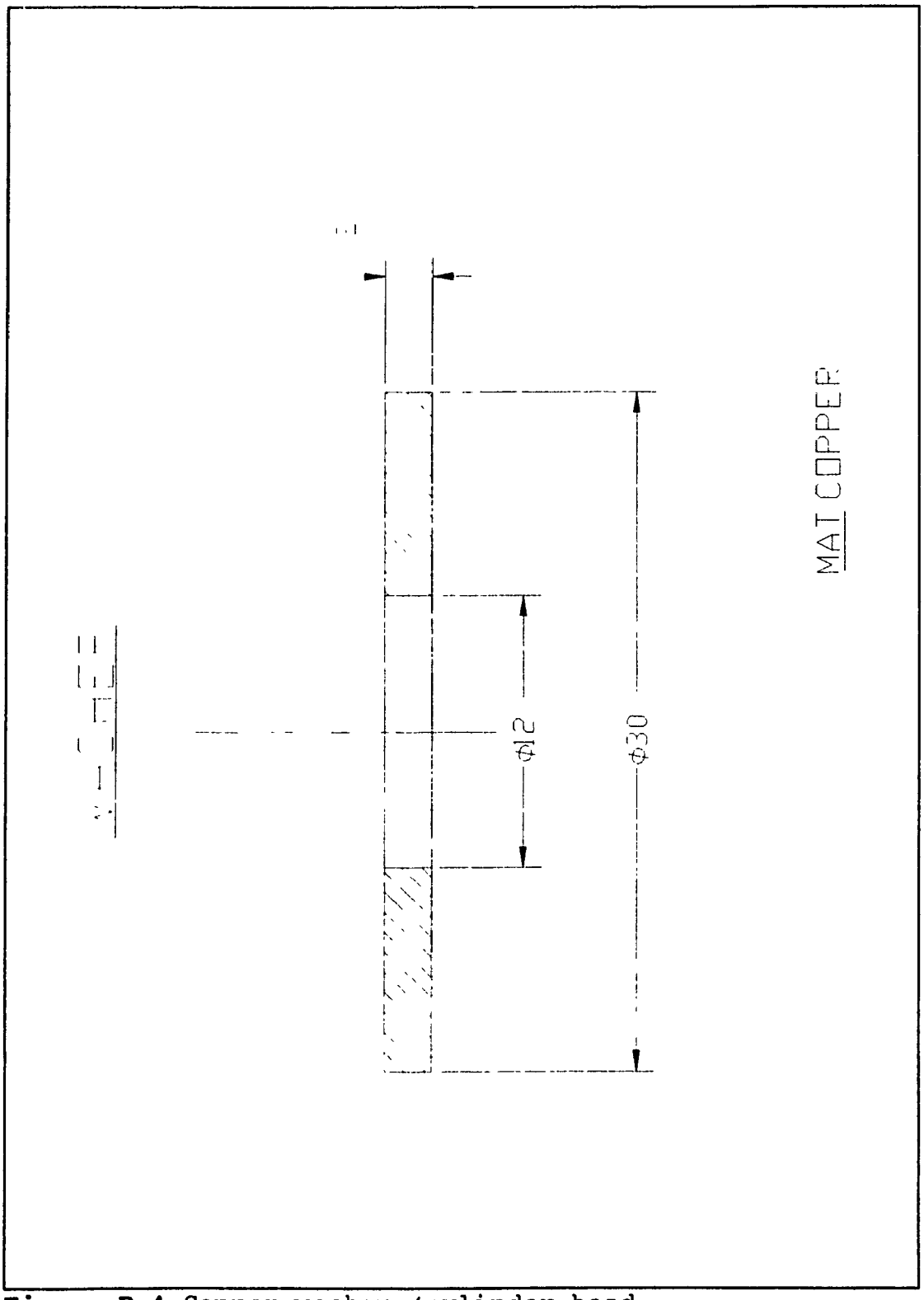

Figure B.4 Copper washer (cylinder head and ignition chamber)

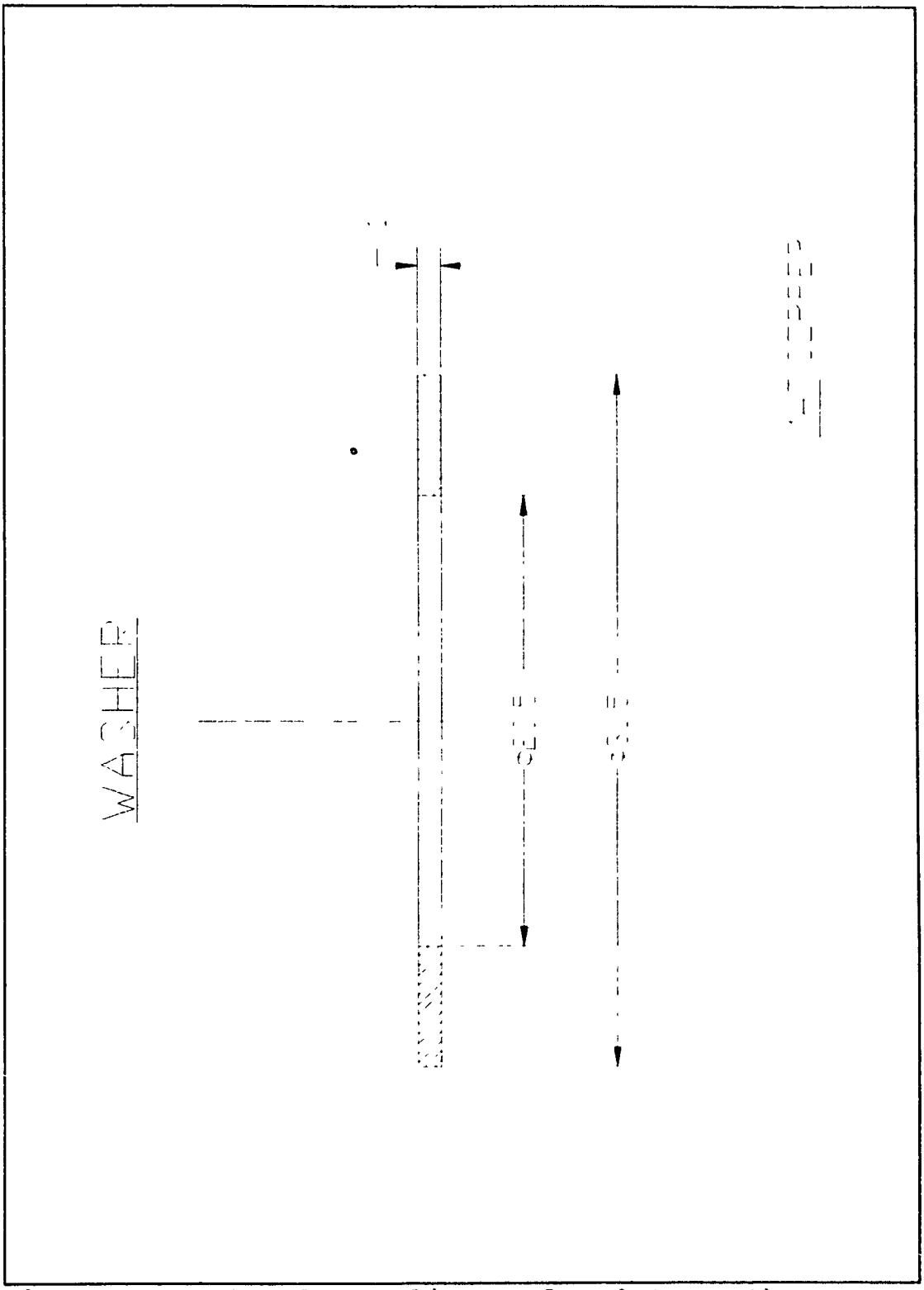

Figure B.5 Washer for sealing surface between the fuel injector spacer and the ignition chamber

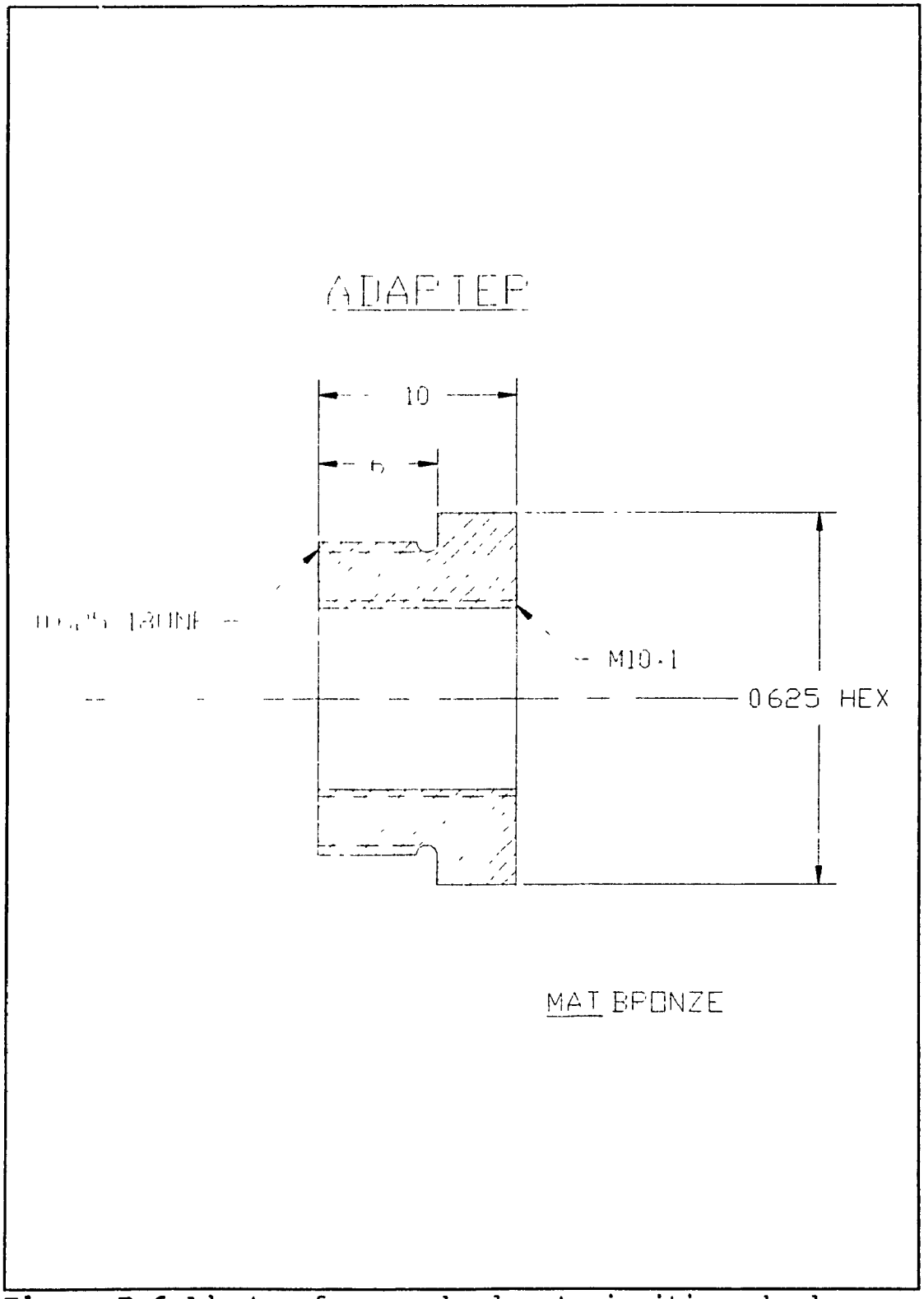

Figure B.6 Adapter for spark plug to ignition chamber

APPENDIX C

The drawings shown in this section represent the different spacer configurations tested on the diesel test engine. For this engine, seven spacers have been machined out of aluminum.

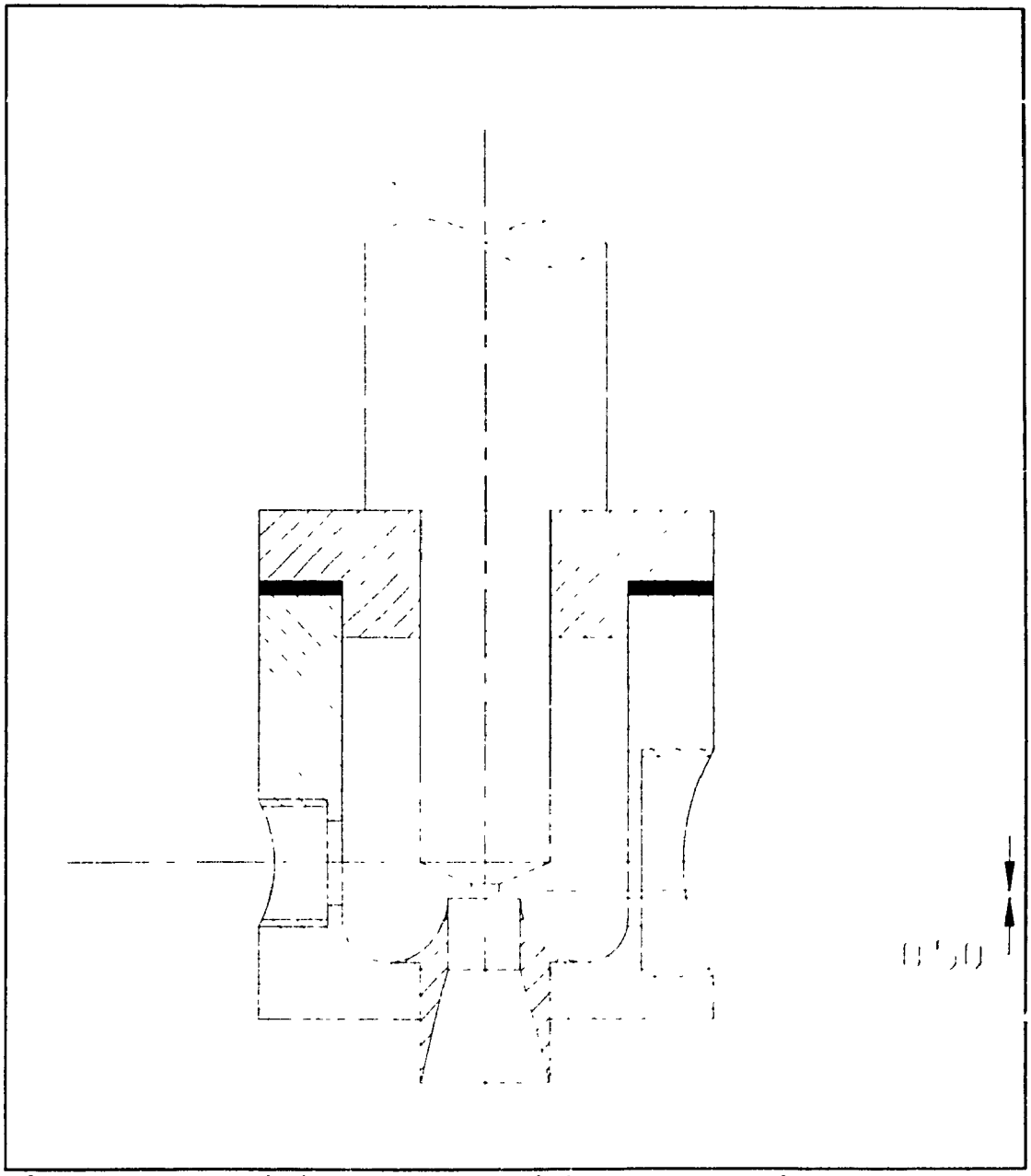

Figure C.1 Ignition chamber with spacer number 1

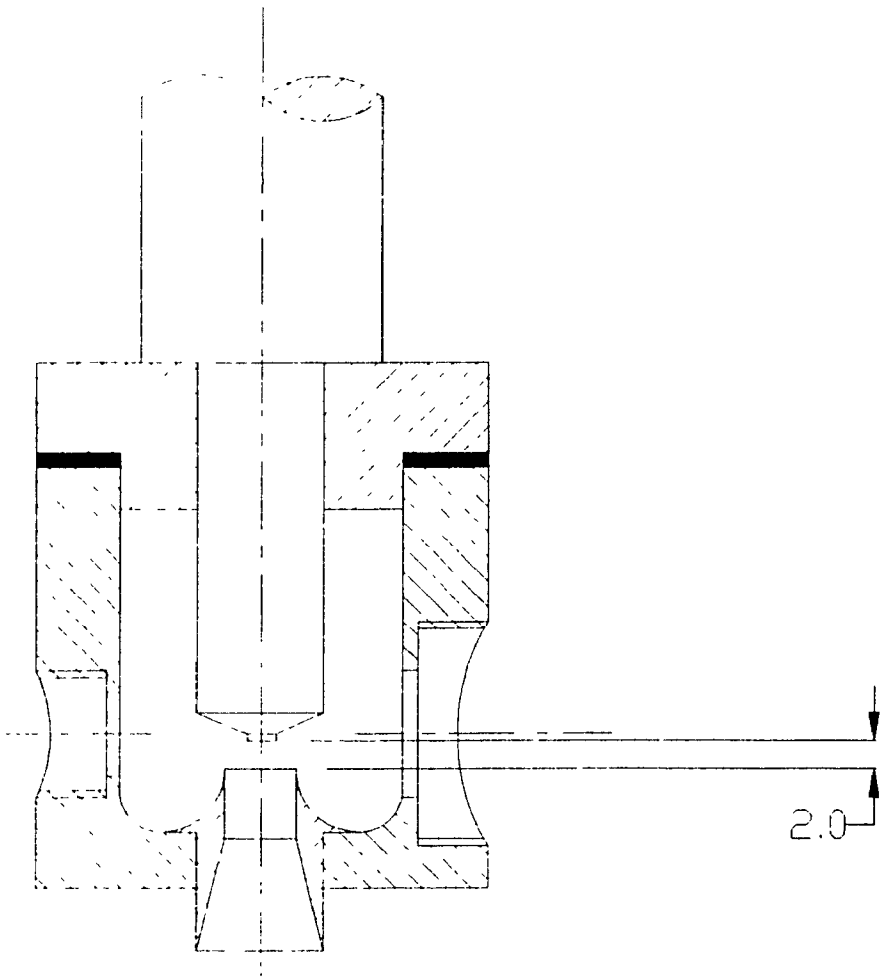

Figure C.2 Ignition chamber with spacer number 2

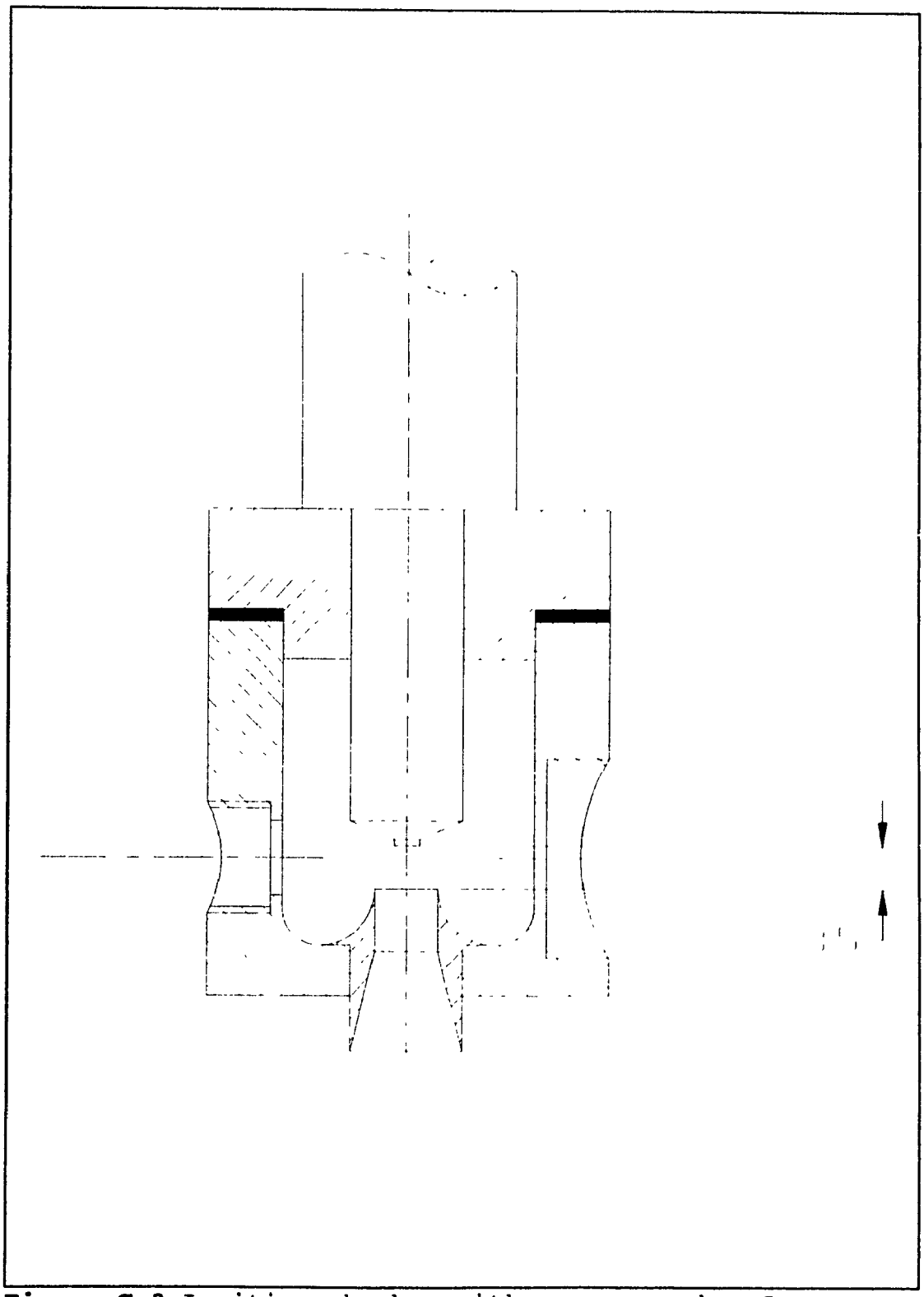

Figure C.3 Ignition chamber with spacer number 3

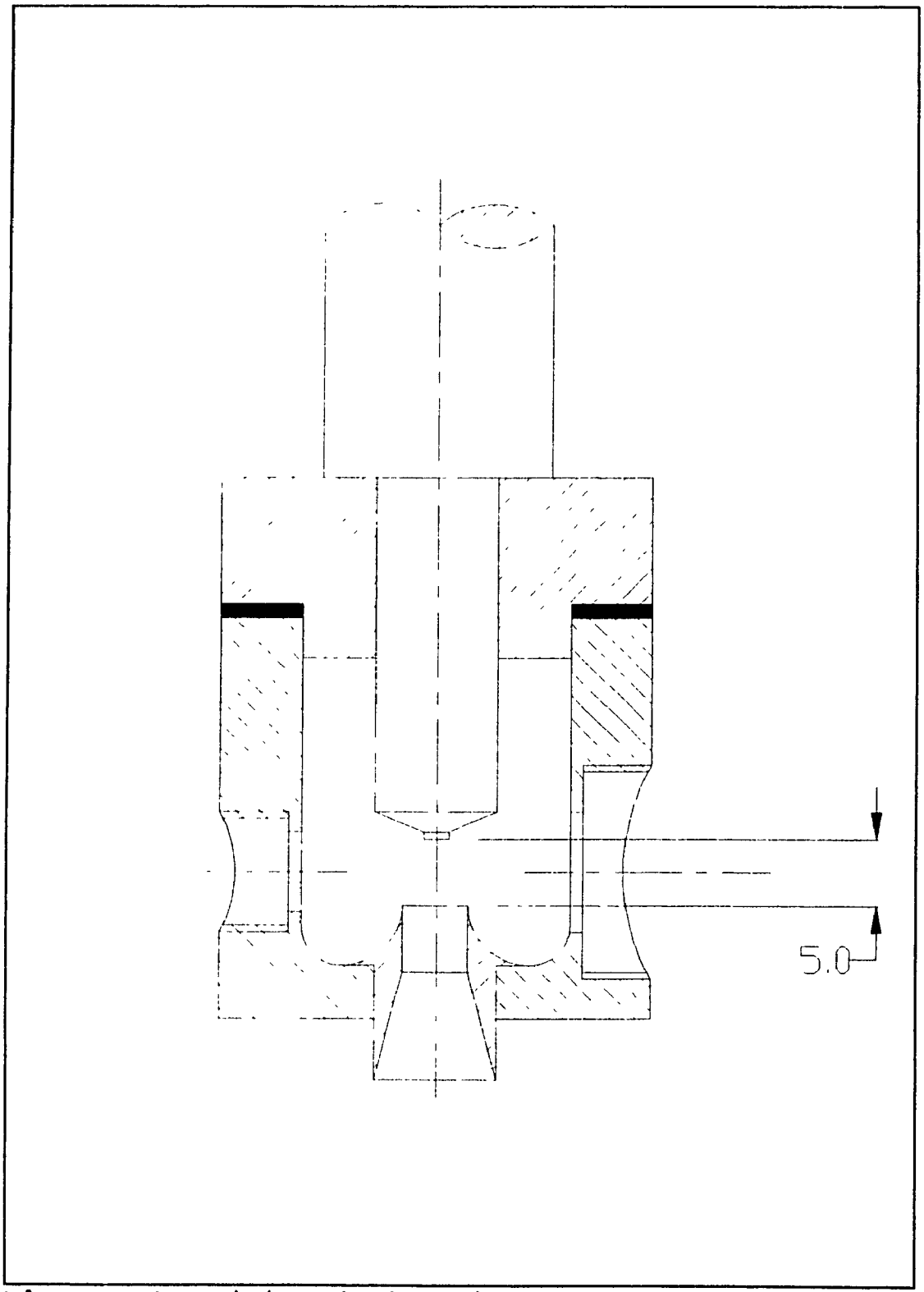

Figure C.4 Ignition chamber with spacer number 4

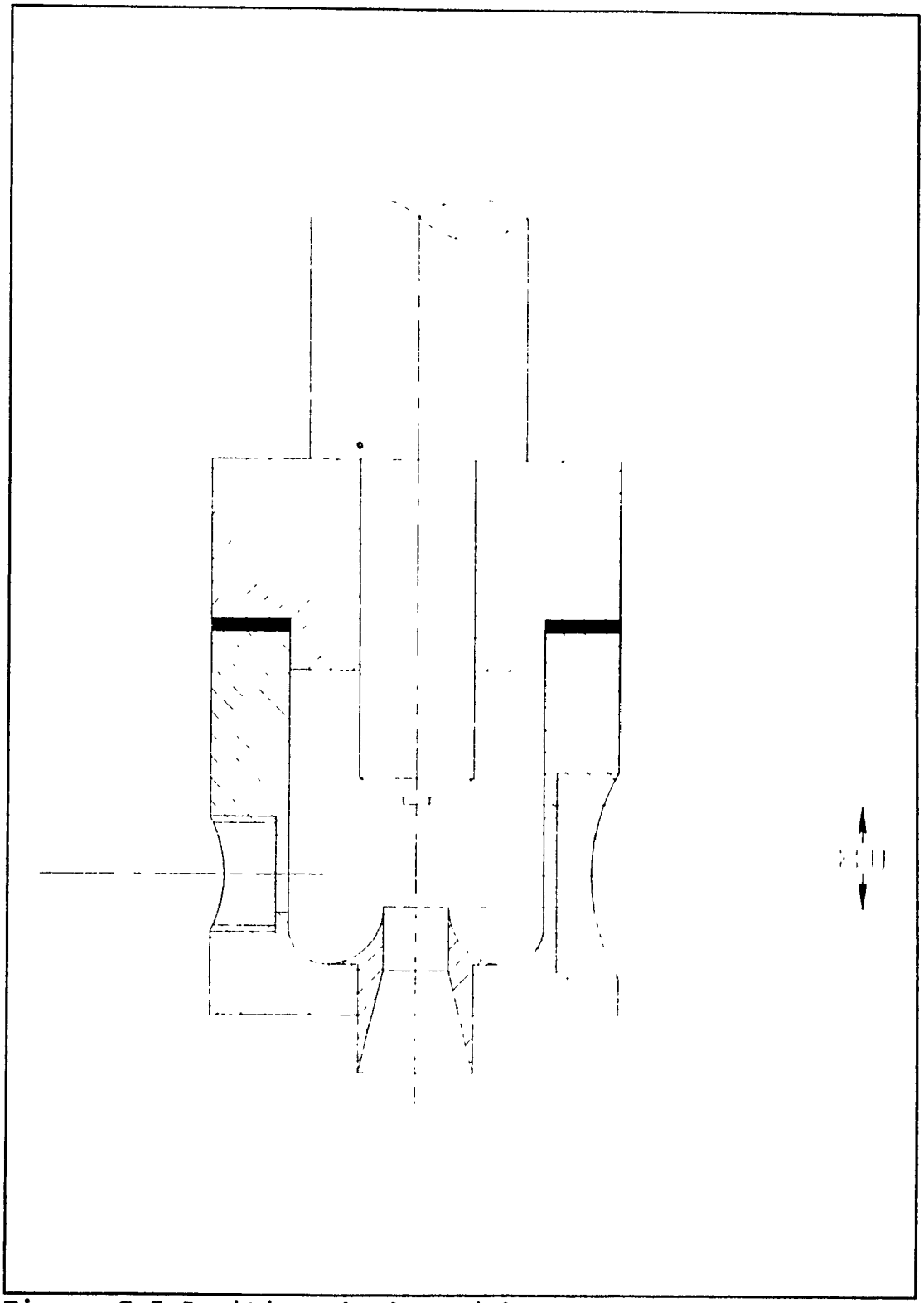

Figure C.5 Ignition chamber with spacer number 5

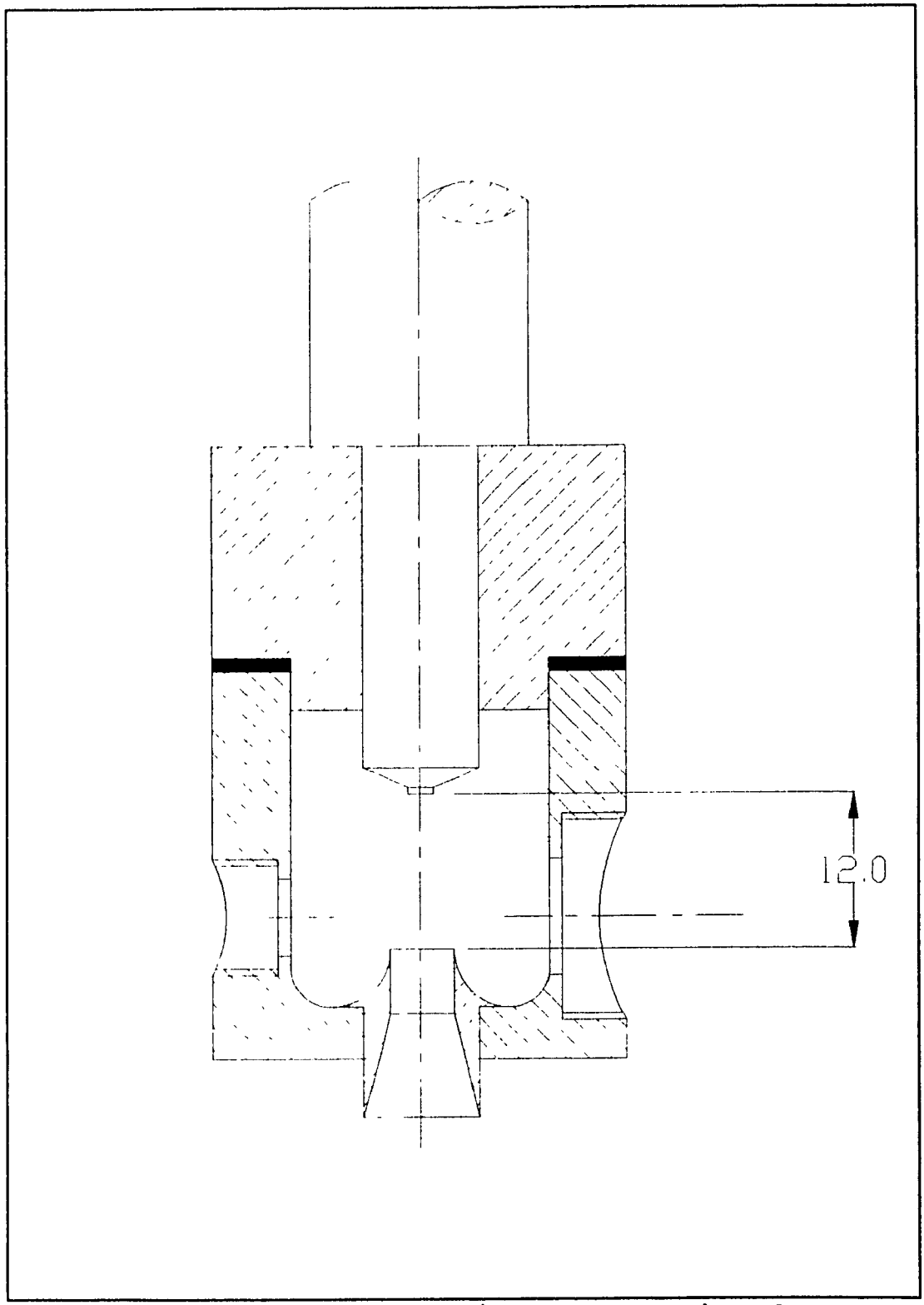

Figure C.6 Ignition chamber with spacer number 6

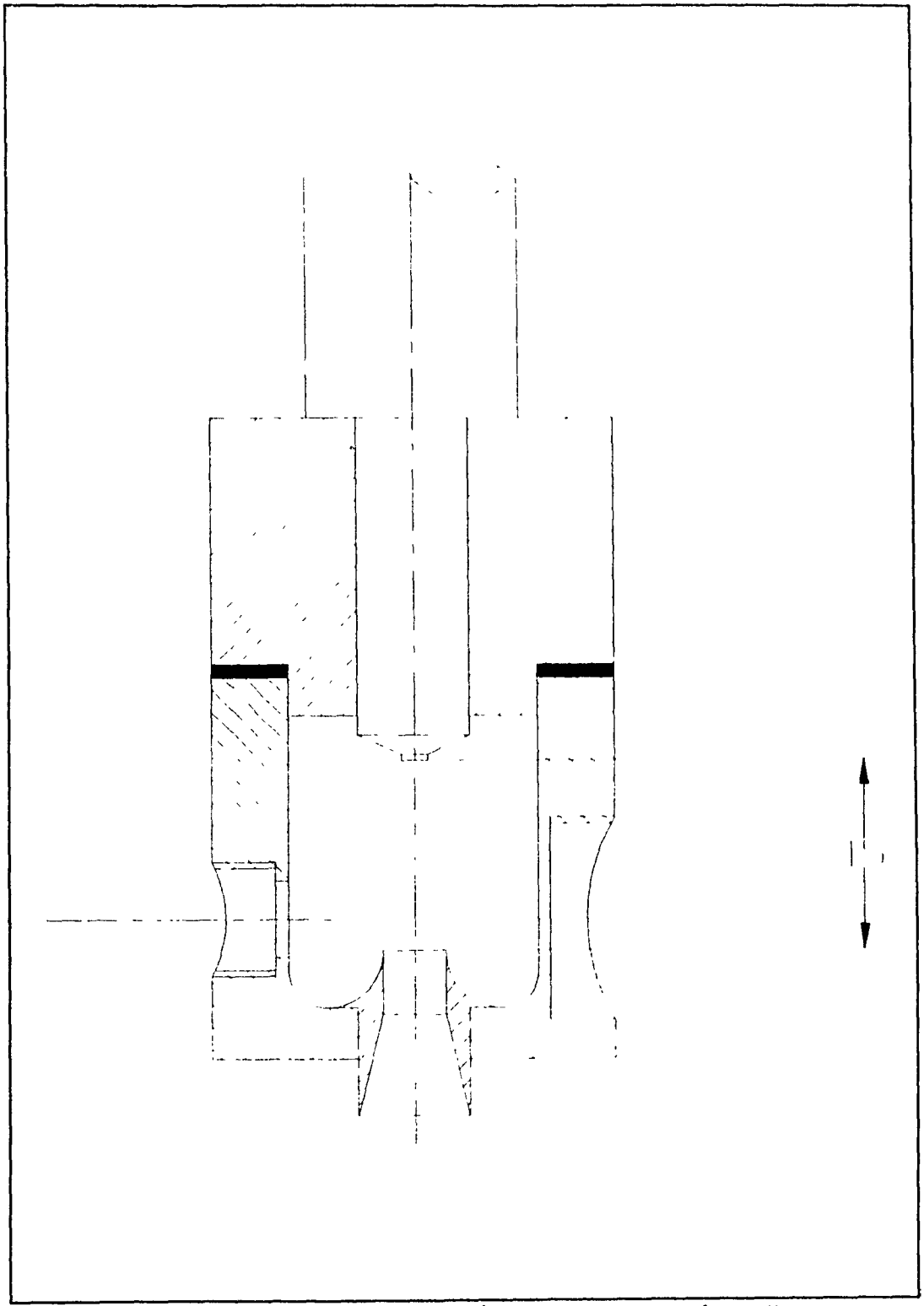

Figure C.7 Ignition chamber with spacer number 7

APPENDIX D

Pressure transducer manufactured by Kistler:

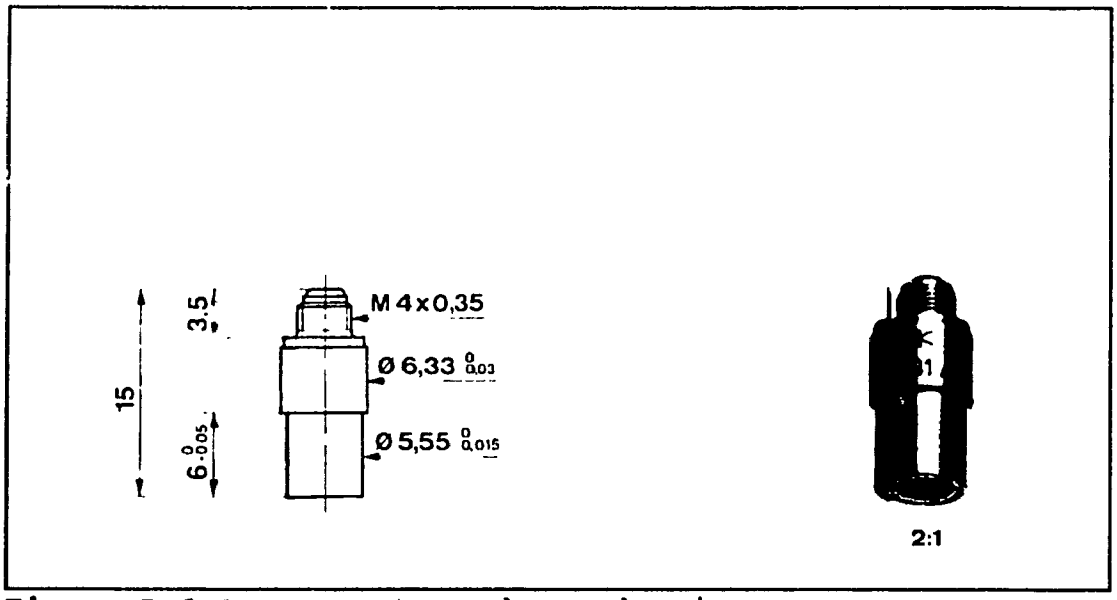

Figure D.1 Pressure transducer drawing

TECHNISCHE DATEN — DONNEES TECHNIQUES — TECHNICAL DATA

Druckaufnehmer	Capteur de pression	Pressure Transducer		601A	601H
Bereich	Gamme	Range	bar	0 ..250	0. 1000
Kalibrierter Teilbereich: 10%	Gamme partielle étalonnée: 10%	Calibrated partial range: 10%	bar	0...25	0. 100
1%	1%	1%	bar	0 .2,5	0.. 10
Ansprechschwelle	Sault de réponse	Threshold	bar	<0,002	<0,002
Überlast	Surcharge	Overload	bar	500	1200
Empfindlichkeit	Sensibilité	Sensitivity	pC/bar	≈ −16	≈ −16
Kraft-Empfindlichkeit	Sensibilité à la force	Force-sensitivity	pC/N	≈ −13	≈ −13
Eigenfrequenz	Fréquence propre	Natural frequency	kHz	>150	>150
Anstiegszeit	Temps de montée	Rise time	µs	3	3
Linearität	Linéarité	Linearity	%FSO	≤±0,5	≤±0,8
Isolationswiderstand	Résistance d'isolement	Insulation resistance	TΩ	100	100
Kapazität	Capacité	Capacitance	pF	5	5
Beschleunigungsempfindlichkeit	Sensibilité aux accélérations	Acceleration sensitivity	bar/g	0,001	0,001
Temperaturkoeffizient der Empfindlichkeit	Coefficient de température de la sensibilité	Temperature coefficient of the sensitivity	°C⁻¹	10^{-4}	10^{-4}
Betriebstemperaturbereich	Gamme de température d'utilisation	Operating temperature range	°C	−196 240	−196 240
Stossfestigkeit	Résistance au choc	Shock resistance	g	10'000	10'000
Gewicht	Poids	Weight	g	1,7	1,7

1 bar 10^5 Pa (Pascal) 10^5 N m^{-2} 1,0197 at - 14,503 psi, 1 in 25,4 mm, 1 N - 0,22480 lbf, 1 kg 2,2046.. lb, 1 TΩ (Teraohm) - 10^{12}Ω

Figure D.2 Technical information for the pressure transducer

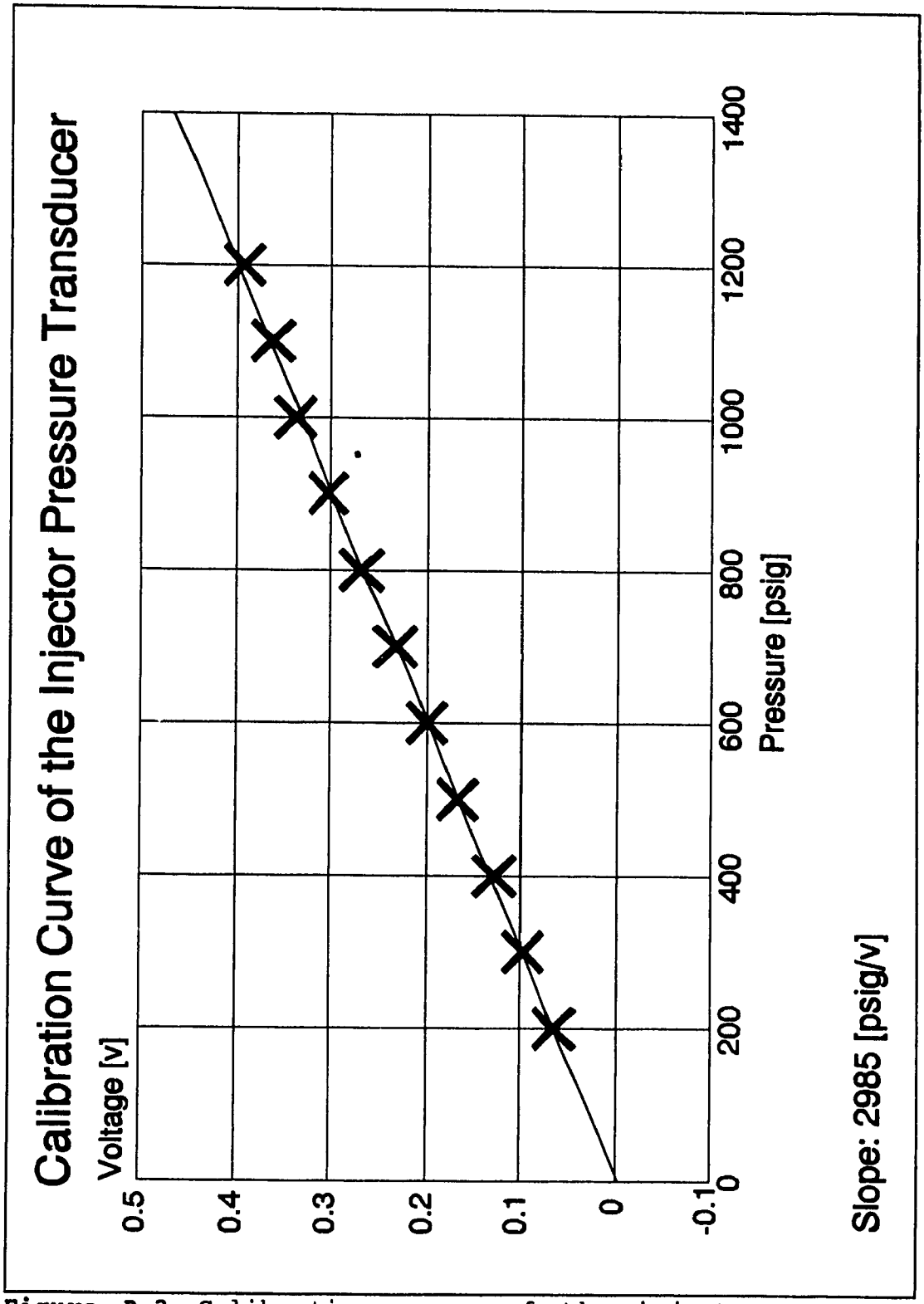

Figure D.3 Calibration curve of the injector pressure transducer

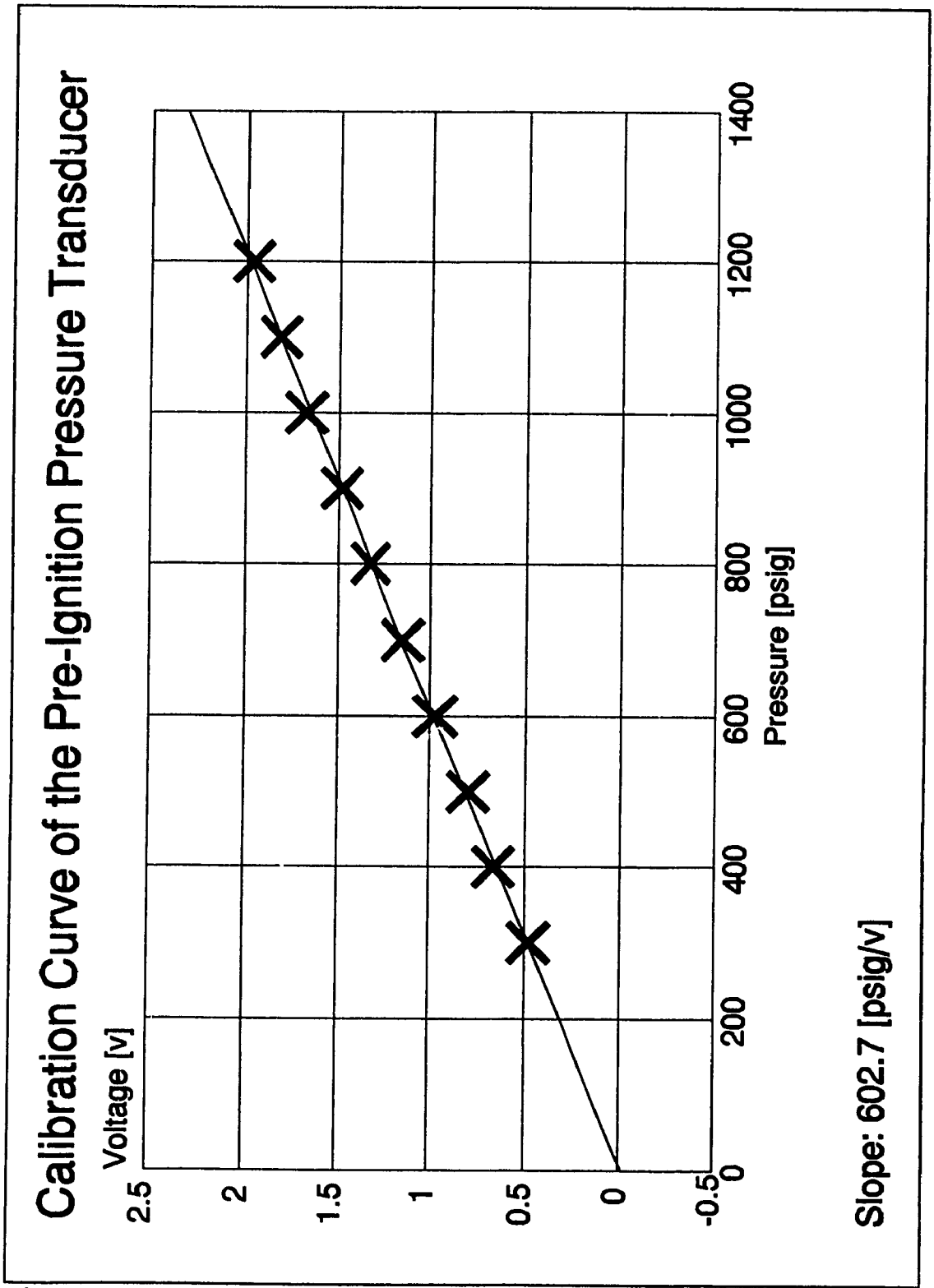

Figure D.4 Calibration curve of the ignition chamber pressure transducer

APPENDIX E

The following list is the specificaiton to the Petters diesel engine.

PH and PHW

General Data

		PH1	PH2	PHW1	PHW2
Injection		Direct			
Rotation Looking on Flywheel		Clockwise and Anti-clockwise Builds			
Bore	mm in	87 465 3.443	87 465 3.443	87 313 3 437	87 313 3 437
Stroke	mm in	110 4 33	110 4 33	110 4 33	110 4 33
Piston Area	cm^2 in^2	60 08 9.313	60 08 9 313	59 89 9 282	59 89 9 283
Cylinder Capacity - total	l cm^3 in^3	0.661 660 9 40.325	1 321 1 321 8 80.65	0 659 659 0 40 20	1 318 1318 0 80 40
Compression Ratio		16 5.1	16.5 1	16 5 1	16 5 1
Mean Piston Speed at 2200 r/min	m/sec ft/min	8 066 1588	8 066 1588	8.066 1588	8 066 1588
Maximum Permissible Crankshaft End Thrust	kg lb	181 8 400.0	181 8 400 0	181 8 400 0	181 8 400 0
Mechanical Efficiency		74%	74%	74%	74%
Brake Thermal Efficiency		32%	32%	32%	32%
Oil Sump Capacity (engine level)	l pt US qt	2.8 5 0 3 0	5 7 10 0 6 0	2 8 5 0 3 0	5 7 10 0 6 0
Lubricating Oil Pressure (minimum at 1000r/min)	bar lbf/in^2	0.8 12	0 8 12	0 8 12	0 8 12
Lubricating Oil Pressure (mean)	bar lbf/in^2	2 8-4 0 40-60	2.8-4 0 40-60	2.8-4.0 40-60	2 8-4 0 40-60
Pressure Relief Valve Setting - when hot	bar lbf/in^2	2 76-3 45 40-50	2 76-3 45 40-50	2 4 35 0	2 4 35 0
Capacity Between Dipstick Marks	l pt US qt	0 57 1 0 0 60	1.81 3.18 1 90	0 57 1 0 0 60	1 81 3 18 1 90
Fuel Tank Capacity (engine mounted)	l pt US qt	6 8/18 0 11.9/31 6 7 1/18 9	6 8/18 11 9/31 6 7.1/18 9	6 8/18 0 11 9/31 6 7 1/18 9	6 8/18 0 11 9/31 6 7 1/18 9
Injector Setting - up to 1100r/min **Injector Setting - above 1100r/min**	bar atmos	155 217	155 217	155 217	155 217
Intake Restriction Before Derating	mmHg inH_2O	20 0 11 0	20 0 11 0	20.0 11 0	20 0 11 0
Exhaust Back Pressure Before Derating	mmHg inH_2O	42 0 23 0	42 0 23 0	42 0 23 0	42 0 23 0
Minimum Idling Speed	r/min	850	850	850	850
Weight of Flywheel	kg lb	59 5 131	59 5 131	59 5 131	59 5 131

Figure E.1 Engine data sheet